2 copies Bulk

GPO PRICE $ _____

CFSTI PRICE(S) $ _____

Hard copy (HC) 1.00

Microfiche (MF) .75

ff 653 July 65

JET PROPULSION LABORATORY
CALIFORNIA INSTITUTE OF TECHNOLOGY
PASADENA, CALIFORNIA

RE-ORDER NO. 64-521

This document consists of 104 pages,
250 copies, Series A

CONCEPTUAL DESIGN STUDIES OF AN ADVANCED MARINER SPACECRAFT

VOLUME I
SUMMARY

Prepared by

RESEARCH AND ADVANCED DEVELOPMENT DIVISION
AVCO CORPORATION
Wilmington, Massachusetts

This work was performed for the Jet Propulsion Laboratory, California Institute of Technology, sponsored by the National Aeronautics and Space Administration under Contract NAS7-100.

RAD-TR-64-36
Contract 950896

28 October 1964

Prepared for

CALIFORNIA INSTITUTE OF TECHNOLOGY
JET PROPULSION LABORATORY
4800 Oak Grove Drive
Pasadena, California

104 PAGES INCLUDE (8 ROMAN NUMERIAL)

SUMMARY

This report presents the results of a 4-month parametric analysis and conceptual design study conducted by the Research and Advanced Development Division of the Avco Corporation for the Jet Propulsion Laboratory. The study objectives included a parametric analysis of the unmanned flyby bus/lander concept for scientific investigation of Mars during the 1969 and 1971 launch opportunities, a conceptual design of the selected configuration, and a development and cost plan indicating the program leading to development and first flight of the Advanced Mariner vehicle in 1969.

The flyby bus/lander final concept utilizes a 1493-pound spacecraft launched by an Atlas Centaur vehicle. The scientific capability of the lander and flyby bus vehicles was determined to obtain a balance between scientific data and overall system complexity commensurate with the first landing mission to Mars.

The lander vehicle separates from the flyby bus vehicle prior to planet encounter, enters the planetary atmsophere, and descends to the surface on a parachute. During atmospheric entry, parachute descent, and surface operations, the lander analyzes the Martian atmosphere and, for 5 hours after impact, determines wind velocity, and also performs a simple life detection experiment. The information is transmitted to Earth via both a direct transmission link to the DSIF, and is also relayed through the flyby bus which has been placed on a delayed flyby trajectory for this purpose. The flyby bus also collects interplanetary data and maps the planet. The lander vehicle has been designed to accommodate the minimum projected atmosphere for Mars (11 millibar surface pressure) and surface winds gusting to 200 ft/sec, resulting in impact loads of up to 1500 g for a landed payload protected by crushable material. The lander is designed to be dry heat sterilized to avoid contamination of Mars with Earth organisms. The flyby bus is placed on a biased trajectory providing a small probability of entering the planetary atmosphere and therefore is not required to be sterilized.

The mission plan shows that a minimum of three launch attempts are necessary to achieve an 84 percent chance of at least one successful mission during the 1969 and 1971 launch opportunities. Hardware development must begin early in 1965 to meet a 1969 launch date.

ILLUSTRATIONS

ILLUSTRATIONS (Cont'd)

ILLUSTRATIONS (Concl'd)

TABLES

1.0 INTRODUCTION

The United States program for interplanetary flight to Mars will begin in November, 1964, with the launch of two NASA/JPL Mariner 64 spacecraft to perform planetary flyby missions. The Atlas-Agena launch vehicle used will limit each of these identical Mariners to an injected weight of approximately 570 pounds. Analytical studies of larger Mariner vehicles launched by the Atlas-Centaur during the 1969 and 1971 launch opportunities were initiated early in 1963 by JPL. The objective of this project, Advanced Mariner, was to investigate the relative merits of two competitive missions: the planetary orbiter and the flyby bus/lander.

A study program concerned with the flyby bus/lander mission was conducted by the Research and Advanced Development Division of the Avco Corporation and is the subject of this report. Two sequential work phases divided the effort: a parametric investigation of all major aspects of the flyby bus/lander mission concept, limited in scope only by the floxed Atlas-Centaur payload capability, and a conceptual design phase which developed a single preferred design configuration, based on mission objectives, which tested the validity of the parametric study. A variety of basically different spacecraft configurations was examined including multiple lander concepts, concepts with a single lander vehicle with several nonimpact-surviving atmospheric probes, and the single large lander concept. The latter was chosen as the most logical way to satisfy all mission objectives and ground rules. Attention was focused on it during the final portion of the Advanced Mariner project.

During the interplanetary trajectory the entire spacecraft consists of a pre-launch-sterilized lander, packaged within a protective canister, and a non-sterilized planetary flyby vehicle. The flyby vehicle acts as a bus for the lander during transit to the planet. Tracking of the early trajectory by the DSIF facilities on Earth provides the guidance information for two midcourse trajectory corrections; these nominally take place 1 and 10 days after spacecraft separation from the Centaur. The final trajectory is biased away from Mars by an amount sufficient to preclude planetary atmospheric contamination by the unsterilized flyby vehicle. (Trajectory dispersions and tracking errors have been analyzed and combined to determine the planet miss distance necessary to provide less than a 1 in 10,000 chance of this occurring.) Prior to Mars encounter, at an Earth-tracking-determined range of 5.0×10^6 to 0.5×10^6 kilometers from the planet, the sterilized lander within its protective canister is separated and propelled away from the flyby bus by a spring device. At a safe distance from the flyby vehicle the lander is spun about its longitudinal axis by solid propellant rockets attached to the sterilization canister. The canister is segmented and shed by centrifugal force. The lander is then thrusted by a solid propellant motor towards the planet. Immediately after lander separation, the flyby bus is reoriented and slowed down by thrust from its main engine. This causes the flyby bus to arrive at Mars periapsis about five hours

after lander entry, thus allowing lander-to-bus communications during the entire projected 5-hour lander mission lifetime. Prior to impact of the lander, atmospheric entry data are collected and stored. During lander parachute descent, these data are played back to the flyby bus via a relay communications link and thence to Earth. All postlanding data are redundantly transmitted to Earth using the relay link and a direct link to the DSIF network. As the flyby bus passes close to the planet, television and infrared mapping data are acquired and stored for subsequent postencounter playback to Earth.

The initial study ground rules proposed by JPL included the use of an Atlas-Centaur launch vehicle with up to 30 percent floxing. The Surveyor ascent shroud configuration was also specified. The choice of lander bus location, together with the shroud constraint, determined the maximum diametral packaging envelope allowable for the lander. Ballistic parameter requirements for suitable atmospheric deceleration were constrained by the characteristics of the Kaplan 11 millibar surface pressure atmosphere. Still another limitation was the atmosphere-dependent projection of surface winds gusting to a maximum velocity of 200 ft/sec. In combination, these factors severely curtailed the payload capability and hence scientific data collection capacity of the lander. The resulting lander-plus-bus spacecraft configuration weight proved to be well within the launch capability of the floxed Atlas-Centaur.

Toward the end of the study, new data obtained by JPL revealed that the development of a floxed Atlas-Centaur capability for 1969 is unlikely; this initiated a review of the overall spacecraft design concept. The injected weight capability for the selected 1971 launch window, 3 May to 3 June, using an unfloxed Atlas-Centaur, is 1550 pounds. For the 1969 launch opportunity, 10 January through 11 February, the corresponding value is 1342 pounds, or 151 pounds less than the flyby bus-lander conceptual design total weight of 1493 pounds. An alternative lunch window for 1969 was developed, 26 January through 25 February, which increases the injected weight capability of the unfloxed Atlas-Centaur to 1470 pounds without serious degradation of the approach trajectory parameters. Further increase of this injected weight capability in the 1969 launch window, however, would seriously reduce the ZAP angle and delay the arrival date beyond the peak of the wave of darkening phenomena at the selected Syrtis Major landing site. If the 10 January through 11 February 1969 launch window were retained, in order to retain its attractive planetary approach parameters, a relaxation of the wind velocity model from the design study value of 200 to 100 ft/sec would allow a reduction in the spacecraft weight from 1493 to 1320 pounds, primarily by reducing the impact attenuation requirement, resulting in a smaller and lighter lander. Alternatively, a relaxation in the atmospheric model from a minimum surface pressure of 11 to 20 millibars reduces the spacecraft weight to 1360 pounds.

Either or both of these basic study ground rule relaxations will reduce the spacecraft weight sufficiently to allow a 1969 launch by the unfloxed Atlas-Centaur. This relaxation of the atmospheric and wind models could conceivably result from telescopic observations of Mars at the next planetary opposition in March 1965, and from data obtained by the Mariner flyby missions in 1964.

2.0 SYSTEMS ANALYSIS

2.1 MISSION OBJECTIVES

The advanced Mariner Study Program provided a 5-month parametric evaluation and conceptual design of the flyby bus/lander mission for the 1969 and 1971 launch opportunities to Mars. To proceed with the study program, mission objectives and constraints were established. These served to direct and restrain the spacecraft design into a size, weight and performance class appropriate for the first unmanned lander mission to another planet. The Jet Propulsion Laboratory specified mission objectives at the initiation of the study program, viz:

1. Demonstrate the capability of successful landing and survival on the planetary surface for several hours

2. Successfully perform a simple biological experiment on the planet's surface for a period of 5 hours

3. Extend the lifetime of the above biological experiment.

Implied in these objectives is successful operation of the flyby bus vehicle through completion of its lander support mission; lander separation, and any subsequent operations necessary for relay communications from the lander through the flyby bus to Earth.

To synthesize reasonable lander scientific payloads for the parametric evaluation and conceptual design studies, the first JPL mission objective was modified to include such diagnostic data as necessary to evaluate spacecraft performance in compliance with the "land and survive" objective.

The third JPL objective was implemented by attempting to augment the simple biological experiment with a second simple biological experiment operating on a different life detection principle while extending the surface lifetime to 24 hours.

A fourth mission objective was added by Avco RAD, viz.:

4. Obtain scientific and engineering design data in support of future lander missions to Mars.

This objective includes the obtainment of data concerning the atmospheric properties, density profile, temperature profile, pressure profile, scale height, wind velocity, and atmospheric composition, as well as surface topographical data, geological data, and engineering design evaluation data. These data should be sufficient to at least partially resolve the many uncertainties concerning the Martian atmospheric and surface properties which presently force an extremely

conservative approach to the design of Martian landers. The design of future landers in the Voyager and manned Martian lander classes is heavily dependent upon good information concerning the entry, descent, impact, and surface operation phases, since these more complex and costly vehicles are necessarily more sensitive to anomalies in the atmospheric and surface properties of the planet.

2.2 MISSION CONSTRAINTS

The parametric evaluation and conceptual design study was significantly regulated in many areas by imposed environmental and operational constraints. These constraints act to limit the range of the parametric analyses and to restrain the conceptual mission and spacecraft designs to be compatible with state-of-the-art technology consistent with the first unmanned planetary entry vehicle.

The atmospheric models used in this study are atmospheres "G" through "K" in a series of atmospheres synthesized at the Jet Propulsion Laboratory. These models vary in surface pressure from 11 to 30 millibars and are typical of the low surface pressure atmospheric models developed by Dr. L. D. Kaplan. The surface wind model employed assumed wind velocities gusting to 200 ft/sec over the near surface atmospheric profile.

An Atlas-Centaur launch vehicle is assumed with Atlas floxing limited to 30 percent, resulting in injected payload capability up to 2358 pounds depending upon the launch window selected. The Surveyor ascent shroud defined the maximum static envelope for the Advanced Mariner spacecraft; however, midway in the study this constraint was relaxed slightly allowing the lower cylindrical section of the shroud to be lengthened.

The lander design was required to survive landing in the high wind environment previously discussed in order to perform a life detection experiment for 5 hours. Only passive impact protection systems were examined with particular emphasis on the use of various crushable materials.

As a safeguard against biological contamination of Mars, the spacecraft and mission design must guarantee a probability of contamination less than 10^{-4}. This requirement implies sterilization of the lander; the dry heat sterilization process chosen at 135°C for 24 hours and the consequent qualification test requirement of three cycles at 145°C for 36 hours place severe constraints on many of the lander subsystems.

The communications, tracking, and command and control subsystems must be compatible with the Deep Space Instrumentation Facility.

2.3 MISSION PROFILE

The sequence of events during a typical Advanced Mariner 1969 mission are shown in figures 1 and 2. After injection into interplanetary transfer orbit for a flyby trajectory by an Atlas Centaur launch vehicle, the solar panels are deployed, and the spacecraft attitude control system maneuvers the spacecraft to acquire the cruise mode attitude references--the Sun, and Canopus. Attitude orientation is maintained during the interplanetary cruise phase of the flight by cold gas reaction jets controlled by the outputs of the Sun sensor and the Canopus tracker. Scientific measurements made during the cruise phase are transmitted to the Deep Space Instrumentation Facility stations on Earth by a 10-watt, S-band transmitter at 33-1/3 bits/sec near Earth through a hemiomni antenna. This bit rate is dropped to 8-1/3 bits/sec approximately 20,000,000 km from Earth and is increased to 133-1/3 bits/sec through the fixed 3-foot by 1-1/2-foot high gain antenna during the post-encounter phase.

The first midcourse correction (to reduce the trajectory dispersion at planetary encounter) is made approximately one day after launch. The proper magnitude and thrust application angle for the first midcourse correction velocity increment are determined by tracking the spacecraft for one day and are then transmitted to the spacecraft. A preprogrammed sequence, initiated by ground command, places the spacecraft on gyro attitude reference to maneuver the spacecraft to the proper attitude for application of the velocity increment. After rocket firing, the vehicle is reoriented to the Sun-Canopus reference frame by the attitude control system in the search and acquisition mode. At this point the cruise mode is resumed and the spacecraft is tracked for a period of about 10 days at which time a second midcourse correction is made, if it is deemed necessary.

Since the star Canopus is not exactly at the southern galactic pole, the cone angle of the Canopus tracker must be continuously updated throughout the interplanetary trajectory to maintain the roll reference. The type II trajectory to Mars in 1969 requires 14 such incremental adjustments of the Canopus tracker cone angle.

At approximately 1,000,000 km from the planet, the lander subsystems are checked out through the bus lander umbilical connector to the bus communications system to Earth. If all lander systems are operating properly, the vehicle is maneuvered into the correct attitude for lander ejection, as determined by the DSIF tracking stations. The lander is spring-ejected, spun up using solid propellant spin rockets, and the rigid sterilization canister is segmented and jettisonned together with the expended spin rocket casings. The lander solid rocket engine is then ignited to impart a velocity increment to the lander, placing it on an impact trajectory. Immediately after termination of rocket burn, the lander is despun by a yo-yo despin system. The lander engine and yo-yo are then jettisonned. Diagnostic and event data recorded during the separation sequence are transmitted from the lander to the flyby bus via a 30-watt relay link at 11.5 bits/sec.

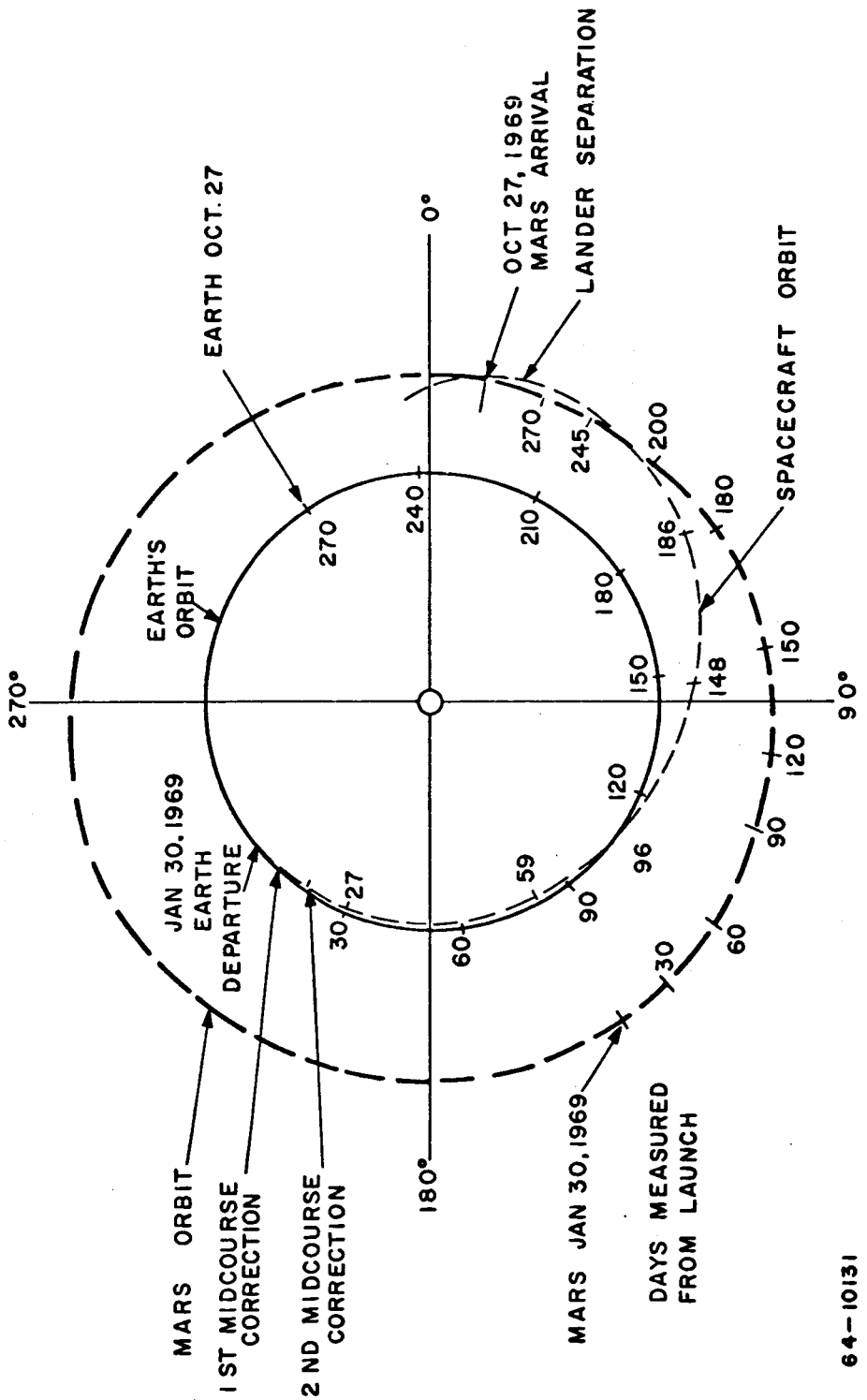

Figure 1 - TYPICAL INTERPLANETARY EARTH TO MARS TRANSFER, TYPE II

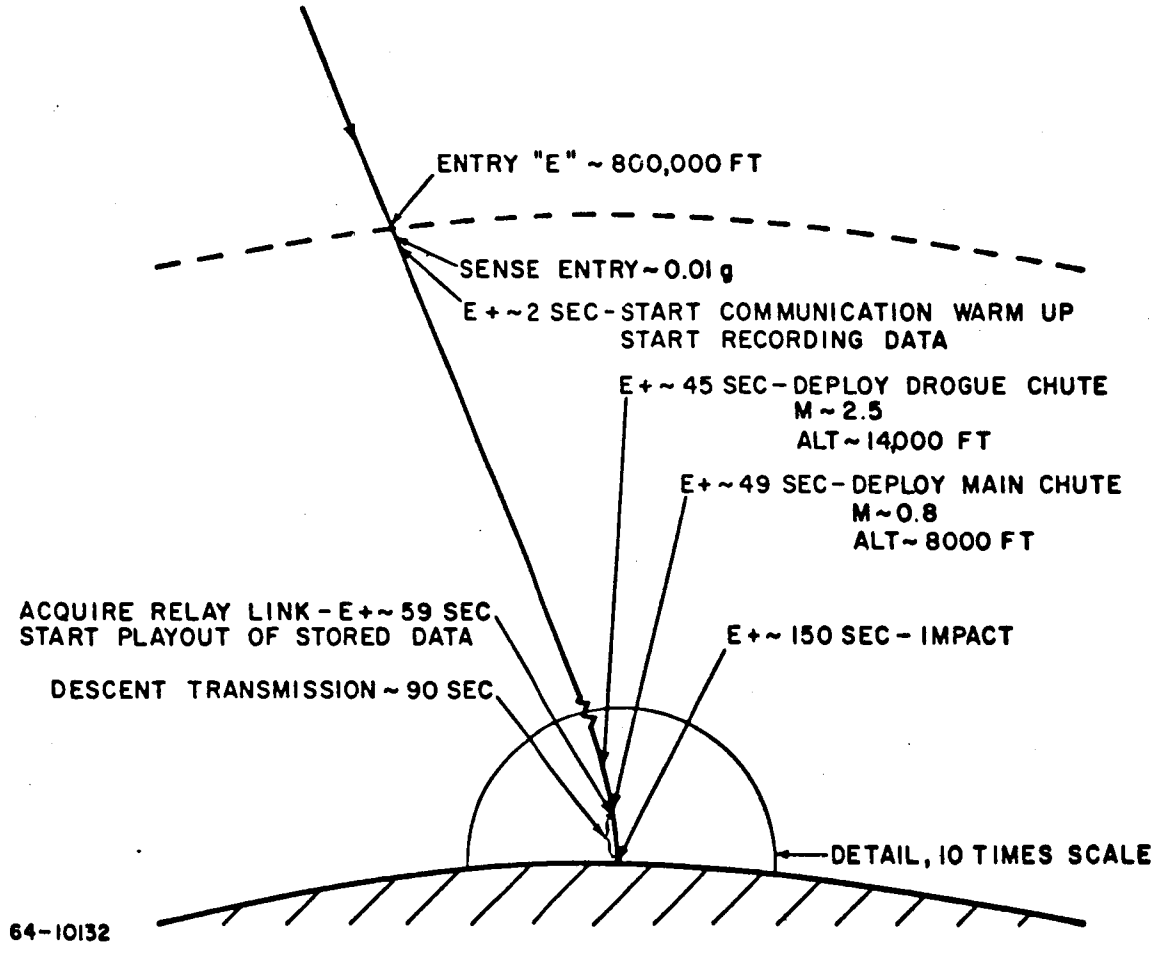

Figure 2 - MARS ENTRY TRAJECTORY

After the lander separation is verified, the flyby bus vehicle is maneuvered into the correct attitude for application of a velocity decrement of approximately 1000 ft/sec., causing the flyby bus to reach the planet about 5-1/2 hours after the lander, such that it remains in radio view for the entire 5-hour lander surface mission.

A second transmission of event data and lander status data is made about 2 hours prior to lander entry via a 30-watt relay communications link to the flyby bus.

During entry blackout, scientific and engineering data are recorded for subsequent playback. At Mach 2.5 the drogue chute is deployed by an inertially activated timer to decelerate the lander to Mach 0.8 where the entry vehicle is jettisoned and the main chute is deployed. During the parachute descent of the payload sphere, for about 90 seconds duration, the stored entry data and data taken during parachute descent are relayed to the flyby bus at 184 bits/sec by a 90-watt, S-band transmitter.

Just prior to impact, the descent communications transmitter and antenna are jettisoned; however, the recorded data are stored for post-impact transmission. The landed payload impacts the planet at velocities up to 210 ft/sec protected by a sphere of aluminum honeycomb crushable material. After impact, the crushable sphere is segmented and jettisoned to allow deployment of the scientific instruments and unencumbered operation of the post-impact communications system. The post-impact communications antenna is erected and locked to the local vertical by a flotation system supporting the entire landed payload sphere.

The post-impact transmission of scientific and engineering data from the lander is accomplished by a single 30-watt S-band communications system transmitting to both the flyby bus and directly to Earth at 11.5 bits/sec. Three such transmissions are made during the 5 hours surface lifetime of the lander--one immediately after impact, one 90 minutes after impact, and one 5 hours after impact--to return data on the surface temperature, pressure, wind velocity, and the life detection experiment. The preimpact stored data are played out once during the first landed transmission.

The spatial-time relationship of the lander and the flyby bus during the 5-hour surface mission of the lander are shown in figure 3 for 1969 and figure 4 for 1971. These figures are Mercator projections of the planetary surface shown in an equatorial coordinate system using the sun line as a longitude reference. The terminator is shown defining the sunlit region of the planet as well as an elliptical area about the Earth line defining the limit of direct link communications to Earth. Planetary surface features pass across the Mercator chart from left to right as the planet rotates, once each Martian day.

The projection of the lander and flyby bus tracks are shown from separation to impact for the lander and from separation through the sunlit region for the flyby

bus. Time markers are shown on each track indicating the relative positions of the two vehicles at separation, lander entry (E), 3 hours after lander entry (E+3), 5 hours after lander entry (E+5), and at flyby periapsis (P). A section of the flyby bus track is shaded where the flyby bus altitude is nominally below 25,000 km, allowing television mapping to occur at a resolution of better than 2 km.

The flyby bus approaches the planet about 5-1/2 hours behind the lander, receiving data from each of the lander transmissions for storage and subsequent transmission to Earth. In the vicinity of planetary periapsis, approximately 100 television pictures are taken and stored for playback to Earth during the next 10-day period. Other planetary scientific data are transmitted in real time to Earth during the encounter phase. After playback of the stored television pictures the flyby bus reverts to the cruise mode and continues its flight through space until one of the spacecraft systems reaches a limiting condition and contact with Earth is lost.

2.4 MISSION PLAN

During the conceptual design phase of the study, the reliability profile for the Advanced Mariner mission was developed. This reliability profile shows the probabilities of successfully accomplishing major events during the mission. Since the development of the reliability profile required the prediction of the system failure contributions, a valuable output from the analysis was the estimate of system mission reliability as well as the reliability of various spacecraft subsystems. An indication of the degree of reliability improvement needed in the program can be obtained by comparing these system reliability predictions with preliminary reliability goals allocated to these same systems as shown in table I. These system goals are associated with a mission success objective of 0.50 and were allocated using the model described in the Voyager Final Report.[1]

In addition to providing success probabilities for the critical events occurring during the mission, the analysis resulted in an estimate of the probability of success for the over-all flyby bus/lander mission. The latter reliability estimate was used to determine the probabilities of obtaining at least one successful mission out of "n" launch attempts. In the Advanced Mariner Program, multilaunches will be employed to enhance program success. From the above analysis, the probability of success for a single flyby bus/lander mission was estimated to be 0.452; i.e., the product of booster reliability (0.75) and spacecraft reliability (0.603). The probabilities of at least one successful mission out of "n" launch attempts are shown graphically in figure 5. There is a better than 90 percent probability that with four launch attempts, there will be at least one successful total flyby bus/lander mission in the Advanced Mariner Program.

*This model, which is based on quantitative factors, is explained on pages 309 and 310 of Volume III—Systems Analysis (part of the Voyager Design Studies, prepared by Avco Corporation under Contract No. NASw 697 (15 October 1963).

TYPICAL LANDER—FLYBY GEOMETRY

$R_s - 10^6$ KM

$V_\infty - 4.0$ KM/SEC

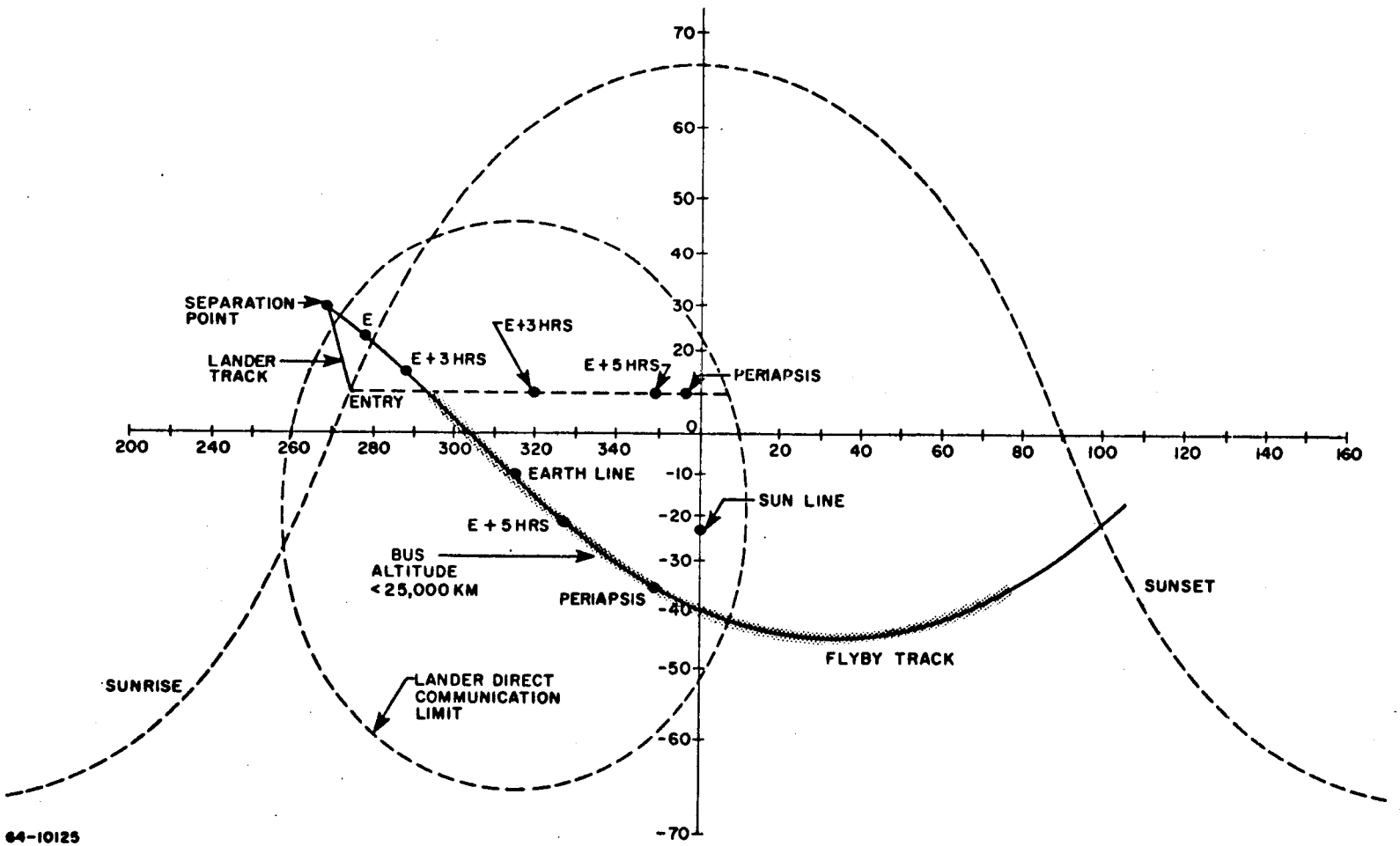

Figure 3 - ENTRY AND FLYBY RELATIONS, 1969 MARS LAUNCH OPPORTUNITY

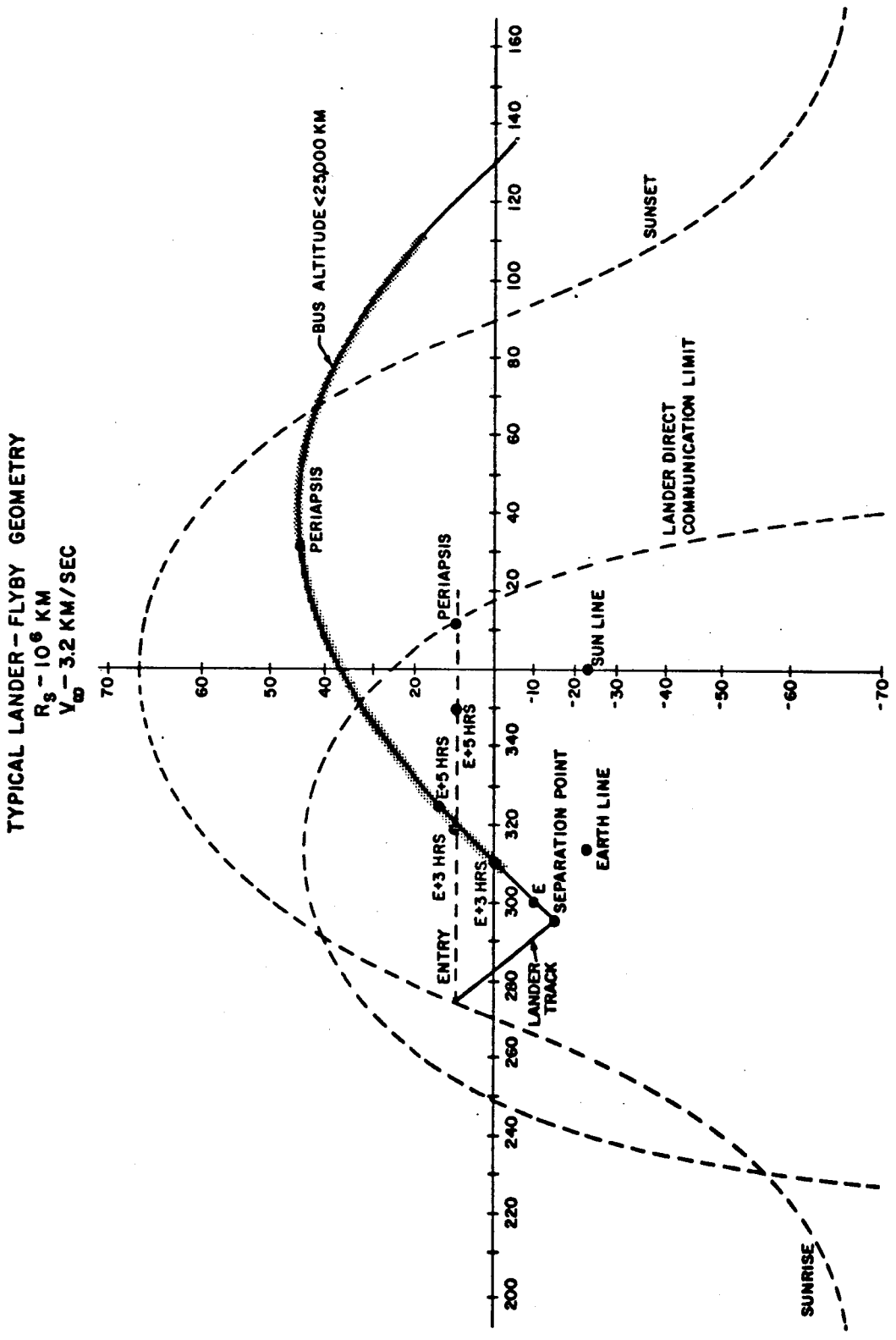

Figure 4 - ENTRY AND FLYBY RELATIONS, 1971 MARS LAUNCH OPPORTUNITY

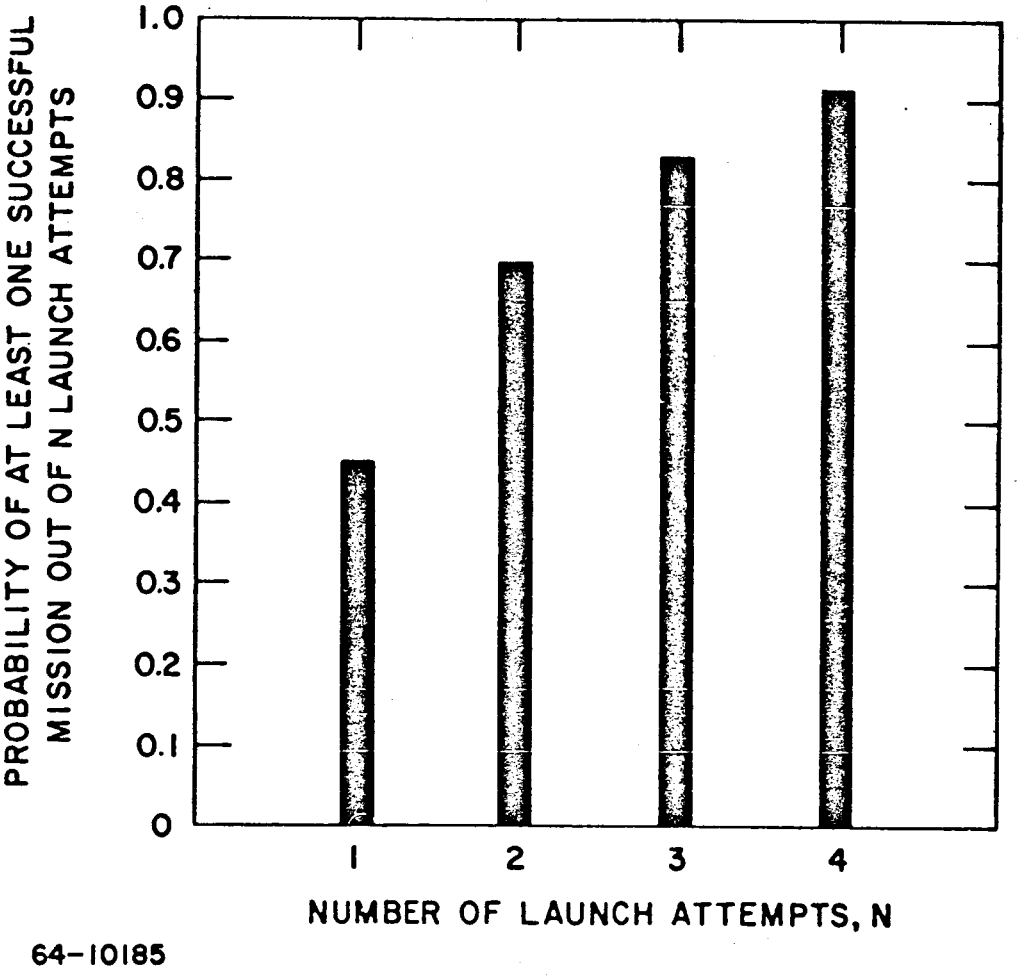

Figure 5 - PROBABILITY OF AT LEAST ONE SUCCESSFUL MISSION

TABLE 1

ADVANCED MARINER SPACECRAFT PREDICTED
AND ALLOCATED SYSTEM RELIABILITY VALUES
(Mission Success Objective: 0.50)

Spacecraft System	Predicted Reliability Estimates	Allocated Reliability Goals
Flyby Bus	0.6804	0.7343
Science*	0.9757	0.9805
Engineering Mechanics	0.9794	0.9834
Power	0.9276	0.9415
Communications	0.9507	0.9603
Guidance	0.9734	0.9786
Attitude Control	0.8688	0.8933
Separation	0.9808	0.9846
Propulsion	0.9934	0.9947
Central Computer and Sequencer	0.9800	0.9839
Lander	0.8864	0.9078
Science	0.9895	0.9915
Engineering Mechanics	0.9389	0.9506
Communications	0.9590	0.9670
Power	0.9988	0.9990
Propulsion	0.9961	0.9969
Over-all Spacecraft	0.603	0.667

*Does not include the reliability of Government-furnished equipment used during the transit cruise phase.

2.5 LAUNCH WINDOW ANALYSIS

For any interplanetary mission the optimum launch window within a given launch opportunity is a function of the vehicle configuration, i.e., flyby bus/lander, orbiter, orbiter/lander, and the scientific mission requirements. In the case of a flyby bus/lander vehicle, with no major retropropulsion requirements in the vicinity of the target planet, the injected payload, exclusive of propulsion, is maximized when the minimum departure velocity is employed. However, the Advanced Mariner mission requirements of a sunrise landing at Syrtis Major near the peak of the wave of darkening phenomena dictated the selection of a launch window other than the minimum departure velocity window centered about 2 April 1969. The desirability of arriving near the peak of the wave of darkening is obvious since this maximizes the likelihood of determining the existence of life, whereas the sunrise landing requirement tends to maximize the direct link lander communication period.

An examination of the pertinent trajectory parameters associated with the 1969 minimum departure velocity window indicated that significant improvements in the arrival date, ZAP angle, approach velocity, communication range, and time of flight could be realized for an earlier launch date with a corresponding injected payload penalty. Based upon this trajectory parameter analysis, a tentative launch window was selected between 10 January and 11 February. Specific advantages associated with this selected launch window over the minimum departure velocity launch window include:

1. Arrival data within one month of the peak of the wave of darkening rather than 2 to 3 months subsequent to the peak of the wave of darkening

2. An approach asymptote near the terminator plane which maximizes the entry angle and minimizes the dispersion associated with a Syrtis Major impact, instead of an approach asymptote within 40 degrees of the sunline

3. A reduction of 25 percent in the approach velocity which reduces the lander entry velocity, reduces the velocity requirement to affect the separation and slowdown maneuvers, and increases the flyby dwell time in vicinity of Mars

4. A reduction of 35 percent in the communication range

5. A reduction of 10 percent in time of flight.

The parameters associated with these specific windows are presented in table II. The payload penalty of 340 pounds associated with the design launch window in January was not considered significant since the spacecraft weight is considerably less than the maximum capability of the floxed Atlas Centaur. However, if the floxed Atlas Centaur boost vehicle is unavailable for this mission, minor shifts in the launch window back into February could recoup at

least 50 percent of the present payload penalty without introducing significant perturbations in the remaining trajectory parameters.

Pertinent systems studies conducted for the selected design launch window indicated that this window satisfies the occultation, relay communication, and entry dispersion requirements. For this launch opportunity the nominal periapsis altitude was based upon a sterilization requirement that the minimum passing distance be in excess of 1500 km.

The 1971 launch opportunity produces the most favorable trajectory characteristics of any opportunity during the 15-year metonic cycle. The minimum departure velocity window affords an excellent starting point in quest of the optimum window for the Mariner mission. An analysis of the trajectory parameters associated with this window indicated that the major difficulty centered about the arrival date, 1 to 3 months subsequent to the peak of the wave of darkening. The characteristics of the optimum arrival date window indicated that since the approach asymptote was along the Earth-Mars line, difficulty would be encountered in the areas of Earth occultation, relay communications, and entry dispersion. These problem areas are greatly alleviated in selecting an arrival date 4 weeks subsequent to the peak of the wave of darkening in that the approach asymptote shifts approximately 25 degrees from the Mars-Earth line towards the sunrise terminator plane.

A comparison of the trajectory parameters associated with both the minimum departure velocity window and the selected design window is presented in table III. It is interesting to note that the launch dates associated with these two windows are essentially the same and that increased departure velocity requirements are employed to produce the faster transfer trips required to shift the arrival date window. The payload penalty associated with the 1971 design window is approximately 70 pounds. The periapsis altitude for the minimum departure velocity launch window is based upon a sterilization requirement of 1500 km, whereas the minimum passing altitude associated with the design window satisfies an Earth occultation constraint of 4000 km.

TABLE 2

COMPARISON OF TRAJECTORY PARAMETERS
1969 LAUNCH OPPORTUNITY

Parameter	Minimum Departure Velocity Window	Design Window
Departure Date	17 Mar - 16 Apr	10 Jan - 11 Feb
Arrival Date	5 Jan - 10 Feb (1970)	15 Oct - 2 Nov
Time of Flight (days)	294-300	264-278
Departure Velocity (km/sec)	2.82-2.87	3.35-3.72
Approach Velocity (km/sec)	4.94-5.31	3.74-4.20
Atlas Centaur Injected Payload (lb)		
0 percent flox	1,680	1,342
20 percent flox	2,125	1,756
30 percent flox	2,358	1,965
Flyby/Lander Separation Range (10^6 km)	----	1-5
Communication Range (10^6 km)	240-279	160-176
ZAP Angle (deg)	33-42	72-83
Vehicle Longitude wrt Sunline (deg)	214-226	264-275
Minimum Inclination (deg)	14-24	28-40
Flyby Design Inclination (deg)	----	45 nominal
Lander Entry Angle (Syrtis Major)	-34. → -43.	-66. → -74.
Lander Entry Velocity (ft/sec)	23,130-24,000	20,560-21,500
Periapsis Altitude (km)		
One midcourse correction	42,800 ± 30,975	32,340 ± 23,133
Two midcourse corrections	7,144 ± 4,233	6,328 ± 3,621

TABLE 3

COMPARISON OF TRAJECTORY PARAMETERS
1971 LAUNCH OPPORTUNITY

Parameter	Minimum Departure Velocity Window	Design Window
Departure Date	8 May - 9 Jun	2 May - 3 Jun
Arrival Date	18 Nov - 15 Jan	12 Nov
Time of Flight (days)	194-220	162-194
Departure Velocity (km/sec)	2.82-3.03	2.92-3.20
Approach Velocity (km/sec)	2.82-3.06	3.17-3.32
Atlas Centaur Injected Payload (lb)		
0 percent flox	1,620	1,550
20 percent flox	2,060	1,985
30 percent flox	2,290	2,215
Flyby/Lander Separation Range (10^6 km)	----	1-5
Communication Range (10^6 km)	125-197	119
ZAP Angle (deg)	66-109	113-120
Vehicle Longitude wrt Sunline (deg)	245-284	287-297
Minimum Inclination (deg)	0-18	13-21
Flyby Design Inclination (deg)	----	45 nominal
Lander Entry Angle (Syrtis Major)	-66 → -73	-61
Lander Entry Velocity (ft/sec)	18,910-19,310	19,500-19,770
Periapsis Altitude (km)		
One midcourse correction	21,124 ± 14,718	7,348 ● 3,348
Two midcourse corrections	3,880 ● 1,788	5,521 ● 1,521

3.0 SYSTEM DESIGN -- LANDER

The primary objective of the lander study was to conduct a sufficiently detailed parametric evaluation of the lander and its various subsystems to allow a conceptual design to be easily synthesized for any selected lander mission objective. Each major subsystem of the lander was examined individually and in combination with its interfacing subsystems to determine the significant parameters for overall systems optimization analyses.

The conceptual design analysis represents a detailed study of one possible lander system to evaluate the accuracy of the parametric data and to investigate in more depth some of the design problems which cannot easily be treated parametrically. While the design resulting from this study is representative of the capability of Mars landers in the Advanced Mariner weight class, considerable flexibility remains. The data output of the relay link could be increased by several orders of magnitude, or the mission lifetime on the planet's surface could be extended without seriously affecting the overall spacecraft configuration. In addition, the scientific instrument selection can be modified, within limits, to reflect different overall mission objectives.

The design presented is most seriously constrained by the large variation within the specified atmospheric models, and the postulated wind velocity model. The Kaplan atmospheric model "G", which has the minimum scale height, designs the structure, atmosphere "K", which has the maximum scale height, designs the heat shield, and atmosphere "H", which has the minimum surface pressure together with high temperatures, is the most critical for drogue chute deployment. The high wind model forces the use of a heavy impact attenuator of aluminum honeycomb crushable material with its attendant penalty in landed payload weight.

3.1 DESIGN

Figure 6 shows the final conceptual design of the Advanced Mariner lander; more detailed drawings can be found in volume III -- Lander.

The lander is a 90-inch-diameter, modified Apollo shape; the afterbody cone angle has been reduced to 30 degrees. The design entry weight is 516 pounds resulting in a ballistic coefficient of 0.25 slug/ft^2. The lander external configuration is composed of a forebody heat shield system consisting of an ablative heat shield (Avco 5026) with an aluminum honeycomb substructure, and a thin-shelled beryllium, hot structure afterbody with rings and longeron stiffeners.

The selection of a 90-inch lander diameter resulted from comparing the available internal weight as a function of lander diameter shown in figure 7 with the

required equivalent internal weight resulting from the payload conceptual design studies. Equivalent internal weight is the sum of the internal weight, and the descent payload and associated structure modified by an appropriate factor to account for the absence of impact attenuator on the descent payload.

Embedded in the forebody substructure is a support ring for the landed sphere, associated structural hardware, and the descent communications and science equipment. Also, mounted on the forebody are the pre-entry communications system, multichannel radiometer, and three pressure transducers. The lander descent parachute systems are mounted to the afterbody at diametrically opposite locations. The drogue chute attachment is located at the apex of the afterbody with the riser lines embedded in the afterbody within a thermally insulated longeron. The main chute canister is mounted to the afterbody, but the chute itself rests on the forebody for ease in chute deployment.

The internal configuration is primarily composed of the landed sphere and the support ring. The landed sphere support ring is a short, truncated cone which also provides the separation system between the lander forebody and the descent payload. The separation system consists of simple tension cables incorporating three cable cutters, any one of which can cause separation. The main chute is attached to the landed sphere by a six-lead bridle harness, separated from the sphere by a similar cable separation system. The descent communication horn antenna is also attached to this harness. The landed sphere is approximately 21.5 inches in outer radius, 13 inches of which constitute an aluminum honeycomb impact attenuator. The impact attenuator is constructed in 14 segments which are secured to an outer spherical shell which is, in turn, fastened to a flotation shell. The outer spherical shell separates with the impact attenuator after impact; however, the 14 segments are retained near the flotation shell after separation by elastic lanyard lines and tend to anchor the shell as shown in figure 8. Inside the fiberglass flotation shell is an inner sphere suspended in a flotation fluid. The inner sphere houses the landed scientific, communications, and power equipment. Both the flotation sphere and the inner sphere are dielectric since they contain the communications antenna.

After the lander has successfully completed atmospheric entry, drogue chute actuation is accomplished at Mach 2.5 by an inertially actuated timer. The drogue is mortared out of the side of the afterbody and suspends the entire lander by attachments on the apex of the afterbody. At Mach 0.8, the timer initiates the main chute deployment sequence: the afterbody is separated by a linear shaped charge located at the forebody-afterbody ring and is pulled away by the drogue chute. At the same time, the forebody is jettisoned by release at the support ring. As the afterbody is pulled away, it deploys the main chute which suspends the landed sphere and support ring. After 90 seconds of descent, communication is completed, the support ring, along with the descent payload, is jettisoned.

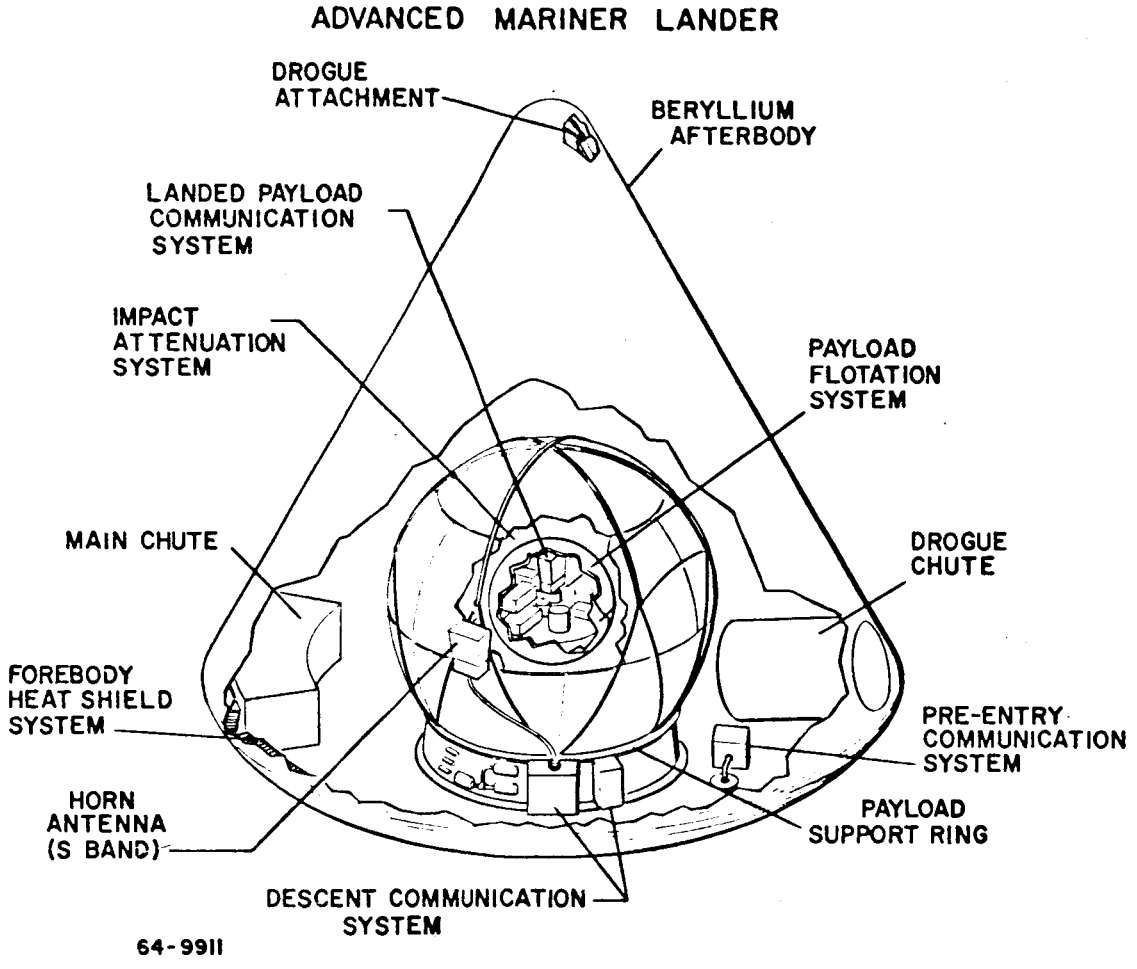

Figure 6 - ADVANCED MARINER LANDER

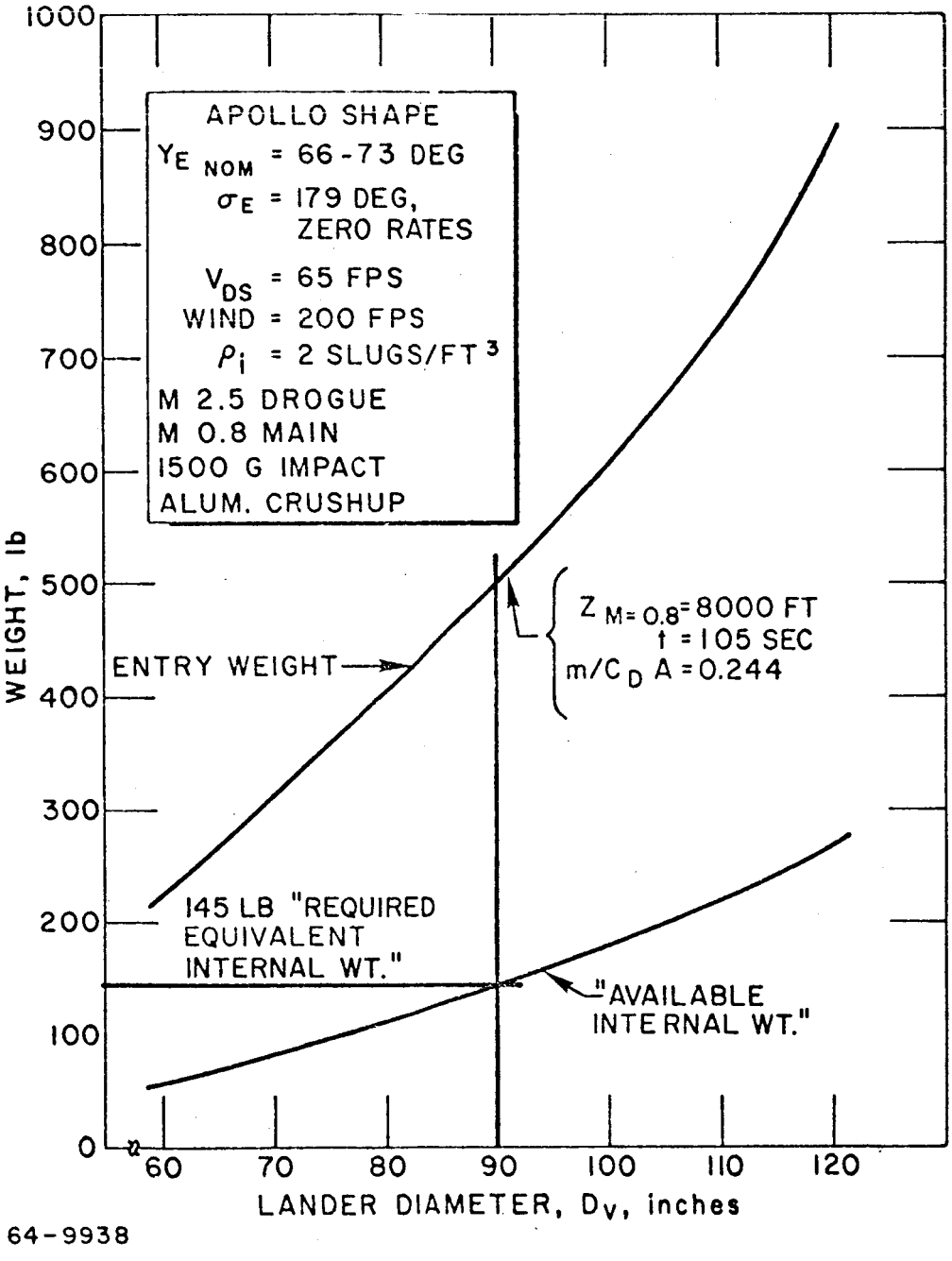

Figure 7 - AVAILABLE INTERNAL WEIGHT VERSUS LANDER DIAMETER

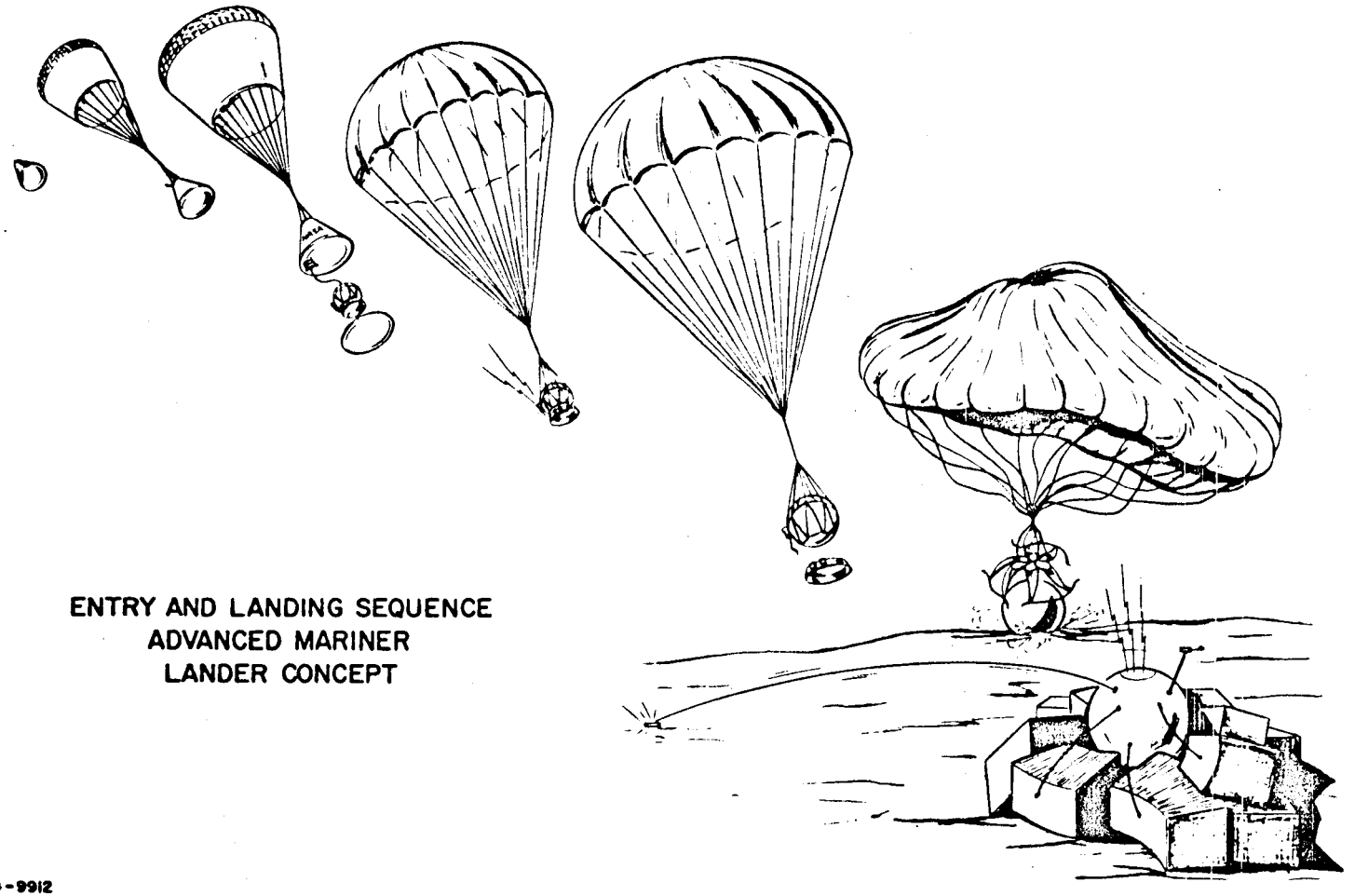

Figure 8 - ENTRY AND LANDING SEQUENCE, ADVANCED MARINER LANDER CONCEPT

At impact, the main chute attachment harness is jettisoned by an impact switch. After the sphere has rolled to a stop, the impact attenuator is segmented by a linear shaped charge into 14 sections. These segments are attached to the internal sphere by elastic lanyard lines to anchor the sphere. The weighted inner sphere has previously been uncaged and is free to rotate to an upright position erecting the antenna. Once this position has been secured, the scientific equipment is deployed, recaging the inner sphere for future operations.

The lander functional diagram is shown in figure 9 and the lander weight summary is shown in table 4.

3.2 HEAT SHIELD SYSTEM

The heat shield system consists of an ablative heat shield and a load-bearing substructure which supports the heat shield. In the design of the heat shield system, the entry conditions, lander shape and diameter, and heat shield and substructure materials were evaluated to assess the impact of the heat shield upon the overall lander design. Several heat shield systems were investigated ranging from a high-temperature charring ablator with an aluminum honeycomb substructure to very low temperature ablators (sublimers) with a fiberglass substructure. Material selection was based on the capability of the system to meet the design requirements of sterilizability, minimum weight, communication RF transparency, and state-of-the-art technology. These results are shown in figure 10. It is evident that the RF transparency requirement is too severe a weight penalty since the heat shield/structure weight fraction is much too large for the LT_{α}/fiberglass and Teflon/fiberglass systems. High-temperature charring ablators such as Avco 5026 are far more efficient for the forebody design, and beryllium, with no ablator, considerably improves the afterbody design. This combination was used in the conceptual design study.

The Avco 5026 material is a random mixture of silica fibers, epoxy resin, and phenolic microballoons pressed into a fiberglass honeycomb core, giving a continuous, one-piece heat shield surface.

The forebody substructure is an aerodynamic load bearing shell of aluminum honeycomb sandwich construction; the beryllium afterbody is of a thin shell hot structure heat sink design with ring and longeron stiffeners. Analysis of the structural shells considered general and local instability under aerodynamic pressure loads as the modes of failure. A very detailed axisymmetric, orthotropic shell analysis was conducted,which revealed that the bending stress levels were well below the material allowables.

The entry conditions strongly affect the heat shield system design in the prediction of the heat and pressure loading distributions over the vehicle. It is apparent that a minimum weight design would result from a -90 degree entry angle and zero angle of attack with no spin or pitch rates. However, the design entry conditions resulting from mission studies are:

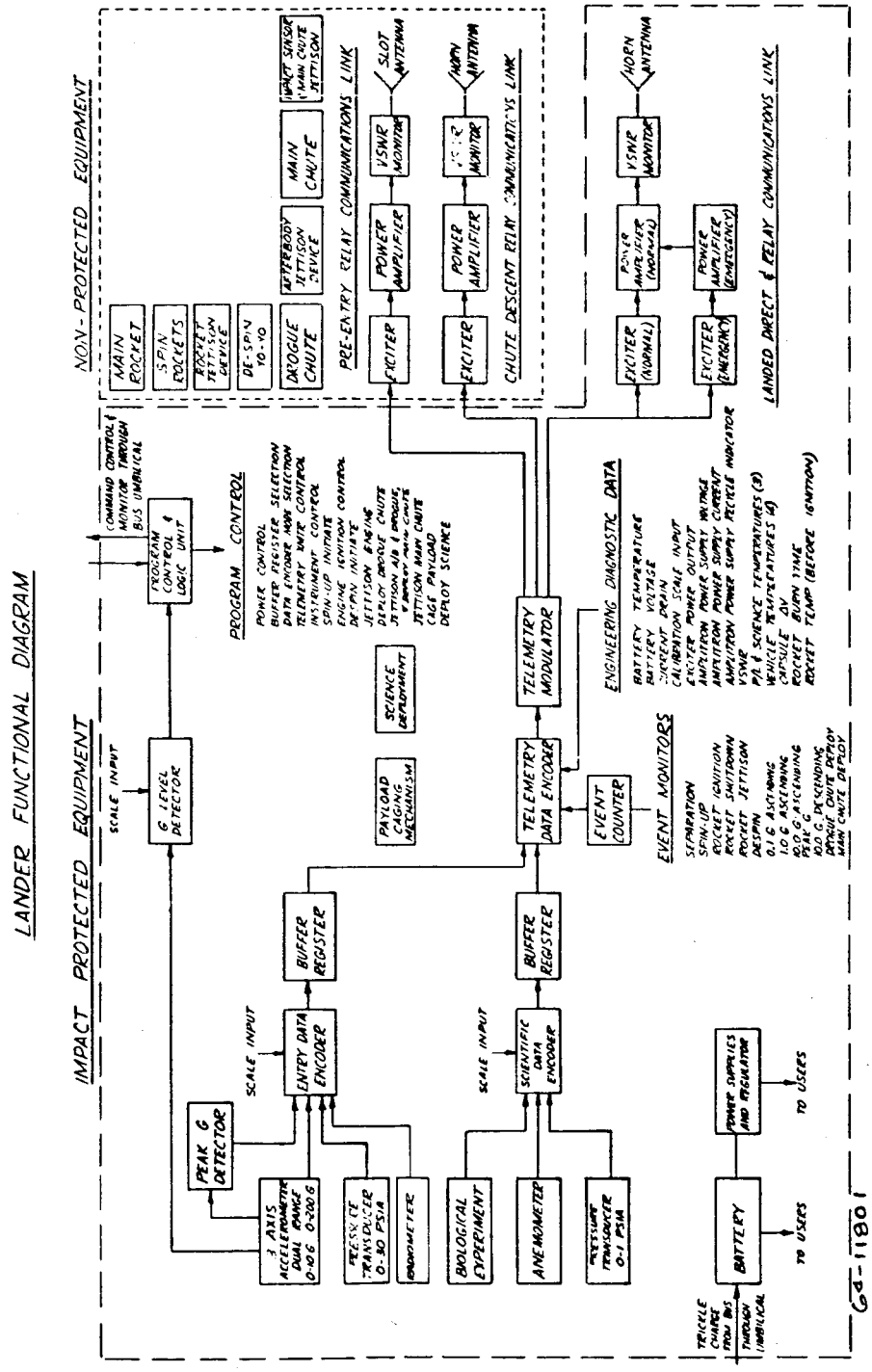

Figure 9 - LANDER FUNCTIONAL DIAGRAM

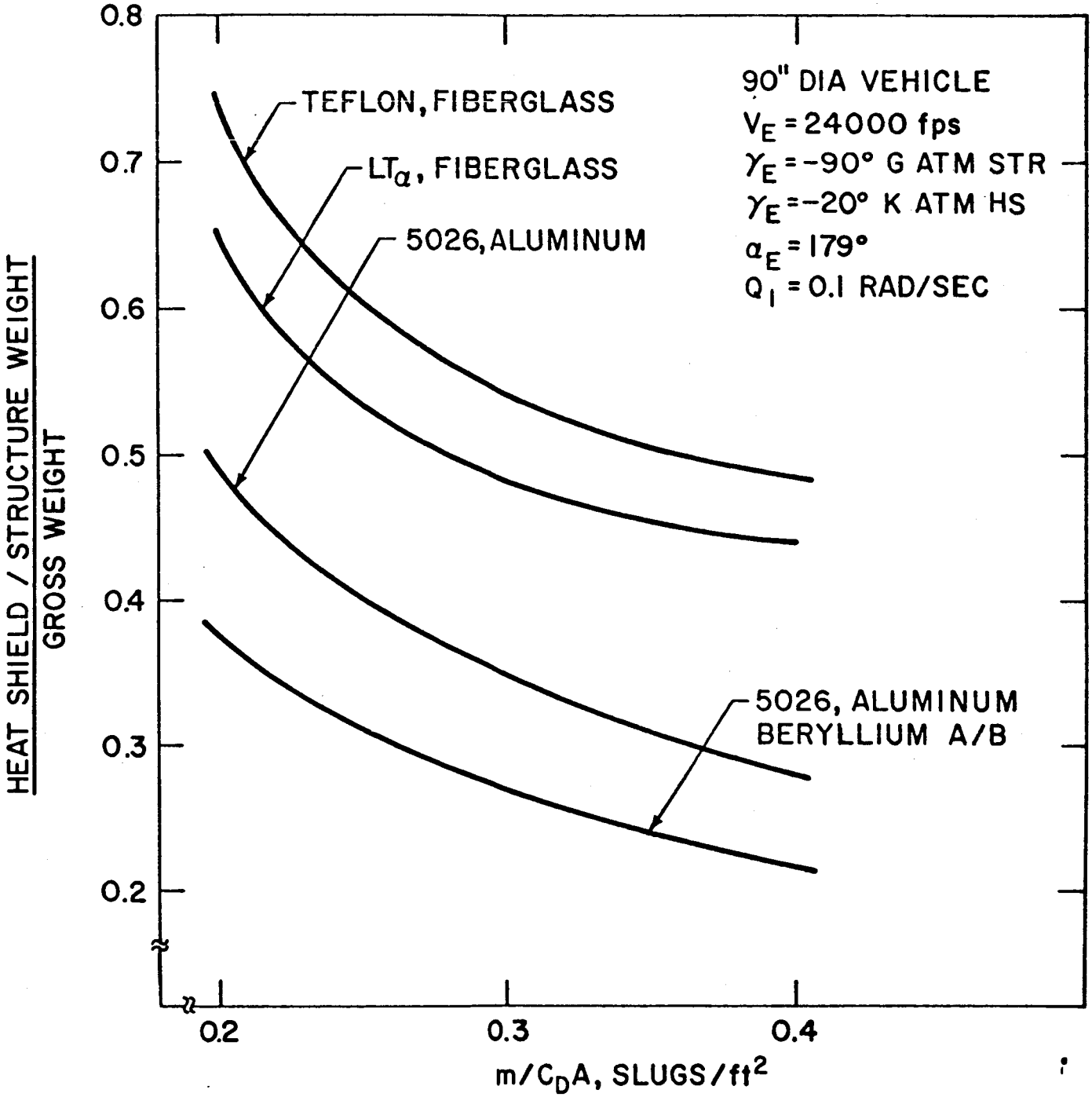

64-9967

Figure 10 - HEAT SHIELD/STRUCTURE MATERIALS STUDY

TABLE 4

LANDER WEIGHT SUMMARY
(pounds)

Internal Weight			126.3 lb.
1. Landed Payload		86.3	
a. Communication	52.5		
b. Power	25.3		
c. Science	8.5		
2. Structure and Deployment		27.9	
3. Thermal Control		2.1	
4. Umbilicals, Wiring, and Pyrotechnics		10.0	
Landed Weight			258.0 lb.
1. Attenuator		126.7	
a. Support Structure	16.7		
b. Aluminum H/C	110.0		
2. Umbilicals, Wiring, and Pyrotechnics		5.0	
Suspended Weight			312.3 lb.
1. Descent Payload		41.1	
a. Communication	37.8		
b. Science	3.3		
2. Structure		9.2	
3. Umbilicals, Wiring, and Pyrotechnics		4.0	
Entry Weight			516.5 lb.
1. Heat Shield		70.4	
2. Structure		66.7	
3. Drogue Chute		30.1	
4. Main Chute		26.7	
5. Thermal Control		10.3	

V_E	=	21,500 ft/sec
γ_E	=	-52 to -88 degrees
α_E	=	179 degrees
Spin Rate	=	0 deg/sec
Pitch Rate	=	0 deg/sec

The heat shield is designed by the -52 deg entry angle and the substructure is designed by the -88 deg entry angle. The worst combination of atmospheric models was considered. A rigorous analysis of both the heat shield and structure designs showed a 20 percent safety factor in the final weights, which is well within preliminary design criteria.

3.3 AERODYNAMICS

The aerodynamic analyses conducted for the Advanced Mariner program considered only the Apollo shape with a variety of minor modifications examined to improve the aerodynamic performance. With the Apollo shape, the most serious problem is aerodynamic damping, particularly during the period of decreasing dynamic pressure, which allows the angle of attack envelope to diverge just prior to parachute deployment. Examination of available experimental aerodynamic coefficient data yielded reliable consistent values for all static coefficients; however, damping coefficient (C_{m_q}) data are rather limited and extremely inconsistent. Based on data from several sources, conservative estimates of this coefficient were tabulated over the entire range of Mach numbers and angles of attack. To evaluate the sensitivity of the lander aerodynamic performance to damping, C_{m_q} was varied from zero to Newtonian values; the resultant angle-of-attack profiles are shown in figure 11. It was found that the lack of damping is critical but that the sensitivity to the damping coefficient can be minimized through the use of spin stabilization.

The large variation in drag coefficient with angle of attack for the Apollo shape causes the altitude for drogue chute deployment ($M \leq 2.5$) to be much lower for dynamic than for particle trajectories. This emphasized the need for better damping and created a new parameter -- effective m/C_DA -- to describe the vehicle performance. Effective m/C_DA is the parameter which compares the dynamic performance of the vehicle with the performance possible at constant zero angle of attack. It is thus always higher than the static hypersonic m/C_DA normally used to describe the vehicle performance and is defined in this study as the m/C_DA required in a particle trajectory to achieve a given minimum altitude at Mach 2.5. An effective m/C_DA of 0.285, based on a drogue chute deployment altitude of 14,000 feet, was selected for the conceptual design.

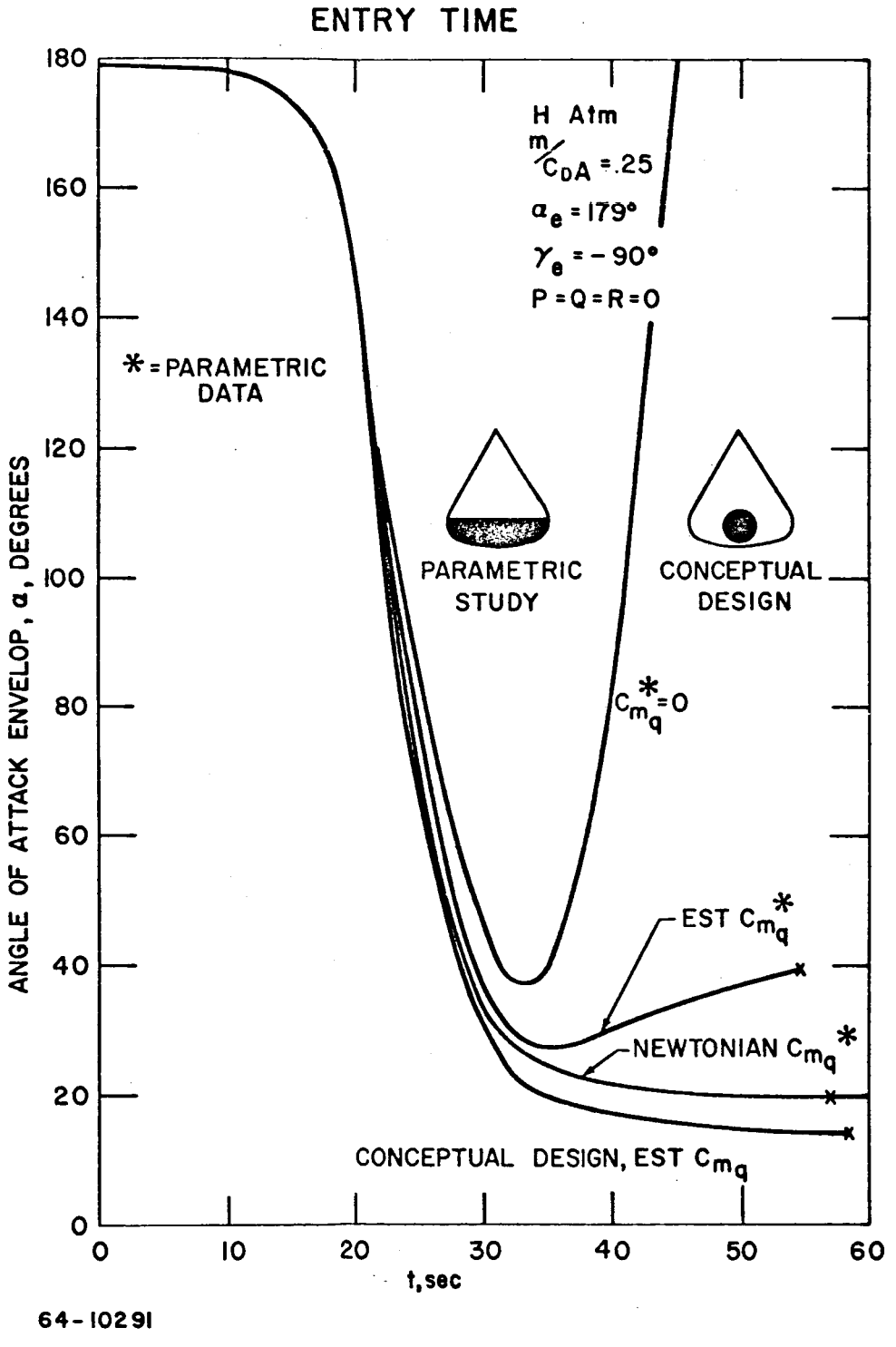

Figure 11 - ANGLE OF ATTACK VERSUS ENTRY TIME

As the internal design of the Advanced Mariner lander progressed, the center of gravity moved from 0.17D to 0.21D necessitating a change in the afterbody design to prevent rearward stability during entry. The moments of inertia also decreased, and the difference between axial and transverse moments of inertia became too small for effective spin stabilization. A beneficial effect of the reduced moments of inertia is increased damping, with resultant improvement in the effective m/C_DA. The improvement in performance of the final conceptual design is compared to that of the parametric studies in figure 11.

Heating studies indicated that the most critical entry conditions for design of the heat shield occur at a flight path angle of -52 degrees in the "K" atmosphere, which results in a total stagnation point heating of 1804 Btu/ft^2.

The maximum convective heating rate of 101 Btu/ft^2-sec is reached in the "G" atmosphere, and a maximum radiative heating rate of 288 Btu/ft^2-sec is obtained in the "J" atmosphere, both occurring at the steepest entry flight path angle of -88 degrees.

3.4 DESCENT SYSTEM

The design of the descent system is dictated by the requirement to reduce the impact velocity of the landed payload to tolerable levels and to provide adequate time during parachute descent to allow communications of the stored entry data prior to impact. A two-chute system was selected rather than a single-chute system to satisfy the descent time requirements, to provide a method of jettisoning the vehicle afterbody, and finally to avoid the necessity of a 35- to 40-foot diameter drogue chute, which is beyond the present state of the art.

A hyperflo drogue chute and a ring-sail main chute were selected because of their good stability and drag area characteristics at the desired deployment Mach numbers. Both the drogue chute and the main chute canopies are of nylon fabric, which is the lightest material able to sustain the aerodynamic heating and loads encountered. The choice of a drogue chute deployment Mach number must consider the lander entry angle, the atmospheric model, the chute actuation system, and the fabric thermal limits. A nominal deployment at Mach 2.5 was selected with an actuation system design which allowed deployment to occur between Mach 2.0 and Mach 3.07 for all combinations of entry angle and atmospheric model. At the upper deployment Mach number of 3.07, the aerodynamic heating and loading on the nylon fabric is just below material limits.

A nominal deployment Mach number of 0.8 was chosen for the main chute in order to ensure subsonic deployment for all combinations of entry angle and atmospheric model. The selected actuation technique assures deployment between Mach 0.61 and Mach 0.88 and maintains the nylon canopy fabric within temperature and loading limitations.

The two-chute system allows optimization of the ballistic coefficient and/or suspended weight. The drogue chute system weight is the parameter which forces optimization. For drogue chute deployment at Mach 2.5, trajectory data predict the ratio of drogue chute area to vehicle area necessary to decelerate the vehicle to Mach 0.8 at the desired main chute deployment altitude. The second quadrant of figure 12 presents the above mentioned trajectory data for a range of m/C_DA, such that the drogue chute weight can readily be determined for a particular set of conditions. For a given main chute deployment altitude, the drogue chute size increases with increasing m/C_DA such that at some point the drogue chute weight becomes so large that it causes a decrease in suspended weight. This result is shown in the fourth quadrant of figure 12.

The main chute is sized on the basis of impact velocity and/or descent time. The first quadrant of figure 12 presents a curve of impact velocity versus main chute area over suspended weight. From this curve one can assess the necessary area and/or weight of a main chute to land a given weight at a particular impact velocity; this result is independent of m/C_DA and deployment altitude. The weight components of an entry vehicle are as follows:

$$W_E = W_{H/S} + W_D + W_S + W_{MC}$$

where:

W_E	=	gross entry weight
$W_{H/S}$	=	heat shield and structure weight
W_D	=	drogue chute weight
W_S	=	suspended weight (payload plus impact attenuator)
W_{MC}	=	main chute weight.

Rearranging the above expression and solving for the suspended weight,

$$W_S = \frac{W_E - W_{H/S} - W_D}{1 + \frac{A_{MC}}{W_S}(0.013)}$$

where

$$W_{MC} = 0.013\, A_{MC}.$$

For a given m/C_DA and vehicle diameter the above expression can be solved for the suspended weight (W_S) such that optimum curves, as those presented in quadrant four of figure 12 can be evolved.

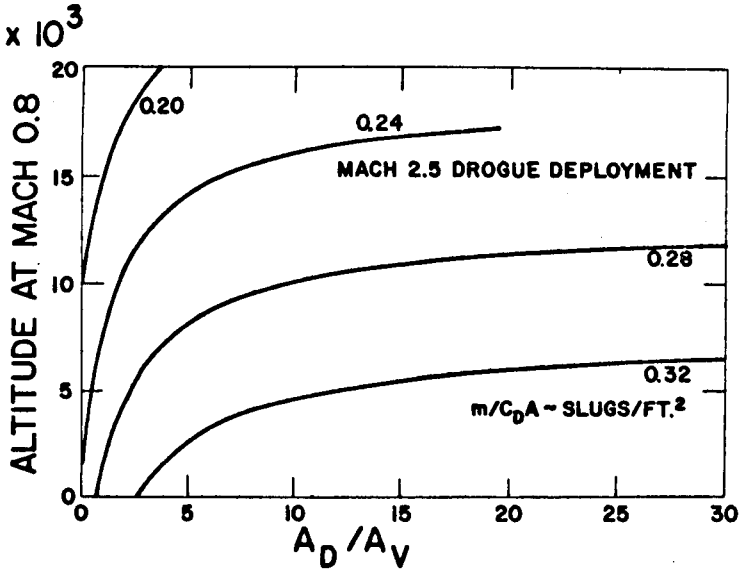

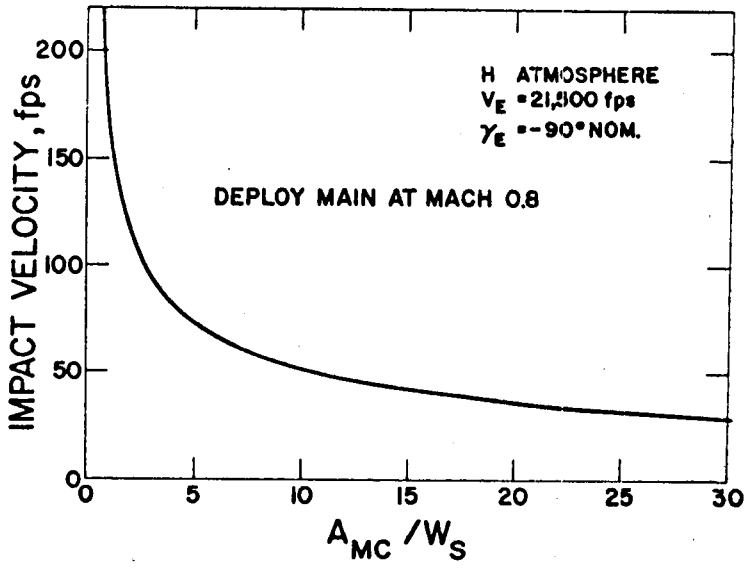

$$\text{SUSPENDED WEIGHT} \sim W_S$$

$$W_S = \frac{W_E - W_{H/S} - W_D}{1 + \frac{A_{MC}}{W_S}(0.013)}$$

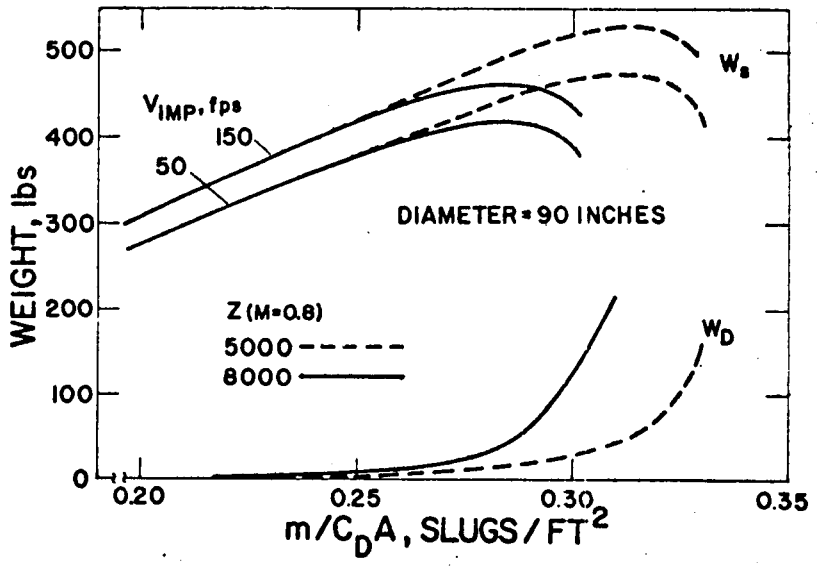

64-9970

Figure 12 - TWO-CHUTE PARAMETRIC STUDY

3.5 IMPACT ATTENUATION SYSTEM

The impact attenuation system selected for the Advanced Mariner conceptual design consists of aluminum honeycomb in the form of a thick spherical covering which surrounds the internal payload to provide omnidirectional impact protection. In detail it is an expanded honeycomb of 5052 aluminum, with 1/8-inch cell size, and 0.001-inch foil gage. It is designed to absorb the kinetic energy of the landed weight at an impact velocity of 210 ft/sec in any orientation and to accomplish this energy absorption while limiting the peak decelerations to the order of 1500 g.

Figure 13 indicates the important parameters in the impact attenuator analysis, such as peak deceleration level and material efficiency (i.e., ratio of payload weight to total landed weight). A spherical rather than lenticular geometry is used, since the sphere yields much lower decelerations. Increasing the packaging density in the internal payload results in a higher payload ratio; in the present conceptual design a density of 3.2 slug/ft^3 is attained.

Three groups of energy absorption materials were studied parametrically (as shown in figure 13). The plastic foams group was found to be too inefficient in that some plastic foams can barely absorb their own kinetic energy at the impact velocities of interest. On the other hand, balsa wood is too efficient; it can absorb the impact energy with a relatively small amount of material, but does so at relatively high deceleration levels. Of the energy absorption materials presently available, aluminum honeycomb appears to effect an adequate compromise between material efficiency and deceleration level.

The 210-ft/sec impact velocity results from a tradeoff study utilizing a two-parachute system; the optimum payload is obtained when the terminal vertical velocity is 65 ft/sec, which with the postulated 200-ft/sec-surface winds on Mars, yields a total impact velocity of 210 ft/sec. At higher descent velocities the increase in impact system weight required is greater than the weight saved in the parachute system. At lower vertical velocities the opposite situation occurs.

In other studies performed on the conceptual design, it was determined that internal components of the payload whose natural frequencies are of the order of 100 cps are liable to experience higher g's than 1500, because of the nature of the shock loading during impact.

It was also determined that this design should not deeply penetrate soft sand on the Martian surface, assuming its characteristics are similar to those displayed by Earth-type sands.

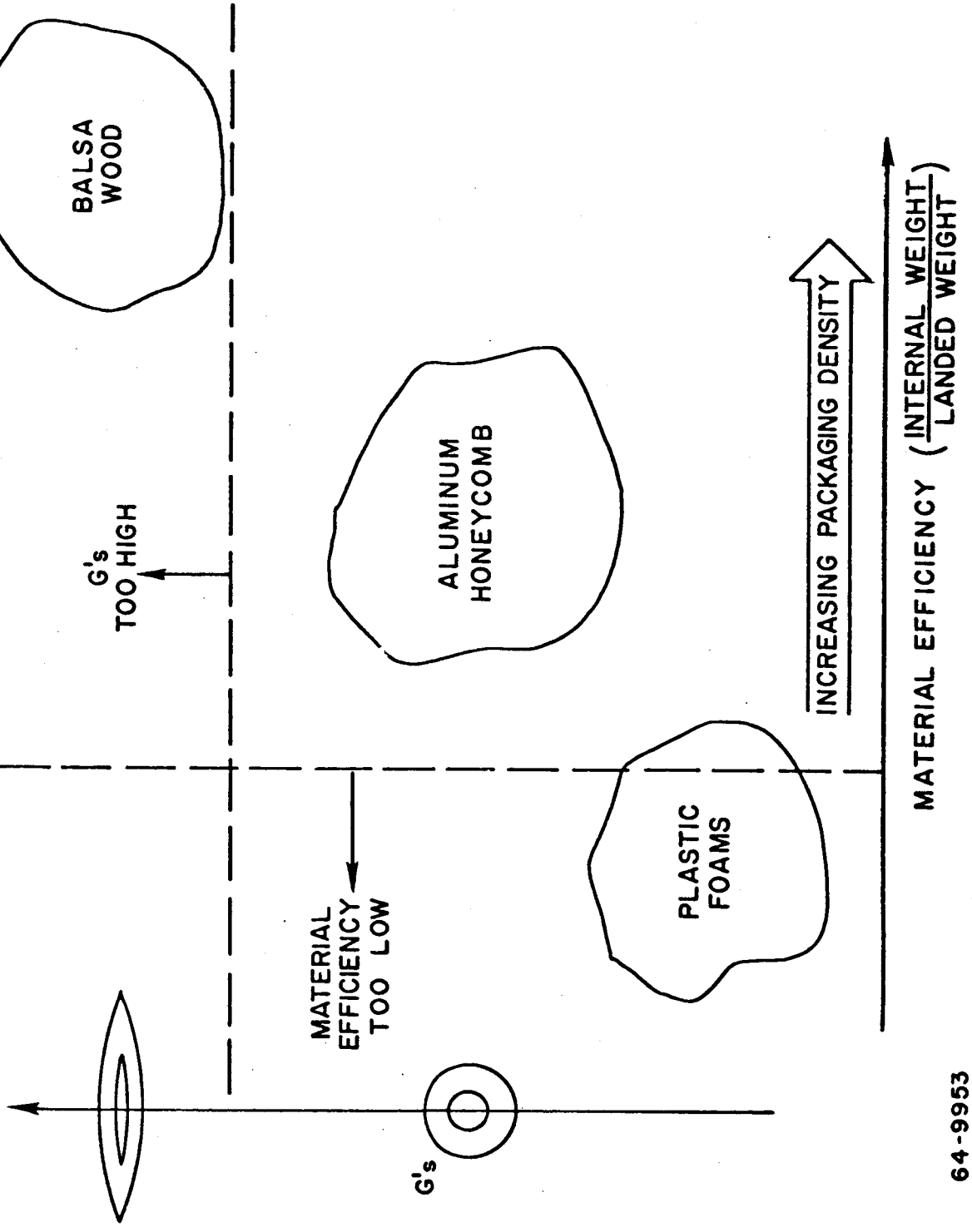

Figure 13 - IMPACT SYSTEM BASIC TRADEOFF DECISIONS

3.6 THERMAL CONTROL

The lander is exposed to five different flight phases which are significant from the viewpoint of the Thermal Control System; (1) near Earth, (2) cruise (3) post-separation, (4) Mars entry and descent, and (5) post-landing.

Near Earth the lander may be exposed to direct heating from the sun during injection, acquisition, and midcourse maneuvers. The response of the surface is rapid to these fluctuating conditions and a low value of α_S / ϵ (less than 1) is desirable if the solar exposure time is prolonged. Systems studies indicate that the lander will not be exposed to the sun for more than one hour. The design concept for the lander provides a large time constant for the internal payload package (on the order of a day) so that large excursions in the canister temperature have negligible influence on the internal payload.

In the cruise phase, the lander is in the shadow of the bus and receives heat by radiation and conduction from the bus. In addition, power is supplied by the bus solar panels to the lander to maintain the internal payload package within the temperature limits of 40 and 100 °F. Twenty watts of power were found to be adequate with an afterbody emissivity of 0.05. The lower limit on lander surface temperatures during cruise is expected to be -60 °F, quite compatible with the spin rocket and separation squib requirements so that additional external heaters would not be required. Additional heaters may be required for the lander main propulsion engine if a sterilizable engine cannot be developed to withstand this cold soak limit. The cold soak limit of -60 °F is felt to be acceptable for the heat shield.

Upon separation, the sterilization canister is discarded and the lander has the requisite thermal control coatings for the near Mars phase of flight. Utilizing higher ratios of α_S / ϵ on the afterbody than on the forebody can negate much of the adverse effect of variable attitude. Here again, it was found desirable to isolate the internal payload. The α_S / ϵ ratios necessary near Mars run from 2.5 to 3.0. Techniques for coating the beryllium afterbody and the heat shield are important development areas. The beryllium afterbody is favorable from the thermal control viewpoint in providing good conduction, thereby minimizing the temperature gradients about the vehicle.

During the entry phase, the beryllium afterbody reaches a peak temperature of 700 °F; however, the temperature rise of the internal payload is small because of its large time constant. Upon deployment of the chute and jettisoning of the heat shield, the landed payload may be subjected to a cold soak (atmospheric temperatures, as low as 130 °K) for as long as 20 minutes. The long descent time is associated with the possibility of encountering a dense atmosphere with a parachute system suitable for the thinnest atmosphere expected. Here the long time constant of the internal payload prevents significant temperature excursions. The cold temperature during descent, however, may affect the performance of the impact attenuator and the parachute.

During the post-landed phase, the internal payload is isolated from the ambient environment. The internally dissipated heat is then handled separately; only 150 watt-hr of power are dissipated.

The isolation of the internal payload was found to be a key requirement in the thermal control studies; however, this runs counter to the requirements of terminal dry heat sterilization. Because of the high internal resistance to the flow of heat, heaters would be required internally during the sterilization phase.

3.7 SCIENTIFIC INSTRUMENTATION

The scientific instruments carried in the lander are used during planetary entry, parachute descent, and for surface measurements during the 5-hour lifetime of the lander. During entry, a six-channel radiometer is used to examine the shock-heated atmosphere in thermodynamic equilibrium behind the shock front in the stagnation region. Measurement of preselected emission bands will permit quantitative determination of the ratios of carbon dioxide, nitrogen, and argon.

A three-axis accelerometer package measures the entry deceleration to determine the atmospheric density profile and the atmospheric scale height. During entry and descent, pressure and temperature measurements are made.

The surface instrumentation consists of a Gulliver biological experiment, surface pressure and temperature measurements, and an anemometer to measure surface wind velocity. The Gulliver experiment employs culture media seeded with radio carbon which is emitted as carbon dioxide through the metabolic processes associated with growth of living organisms. This radio carbon is then detected by a radiation detector as an indication of the presence of life.

3.8 COMMUNICATION AND POWER SYSTEM

The communication requirements for the Advanced Mariner lander include telemetry during the pre-entry, descent, and landed mission phases. Figure 14 shows a block diagram of the system. A direct link to Earth and a redundant relay link through the flyby bus to Earth are both employed during the landed mission phase. Since the lander can assume any orientation on landing, several methods were examined to erect the lander antenna to the local vertical. Gimballing the landed payload by means of a flotation fluid between two concentric spheres of dielectric material was the selected technique. This antenna orientation method, coupled with size constraints, prevented the use of separate antennas for each telemetry link. The antenna selected is a horn having a center frequency of 2295 mc to be compatible with the DSIF. This antenna satisfied the look-angle requirements for both links. Using the direct link equipment at 2295 mc results in a relay link performance margin of 7.1 db at the worst case range and look-angle.

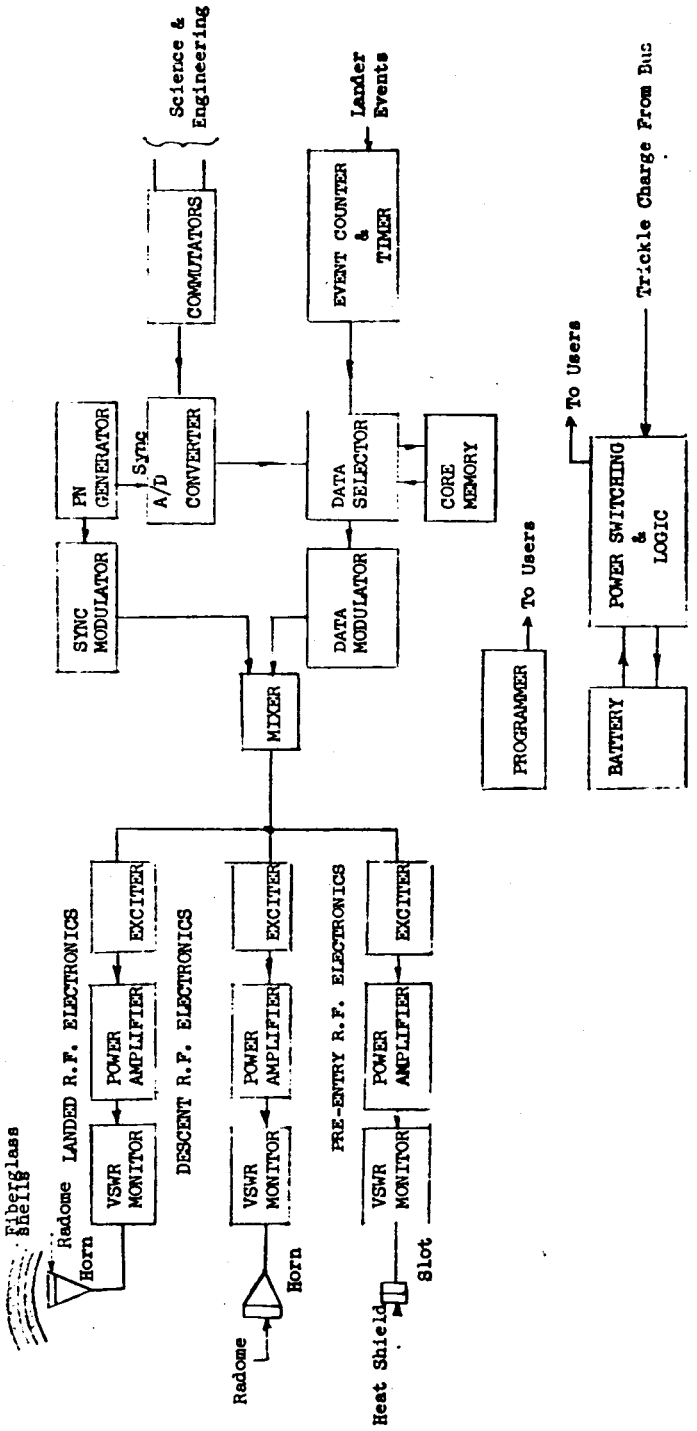

CA-11202

Figure 14 - ADVANCED MARINER LANDER-COMMUNICATION AND POWER SUBSYSTEM BLOCK DIAGRAM

The pre-entry and descent links are relay since a direct link cannot accommodate these mission phases. The carrier frequency is 2295 mc, to be compatible with the landed relay link and thus simplify the flyby bus receiving equipment. The descent transmitter and antenna are located external to the landed payload since the landed antenna is covered by the nondielectric impact attenuator which is jettisoned after impact. The descent antenna is identical to the landed horn. The pre-entry antenna is a cavity backed crossed slot to accommodate the wide look-angle variation between time of separation and entry.

The power amplifiers selected for the three links are amplitron types manufactured by the Raytheon Company. Other amplifier types, such as ceramic triodes or traveling wave tubes (TWT's), could also be used. In the pre-entry and descent links, a non-redundant amplifier is used while in the landed link, redundant amplifiers are used to minimize a possible failure mode at impact. Varactor multiplier exciters are used as drive stages for the three power amplifiers.

The telemetry subsystem and programmer are assumed to be of integrated circuit design. The storage subsystem is a core memory. Other storage systems, typically tape recorders, have basic design problems in surviving the dry heat sterilization and impact shock environments.

The lander power requirements are best accommodated by a battery. A NiCad battery is used since it is the only type presently known which can survive the dry heat sterilization environment.

A summary of the communication and power system characteristics is given in table 5.

3.9 PAYLOAD SYNTHESIS

During the parametric analyses, various lander payload packages were synthesized utilizing the JPL-supplied and Avco-supplemented, instrumentation lists with subsystem parametric tradeoff curves. Communication subsystem selections were made based on range, trajectory geometry, antenna characteristics, bit rates, and data requirements for application to a relay communication capability from lander to bus to DSIF and/or a direct link from lander to DSIF. Three power supply subsystems were considered: battery, fuel cell, and an RTG/battery combination.

Fifteen lander payloads were initially formulated, parametrically, (with variations within each) which satisifed objectives ranging from simple "land and survive" missions to landed lifetimes of from 12 to 48 hours' duration and total data outputs in excess of 1,000,000 bits. Some of these payload formulations were too ambitious for the Advanced Mariner concept and were dropped. Those payloads which were continued as candidates for the conceptual design are listed in figure 15 in order of their increasing complexity. Payload 16, the conceptual design payload, is shown in this chart to indicate its relative capability and complexity.

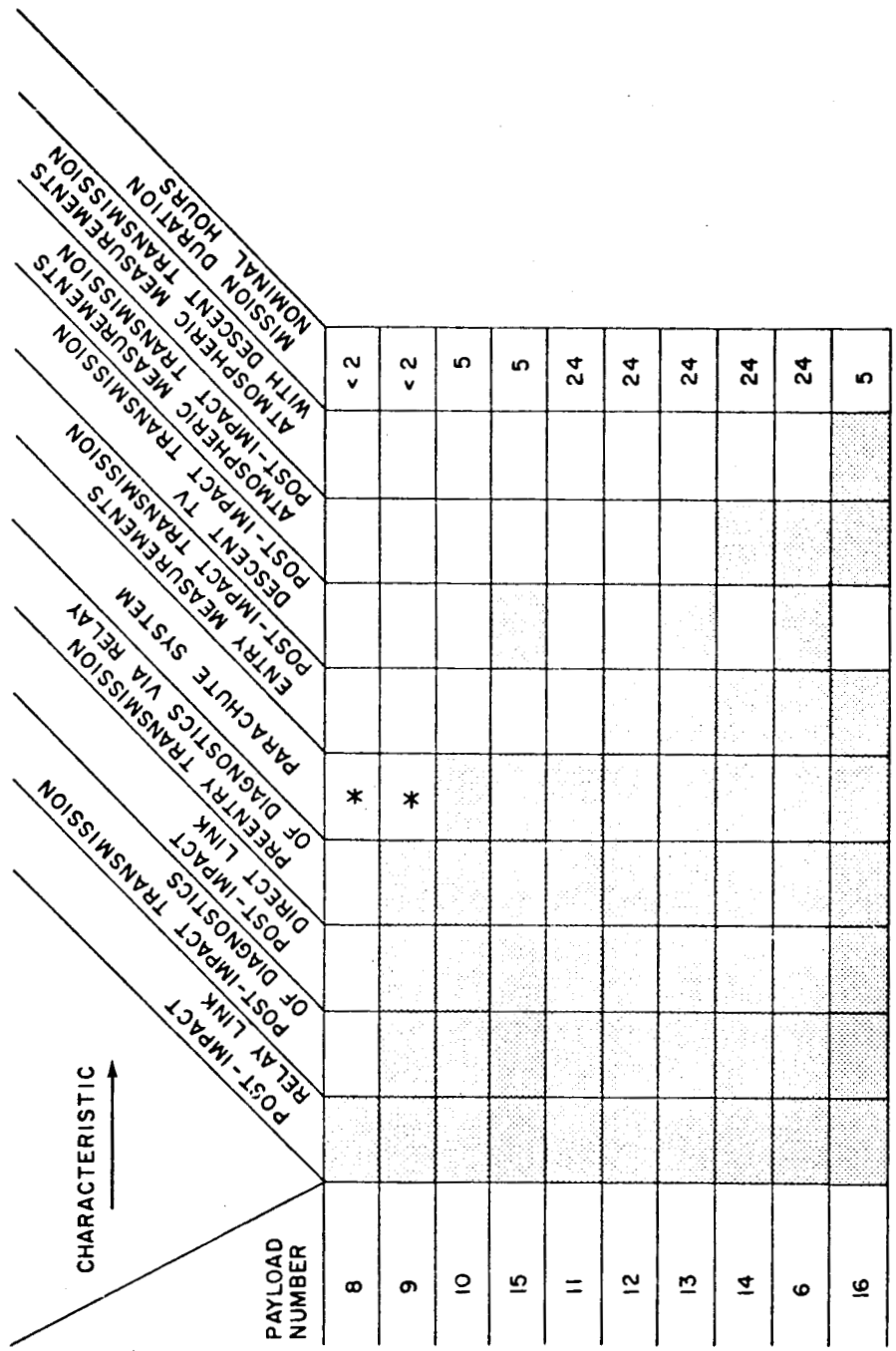

Figure 15 - PARAMETRIC PAYLOAD CHARACTERISTICS

TABLE 5

LANDER COMMUNICATION AND POWER SYSTEM CHARACTERISTICS

Carrier Frequency (all links)	2295 mc
Modulation Scheme (all links)	Coherent PSK/PM
Bit Error Probability (all links)	1×10^{-3}
Antenna Polarization (all links)	Circular
Data Storage	10,000-bit core memory
Primary Power Source	153 watt-hour NiCad battery
Pre-entry Antenna	Crossed slots
Power amplifier	30-watt amplitron
Bit rate	11.5 bps
Descent Antenna	horn (74 deg)
Power amplifier	90-watt amplitron
Bit rate	184 bps
Landed Antenna	horn (74 deg)
Power amplifier	30-watt amplitron (redundant)
Bit rate	11.5 bps (relay and direct)
Battery Weight	25.4 lb
Communication Weight	83.6 lb

The least complex of these payloads--payload 8--represents the minimal "land and survive" mission. Its post-impact relay link transmits only the data indicating the success of the lander in surviving entry and impact through a simple surface pressure measurement. The landed payload was designed to withstand 6000 g at impact; therefore, no parachute system was needed. However, as an added experiment, a parachute backup mode was included which, if successful, would reduce the landing shock to 1500 g.

Payload 9 added engineering instrumentation and a subsystem diagnostic capability (to gather data for future missions in the event of lander failure). The relay link was designed to operate before entry as well as on the surface. A direct link was added as a redundant mode of post-impact transmission. The diagnostic data were relayed before entry and transmitted after impact over both a relay and direct link. This payload was again designed to survive a 6000-g impact with the parachute system as a backup mode. In payloads 8 and 9, the short relay and/or direct transmission time did not require a flyby bus slowdown, nor was a preselected landing site necessary, since no biological experiment was included. The balance of the payloads (shown on figure 15) require a flyby bus slowdown maneuver, extending available relay communication time for bioexperiment data read-out. Syrtis Major was selected as the landing site to maximize the return from the biological experiments. The parachute descent system was no longer considered a backup mode for payloads more complex than payload 9, since a lower impact velocity and consequent lower impact loads were necessary to accommodate the biological experiment.

Payload 15 includes a television capability whereby pictures taken during main parachute descent would be stored and retransmitted after impact through a relay link. Payload 11 extended the biological experiment of payload 10 from 5 hrs to 24 hours and added a second biological experiment employing a different life detection technique. Direct transmission of the resulting data was also extended over the 24-hour period. Payload 12 added simple atmospheric measurements to the instruments of payload 11, to be stored during entry and descent for retransmission after impact.

Payload 13 added the same descent television capability as employed in payload 15, while maintaing all other characteristics of payload 12. Payload 14 deleted the descent television measurements and replaced them with more complex atmospheric composition experiments, to be made after impact and to be transmitted over both direct and relay links.

Payload 6 was the most complex of all payloads considered, in that it included all of the characteristics of payload 14 and again added the descent television with post-impact transmission. A parametric weight summary for all of the payloads listed in figure 15 is shown in figure 16. The necessary RF power requirements for each communication phase are also indicated in figure 15.

The conceptual design payload requirements jointly agreed to by JPL and Avco established the scientific instruments to be used during the various phases of the

lander mission. Referring to the characteristics listed in figure 15, payload 16 represents the simple biological mission of payload 10 with added atmospheric measurements taken during atmospheric entry and parachute descent. All of the pre-impact measurements are stored during entry to be transmitted during the main parachute descent phase. A new mode of communication was therefore added to accommodate this descent measurement transmission. The entry-to-impact data were maintained in storage for subsequent redundant retransmission after impact by means of both direct and relay links.

In summary, this selected communication system operates via relay link to the flyby bus for all three phases of the lander mission: separation to entry, entry to impact, and post-impact on the planet's surface. In addition, a direct link system transmits the required data during the post-impact phase. In selecting the total lander communication package, those systems which operate prior to impact were packaged external to the protected payload. Wherever possible, common elements were used without the use of any RF switching devices. Within the time span of the conceptual design study, total subsystem optimization was not attained. Further investigations have since shown several alternate approaches which should be pursued in the preliminary design phase. The communication link calculations assume the worst case conditions of trajectory geometry and antenna transmission pattern, resulting in a significant margin for the nominal mission. Further analysis of the atmospheric measurement data requirements has shown the conceptual design data list to be conservative. Such factors as these, and others, when optimized, should reduce the selected communication subsystem RF power, weight, and complexity considerably, which in turn would reduce the lander payload weight and overall spacecraft complexity.

PAYLOAD	COMM. SYSTEM	POWER SOURCE	TRANSMITTER POWER (WATTS)	INST. WT. (LB)	INST. POWER WT. (LB)	COMM. WT. (LB)	COMM. POWER WT. (LB)	PAYLOAD WT. (LB)
8	RELAY	BATT.	60	0.3	0.1	44.5	2.0	46.9
9	DIRECT+RELAY	BATT.	60	1.3	0.2	59.1	14.3	74.9
10	DIRECT+RELAY	BATT.	60	8.3	3.5	59.1	16.7	87.6
15	DIRECT+RELAY	FUEL CELL	30 / 100	32.3	4.1	60.7	13.4	110.5
11	DIRECT+RELAY	FUEL CELL	60	27.3	8.4	59.1	8.6	103.4
12	DIRECT+RELAY	FUEL CELL	60	59.3	37.6	59.1	11.0	167.0
13	DIRECT+RELAY	FUEL CELL	60	76.3	38.2	59.1	28.6	202.2
14	DIRECT+RELAY	FUEL CELL	60	72.6	39.4	64.5	17.0	180.8
6	DIRECT+RELAY	FUEL CELL	100	92.0	15.0	66.5	28.5	202.0
16	DIRECT + RELAY	BATT.	30 / 30/90	15.8	2.7	86.2	22.7	127.4

64-10022

Figure 16 - COMMUNICATION, INSTRUMENTATION, AND POWER SYSTEMS PARAMETRIC WEIGHTS

4.0 SYSTEM DESIGN -- FLYBY BUS

The primary mission objective of the flyby bus is the delivery of the lander to Mars. Secondary objectives include (1) topographical mapping of Mars during planetary encounter, and (2) measurement of particles and fields at encounter and during the interplanetary transfer.

To conduct the parametric study and conceptual design study, two major constraints were imposed: (1) the dimensional limitations imposed by the Surveyor shroud, and (2) launch weight limitations imposed by the Atlas-Centaur booster. Launch weight can range from the performance of an unfloxed Atlas Centaur to that of the 30-percent floxed launch vehicle. In principle, the upper launch weight boundary should govern the spacecraft design. However, the lower launch weight boundary is also an interesting constraint for it represents the spacecraft weight that can be launched by an unmodified booster. For a spacecraft designed to be launched towards Mars in 1969 and 1971, trajectory analysis indicated that the 1969 launch opportunity would limit the launch weight. It was found that the injected weight capability for a 32-day launch window extending from January 10 to February 11, 1969, would be 1342 pounds for an unfloxed Atlas-Centaur and 1965 pounds for the 30 percent floxed Atlas-Centaur. The study indicated a spacecraft launch weight of about 1500 pounds was required to provide a worthwhile return of scientific information. Table 6 shows the weight distribution for the Advanced Mariner.

TABLE 6

ADVANCED MARINER SPACECRAFT WEIGHTS

Lander	516 pounds
Separation System	110
Flyby Bus	867
	1493

Several different design concepts were studied to maximize the lander diameter, so as to allow for a reasonable landed payload weight and achievement of a low m/C_DA for the lander. The major configurations investigated were (1) a design arrangement which would place the lander in contact with the booster and the flyby bus on top of the lander and (2) an arrangement in which the flyby bus would be attached to the booster and support the lander. A 96-inch lander diameter could be achieved with the former scheme, at the risk of complicating the problem of separation of the lander from the flyby bus. The latter configuration was selected as the reference design and is shown in figure 17. An 85-inch

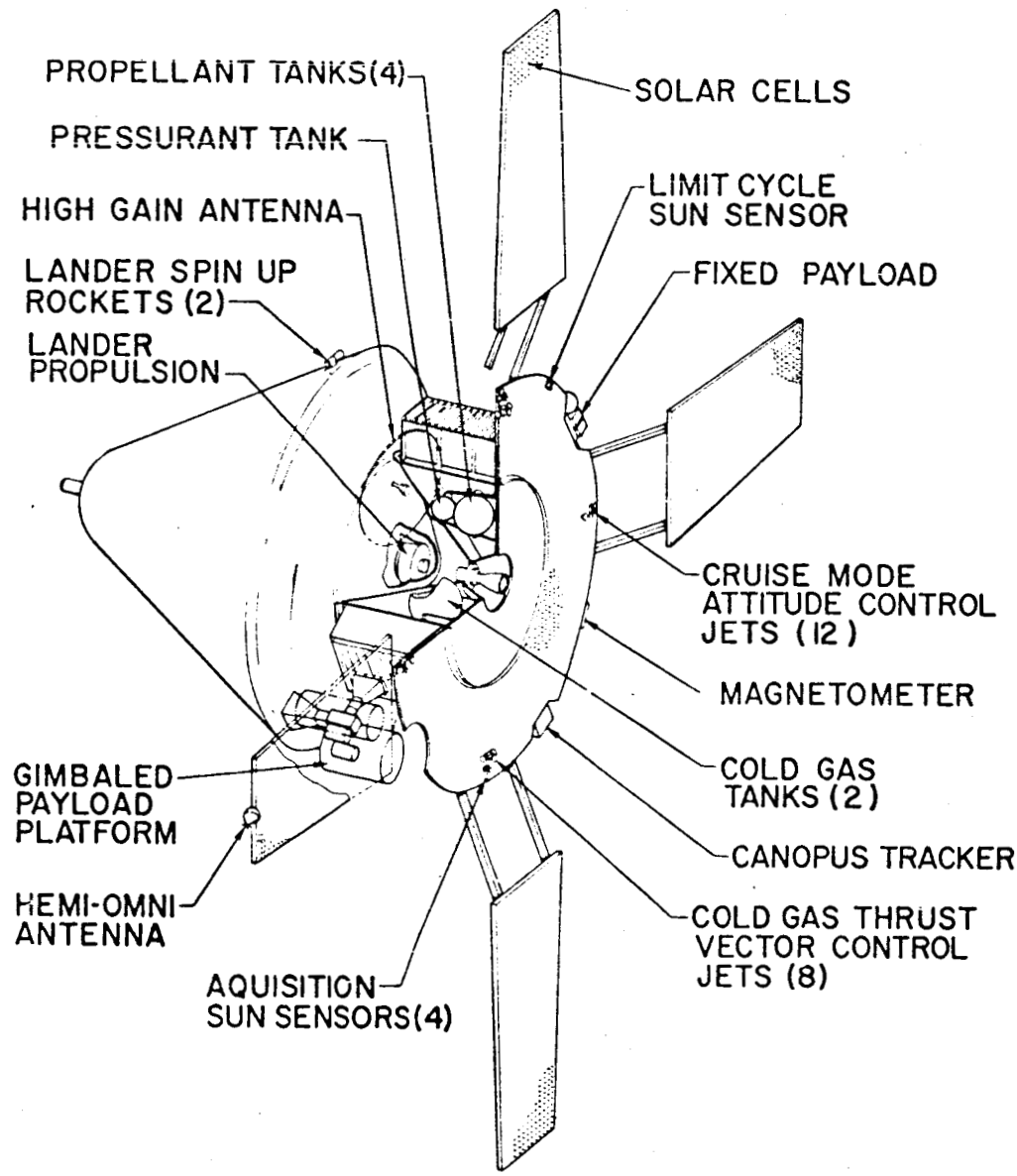

64-9909-2

Figure 17 - ADVANCED MARINER SPACECRAFT CUT-AWAY OF FLYBY BUS LANDER

diameter lander can be accommodated within the Surveyor shroud in this configuration. Lander design studies indicated the requirement for a 90-inch diameter lander to achieve mission objectives. To package a 90-inch diameter lander, it was necessary to increase the cylindrical section of the Surveyor shroud by about 11 inches.

4.1 DESIGN

The overall dimension of the flyby bus in figure 17 is 94 inches in diameter and 26 inches in height. Lander loads are transmitted to the flyby bus through an aluminum cylindrical shell. Propellant and cold gas tanks are housed within this shell, and the system black boxes are housed in six compartments located external to the shell. Thermal control is maintained by use of surface coatings and louvers. The louvers are attached to the exterior of the compartments containing the black boxes. Black box temperature excursions over the mission will range between +94°F and +20°F.

Scientific instruments to measure particles and fields are located on cutouts along the periphery of the rigid solar panel. A gimballed payload platform, which points towards the Martian local vertical during encounter, supports the television mapping system, infrared spectrometer, and horn antenna. Mapping system performance allows a 1-km resolution to be achieved with f8, 12-inch focal length modified Cassegrain optics, and a vidicon detector. The horn antenna receives data relayed from the lander communication system.

A command and telemetry link is maintained by a hemi-omni antenna, which is used from launch to 43,000,000 km from Earth, at which point a crossover to a fixed 3 x 1-1/2 foot antenna occurs. This antenna is fixed to the spacecraft, obviating deployment and gimbal design problems. From launch to approximately 20,000,000 km a bit rate of 33-1/3 bits/sec is maintained. At 20,000,000 km the bit rate is reduced to 8-1/3 bits/sec until post-encounter at which time the bit rate is increased to 133-1/3 bits/sec. The communication system is designed to record information acquired during the encounter mode rather than transmit in real time. A recorder with a 2×10^8-bit storage capacity is used.

Primary power is provided by an oversized solar panel. Sixty square feet of panel area are required to provide the raw power requirements of 240 watts to the spacecraft systems. Four deployable panels and one rigid panel have an area of 85 square feet and a capacity of 340 watts, allowing for power system growth, redundancy, and degradation in performance. Cell performance of 4 w/ft^2 at the Martian distance is assumed. Secondary power is provided by 20 pounds of silver zinc batteries at 37 w-hr/lb; the capacity used is approximately four times the minimum required.

Stabilization and control during the cruise mode is achieved by using nitrogen cold gas reaction control and a Sun-Canopus reference system. Twelve nozzles provide three-axis control. For maneuver a gyro reference system is used,

and during a thrusting mode, thrust vector control is achieved by a set of eight nozzles which draw propellant from the same nitrogen cold gas tanks as the cruise mode reaction control. Nitrogen cold gas is stored within two tanks.

The propulsion system is designed for three cycles of operation, namely: two midcourse maneuvers near Earth with a total ΔV of as much as 110 ft/sec and a flyby bus slowdown maneuver near Mars with a ΔV capability of as much as 919 ft/sec. Inhibited red fuming nitric acid (IRFNA) and unsymmetrical dimethyl hydrazine (UDMH) are loaded into four tanks, two fuel and two oxidizer. A nitrogen pressurant is used for expulsion.

The separation system for the lander includes a rigid sterilization canister to meet the Martian sterilization specification, and a propulsion system to place the lander on an impact trajectory. The lander is attached to the spacecraft at three joints that maintain a sterile interface between the flyby bus and lander. Lander orientation during the thrusting mode is achieved by spin stabilization. Two spin rockets are provided, and a yo-yo despin subsystem is used to reduce the angular rate after propulsion system burnout.

A summary of the flyby bus system characteristics is presented in table 7, the flyby bus functional diagram is shown in figure 18 and a flyby bus weight summary is presented in table 8.

4.2 SCIENTIFIC PAYLOAD

The scientific mission objectives of the flyby bus are to provide topographical mapping of Mars during planetary encounter and measurements of particles and fields at encounter and during interplanetary transfer. A study was conducted to determine the relationship between phenomena that could be detected during encounter and the geophysical information that could be inferred from these measurements. The planet was divided into a number of zones which included (1) the atmosphere, the volume bounded by the solar wind and the planet's surface; (2) the biosphere, taken as distributions of ecologies and individuals in the Martian environment; (3) lithosphere, taken as the solid crust of the planet; and (4) endosphere, taken as the interior. These four zones were further subdivided into regimes of geomorphic order of magnitudes. For example, six regimes of the lithosphere include (1) a first-order regime corresponding to the rotational bulge, (2) a second-order regime corresponding to features of continental dimensions, (3) a third-order regime -- mountain chains or rifts, (4) a fourth-order regime -- volcanic cones or meteor craters, (5) a fifth-order regime -- large boulders, and (6) the sixth-order regime -- objects of sand grain dimension. Target signatures include (1) electromagnetic signatures varying from X-radiation through visible to radar, (2) detection of gravitational, electric, and magnetic fields, and (3) detection of particles varying from corpuscular to molecular to dust. The physical phenomena that is associated with and characteristic of the features are presented. Instruments from the JPL instrument list with which to measure the features are presented. With

TABLE 7

CHARACTERISTICS AND PERFORMANCE OF FLYBY BUS SYTEM

System	Characteristic
Scientific Instrumentation	Television mapping systems; 12-inch focal length; 1-km resolution at 12,000 km; 330 pictures (2×10^8 bits)
	Charged particle detector, ion chamber, cosmic dust detector, micrometeoroid detector, infrared spectrometer
Communication	From launch to 43,000,000 km, 10 watts, S-band, hemi-omni antenna, 33-1/3/8-1/3 bps; from 43,000,000 km; to encounter, 10 watts, S-band, 3-ft x 1-1/2-ft fixed antenna, 8-1/3 bps; from encounter to encounter + 10 days, 10 watts, S-band, 3-ft x 1-1/3-ft fixed antenna, 133-1/3 bps; S-band relay link 34° half-power beam-width horn antenna
Power Supply	Solar cells, 85 $feet^2$, silver-zinc batteries
Guidance	DSIF and two midcourse corrections
Stabilization and Control	Cruise mode: ACS, Sun-Canopus reference, nitrogen cold gas, limit cycle ± 0.1 degree, 88-minute nominal limit cycle period; propulsion mode: gyro reference, nitrogen cold gas TVC
Propulsion	UDMH and IRFNA; 280 I_{sp}; mass fraction 0.7, nitrogen pressurant; surface tension baffles to expel propellants; 25-pound thrust level
Thermal Control	Surface coatings and louvers
Structure	Aluminum shell with six black box compartments

TABLE 8

FLYBY BUS WEIGHT SUMMARY

Science		68.3 lb
Gimballed Payload Platform		20.6
Power Supply		144.5
Batteries (20 lb)		
Solar Panels (102 lb)		
Communications		137.5
Relay Equipment (23.5 lb)		
DAS		8.0
CC&S		15.0
Stabilization And Control		96.9
Nitrogen Cold Gas (31 lb)		
Gas Tanks (31 lb)		
Propulsion		133.0
Propellants (93)		
Thermal Control		36.0
Structure		124.0
Bracketry and Fittings		25.0
Cabling		58.0
	TOTAL	866.8 lb
64-10096		

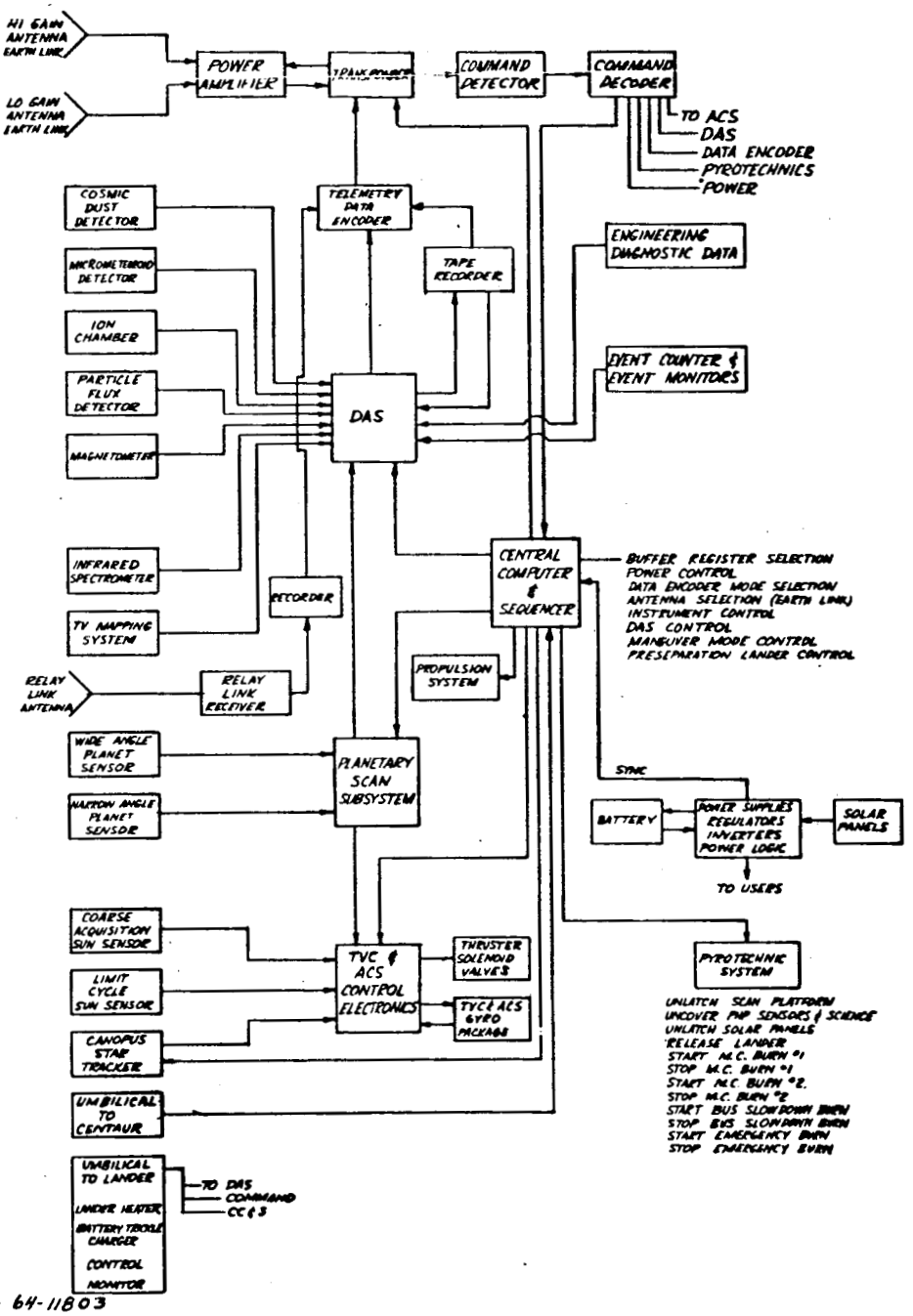

Figure 18 - FLYBY BUS FUNCTIONAL DIAGRAM

these charts and instrumentation list, a ranking of instrumentation can be obtained so that instruments can be added or removed from the flyby bus in an optimal fashion. The group of instruments selected for the flyby bus include an ion chamber, particle flux detector, magnetometer, cosmic dust detector, and micrometeoroid detector, that are fixed to the spacecraft, and an infrared spectrometer and TV mapping system that are attached to a two-axis gimballed payload platform.

An analysis of the mapping system performance using equipment similar to that used for the Mariner 64 television system shows that the expected increase in guidance accuracy allows considerable improvement in resolution. The new system will almost have the exact weight, power, and size as the Mariner 64 system. The camera head can be identical with the Mariner 64 system with the exception of the vidicon tube.

At an altitude of 12,000 km it has been found that the Mariner 64 system can be used with small modification to achieve a resolution of 1 km and a field of view of 220 km. The performance of the present vidicon will be improved to provide a line density increase from 910 to 1360 lines/inch and the photocathode sensitivity will be improved by a factor of 2.

Minor modifications will also be made in the camera control computer and synchronizing circuits, and buffer storage capacity in the data automation system will be expanded by 50 percent to handle the increased data in each television line.

The gimballed payload platform which orients the TV optics and sensor is a servo-controlled mounting platform serving as a base for planet-oriented payload instrumentation and detection equipment. The platform has been designed with freedom to rotate about two orthogonal axes as shown in figure 19. By controlling angular position of the platform about both axes, it is possible to hold the payload in a fixed orientation with respect to the planet. A two-channel horizon sensor mounted on the platform will detect payload orientation with respect to the planet local vertical and will supply error information to position the platform about its azimuth and elevation axes. In this way the payload will be oriented to continuously monitor the surface of the planet during encounter. The gimballed platform will support a television camera, an infrared spectrometer, a relay antenna, a two-axis horizon sensor, and associated electronics. It will be necessary to control the position of this payload with an absolute accuracy of 0.5 degree and with sufficient instantaneous accuracy to hold television camera picture smear within 50 percent of one resolution cell when the camera shutter is open.

4.3 COMMUNICATION AND POWER SYSTEM

The flyby bus communication system characteristics are listed in table 9 and a functional block diagram is presented in figure 20. System studies were

performed using the Mariner 64 spacecraft design as a guide. The flyby bus communication and power systems design will involve a minor modification of the Mariner 64 subsystems.

TABLE 9

FLYBY BUS COMMUNICATION SYSTEM CHARACTERISTICS

System	Characteristic
High-Gain Link Antenna	3-foot major diameter
	0.5 axis ratio
	Gain = 21 db (on axis)
Low-Gain Antenna	Spiral hemi-omni
Relay Link Antenna	Horn
Low-Gain, High-Gain Crossover Range	43,000,000 km
Maximum Post-Encounter Range	190,000,000 km
Data Rates	8-1/3 bps (crossover)
	33-1/3 bps (near Earth)
	133-1/3 bps (post-encounter)
Transmitter Power	10 watts
Communication System Weight	143.5 lb
Power System Weight	146.5 lb

The minimum performance margin in the DSIF-flyby bus channel is 5.2 db and occurs in the command link with the low-gain antenna. The two-way doppler tracking link is always better than the command and telemetry links; therefore designing these links to operate throughout the mission automatically ensures the operation of the tracking link. The telemetry link minimum performance margin, which occurs in the high gain link is 7 db. The link crossover range was based upon antenna pointing losses and minimum transmitter power requirements. A 10-watt transmitter provides adequate telemetry link performance margins.

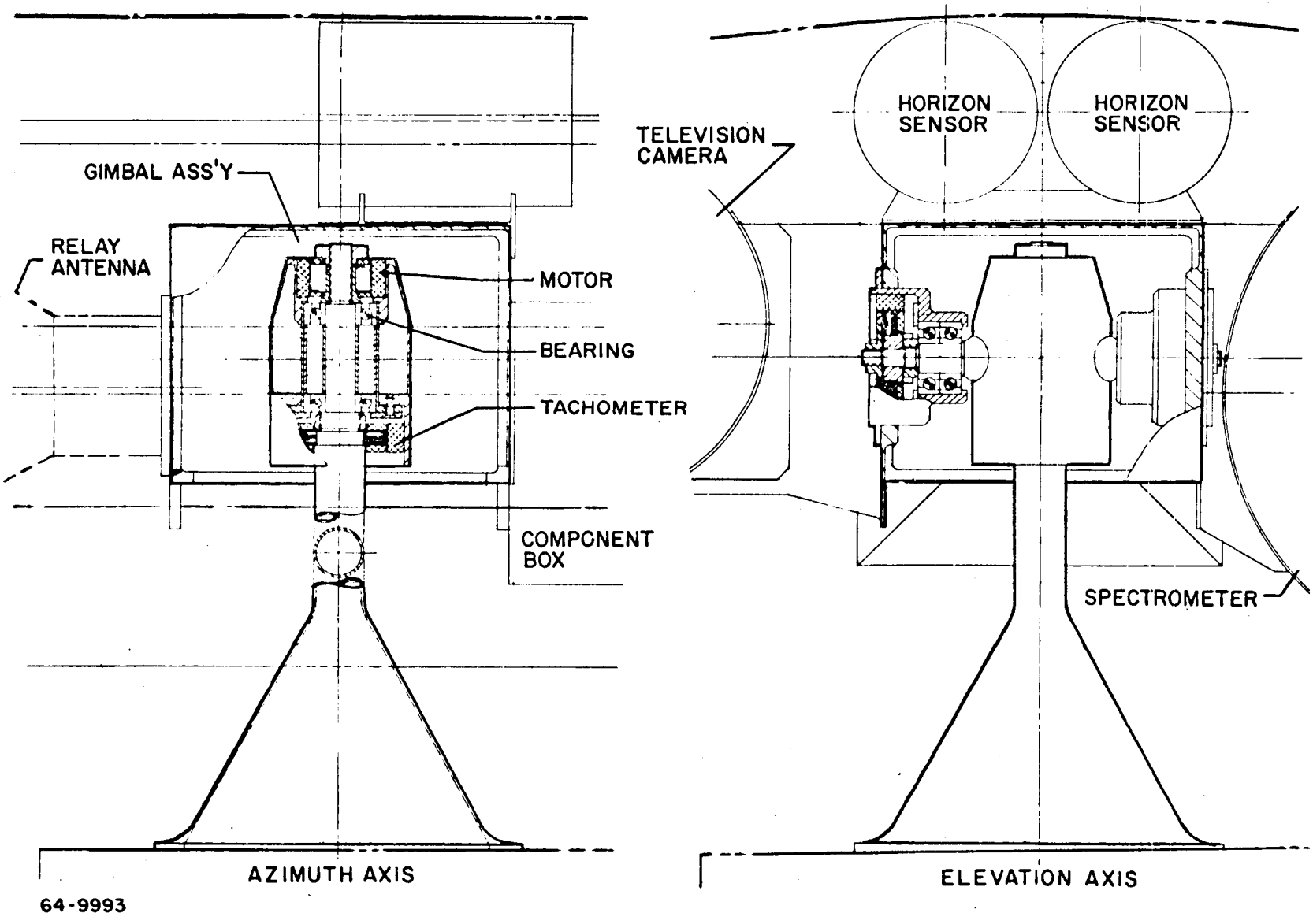

Figure 19 - ADVANCED MARINER FLYBY BUS GIMBALLED PAYLOAD PLATFORM

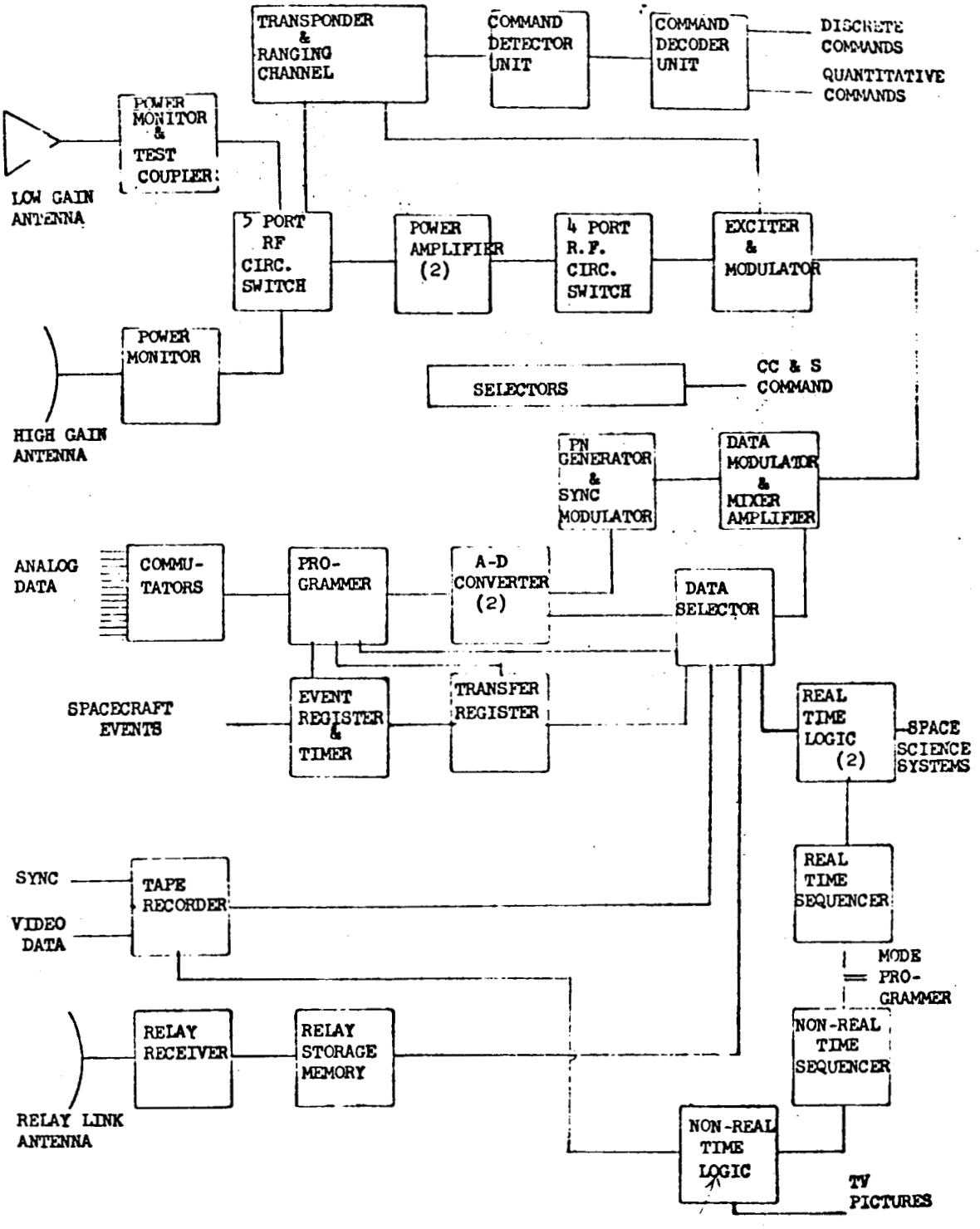

Figure 20 - COMMUNICATION SYSTEM BLOCK DIAGRAM FLYBY BUS

A battery/solar array combination (see functional block diagram presented in figure 21) will supply the raw power for the spacecraft subsystems. The battery requirements will be satisfied by a 20-pound silver-zinc battery with a specific energy of 37 w-hr/lb. Sufficient solar cell panel area is provided so that the battery will be completely recharged in a 24-hour period.

The maximum power demand from the solar array is only 65 percent of the total available power based on an assumed 4 w-hr/ft^2 of solar cell area. Eighty-five square feet of active solar cell area will be distributed on five panels with a weight of 1.2 lb/ft^2 of solar cell area.

The flyby bus communication and power systems hardware list is similar to the Mariner 64 parts list and will also include a receiver, antenna, and storage memory for the relay link. The relay link receiver uses a tunnel diode pre-amplifier and will have automatic acquisition in the carrier and sync loops. The relay link antenna is a horn located on the gimballed payload platform. The relay link memory will have a maximum capacity of 30,000 bits. The RF electronics subsystem will be identical to the Mariner 64 design while the data automation, command, and telemetry subsystems will be slightly modified. The video tape recorder will require an increased storage capacity.

4.4 PROPULSION SYSTEM

The propulsion system is a bi-propellant system having a 25-pound thrust level with a total impulse capability of 26,000 lb-sec. The propellant combination selected is IRFNA/UDMH because of its wide operational temperature range of -56 to 140°F. Propellant specific impulse is a secondary consideration because the total impulse requirement is low; a specific impulse of 280 is attainable.

The bus design allows for a propulsion system installation utilizing a radiation-cooled thrust chamber. The system installation allows the propulsion system to be prepackaged, which is advantageous from a reliability and maintainability viewpoint.

The bus mission requires three start/firing periods of the propulsion system; no solenoid valves are used but a separate flow circuit takes the place of a solenoid valve for each firing. This is accomplished by the use of explosive-operated flow valves in series pairs (one normally open, one normally closed) for each of the three start/firing phases. This concept results in higher system reliability by eliminating valve leakage.

The propulsion system requires positive propellant expulsion; the concept chosen, uses surface tension baffles installed in each of the four propellant tanks. This concept was chosen because there are no bladder systems available that will operate at the propellant freezing point, the metal bellows approach is too heavy, and metal diaphragms are limited to one cycle which prevents system checkout.

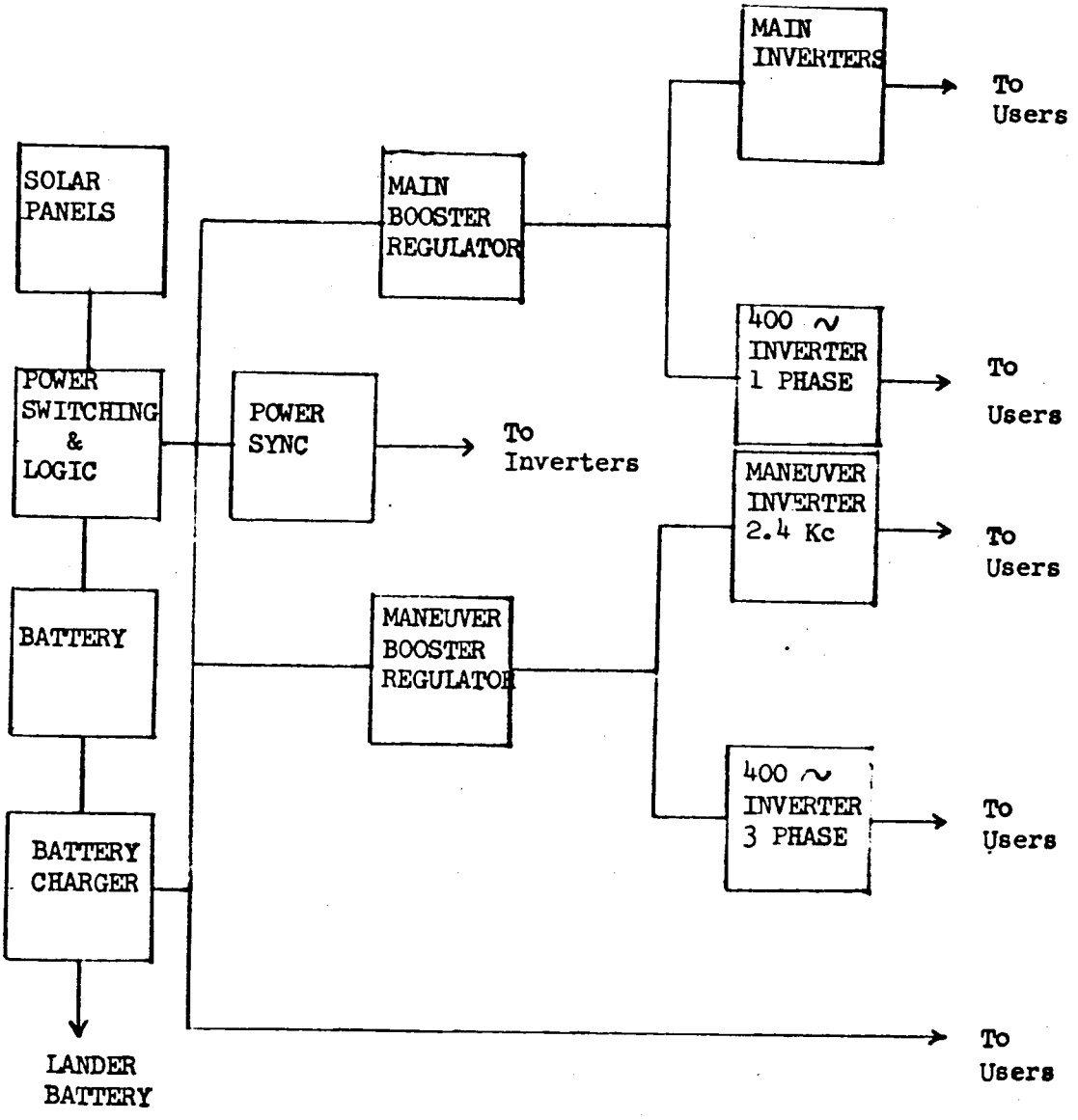

Figure 21 - FUNCTIONAL BLOCK DIAGRAM OF POWER SUPPLY SYSTEM

4.5 SPACECRAFT CONTROL SYSTEM

The conceptual design of an attitude control system for the Advanced Mariner flyby bus was evolved through parametric evaluation of the operational requirements and control system configurations necessary to meet the desired mission objectives. Among the design alternatives considered were cold gas, subliming solid, or cap pistol reaction controls in the basic ACS used for the acquisition, cruise, and orientation modes of operation. For thrust vector control during the thrusting mode of operation, jet vanes, gimballing, secondary injection, and auxiliary reaction jet TVC systems were considered.

Control system total impulse and response characteristics were examined parametrically, and the choice of ACS for the conceptual design was based on rating criteria which included vehicle interface, reliability, system weight, power consumption, controllability, operating history, development time, and development cost.

The ACS conceptual design is built around a cold gas reaction system. Nitrogen jets are used for vehicle attitude control during all phases of the mission. A total of twelve gas jets, four per axis, each having a thrust level of 0.01 pound, provide torque couples for pitch, yaw, and roll rotation in either direction during the acquisition, cruise, and orientation modes of operation. Eight gas jets, two for pitch, two for yaw, and four for roll, each having a thrust level of 0.1 pound are used for thrust vector control of the main propulsion system.

The gyro electronics package includes three floated single-degree-of-freedom gyros used as (a) rate sensors in three axes for damping purposes, and (b) attitude sensors in three axes for attitude hold purposes during spacecraft maneuvering. Also included in the package are evaluation electronics which allow an in-flight evaluation of gyro drift rates so that they may be compensated for during commanded spacecraft maneuvers. The gyro electronics provide the elements necessary to control the gyros in the rate, attitude, and gyro evaluation configurations and to supply an output error signal to the control electronics.

The control electronics package provide the elements necessary to process the error input signals from the gyros or optical sensors and command the appropriate reaction jets when the preset deadband of the on-off level switch is exceeded. Error signal phase determines which polarity of jets is to be energized and error signal amplitude determines when the deadband has been exceeded.

The Canopus star tracker is an electro-optical device which provides electrical signals indicative of the magnitude and direction of the deviation of the star Canopus from a null. An image dissector photomultiplier tube is used as a detector. The mirror of the optics is gimballed to accommodate the apparent motion of Canopus during the Advanced Mariner mission.

The coarse acquisition system consists of four silicon detectors in each spacecraft axis properly mounted on the spacecraft and connected in a bridge. They provide electrical outputs in pitch and yaw indicative of the direction to which the spacecraft must be commanded, to bring the sun within the field of view of the limit cycle sun sensor.

The limit cycle sun sensor is a passive electro-optical device which provides an electrical signal indicative of the direction and magnitude of the Sun's deviation from a null. The optical configuration permits a very sharp null and good scale factor at the expense of a limited field of view.

4.6 STRUCTURES

The flyby bus structural design is essentially based on a semimonocoque construction with major members to support isolated equipment. Aluminum (7075) alloy material was employed for most of the shell structures with magnesium (AS31A) for some support members and fittings.

Structural arrangement of the flyby bus is primarily controlled by the lander and propulsion system design loads which must be redistributed during the launch phase. Basically the structure consists of several major elements:

1. A central support cylinder to transmit launch loads to the launch vehicle adapter

2. A propulsion system support structure which allows the complete removal of the propulsion system as a module

3. A thin non-loadcarrying cover sheet over the top of the central support cylinders to provide meteoroid protection for the propulsion system after lander separation

4. Six electronic package support structures to which are mounted all electronic equipment as modules

5. Four hinged solar panel structures.

The lander and sterilization canister are attached to the flyby bus structure at three points. At each point a special joint is provided that can be heat sterilized with the lander. These joints incorporate a captive explosive separation nut to release the lander and a spring which provides the separation force.

The adapter connecting the spacecraft to the launch vehicle is an aluminum conical shell. A shape charge ring is included for launch vehicle-spacecraft separation.

4.7 THERMAL CONTROL

An analysis of the conceptual design was conducted to determine whether the use of a passive thermal control was feasible. The passive system uses surface coatings and louvers attached to the exterior of the six black box compartments. The black boxes would be mounted on the inside of the compartment flush to the skin; the louvers would be on the outside of the compartment flush to the skin. Control of louver blade angle would be accomplished by the use of bimetallic temperature-actuated springs; this control would not be tied into the command and control system.

Heat loads considered were solar radiation and dissipation of power from the spacecraft system black boxes. Thermal control during the following operational modes was considered: (1) launch pad operation, (2) ascent onto the transfer trajectory, (3) cruise near Earth, (4) maneuver near Earth, (5) cruise near Mars, (6) maneuver near Mars, and (7) cruise after lander separation. It was found that the temperature excursion of the structural skin to which the black boxes are attached can be held between +94°F near Earth and +20°F near Mars. This excursion is based on using a resulting heat capacity of 12 lb/ft^2 of black box. Temperature excursions of the propellant tanks were also held well within their prescribed bounds of -56 to +140°F.

4.8 SEPARATION SYSTEM SUMMARY

The separation system provides the lander with (1) a rigid sterilization canister that maintains the lander in a sterile condition, (2) a separation joint that permits separation from the unsterilized flyby bus without lander being contaminated, (3) a propulsion system to alter the velocity vector of the lander so that when it is released from the flyby bus, it can be accelerated onto an impact trajectory, and (4) a spin stabilization system for attitude control during the thrusting mode.

In the reference configuration (figure 22), the lander is mounted on top of the flyby bus with the lander forebody support ring making contact with the flyby bus adapter section ring. The propulsion system is strapped to the forebody. Yo-yo despin weights are attached to the lander. The weights are released from hooks that are located on a line transverse to the lander longitudinal axis and passing through the center of gravity. The lander, propulsion unit, and yo-yo, are enclosed in an aluminum canister. Attached to the exterior of the canister is a pair of spin rockets.

About 1,000,000 km from the planet the spacecraft leaves the Sun-Canopus reference system and is oriented in a direction such that after separation and acceleration, it will be placed on an impact trajectory. The lander is released and goes through a sequence of events described in the following paragraph. The flyby bus is then oriented in a direction such that it will be slowed down and lag the lander by about 5 hours. After the flyby bus propulsion system performs this maneuver, it returns to the Sun-Canopus reference system.

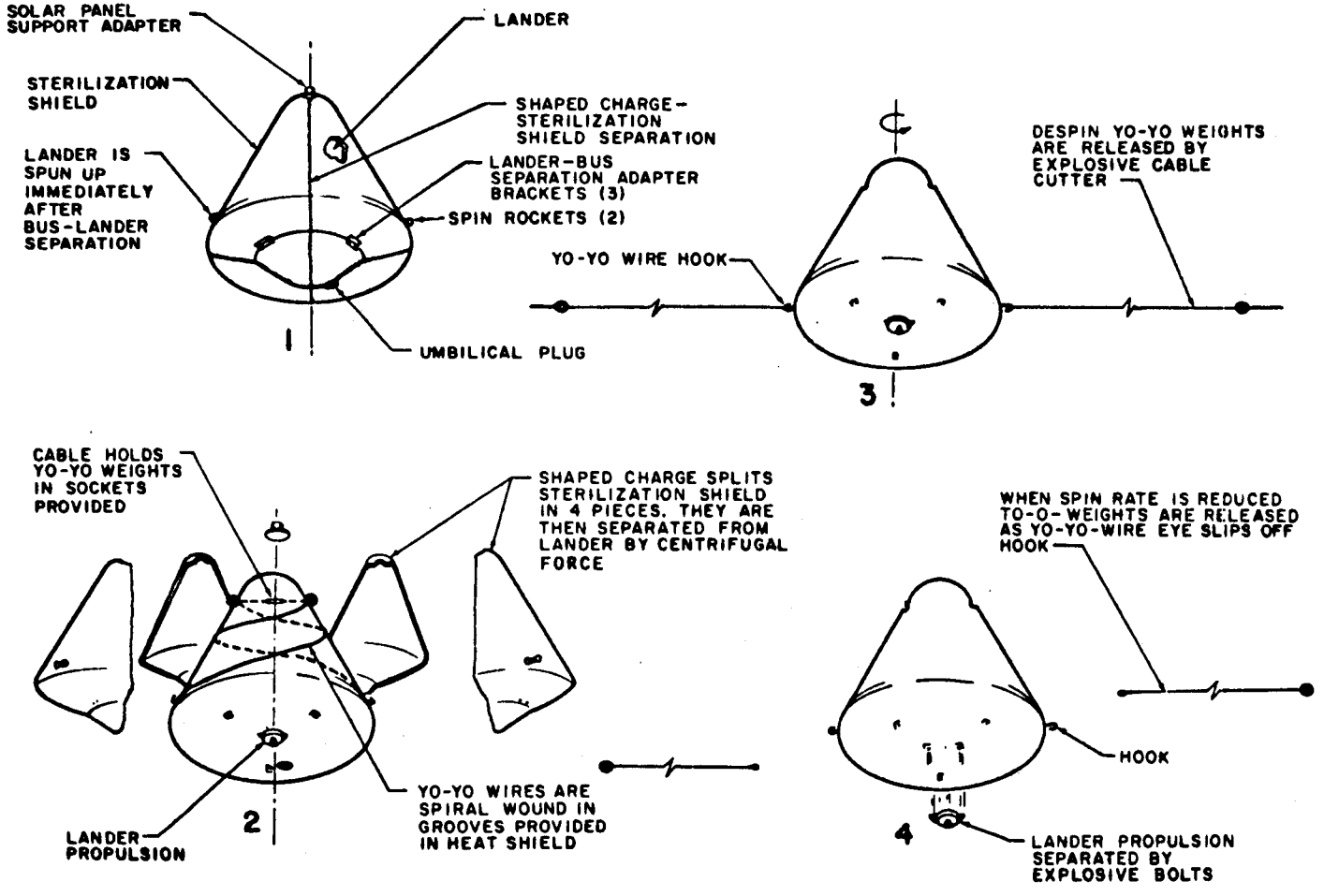

Figure 22 - LANDER SEQUENCE AFTER SEPARATION

The lander sequence after separation is shown in figure 22. On command from the bus an electrical signal energizes the explosive cartridge attached to each of three separation joints. The explosive cartridge breaks the rigid tie-down bolts holding the lander and canister to the flyby bus. Once the bolts are released, three springs are no longer constrained and provide a separation force to displace the lander from the flyby bus. Upon separation, the spin rockets are ignited and accelerate the lander to 20 rpm. When the lander is about 1000 feet from the flyby bus, a shaped charge splits the sterilization canister quadrants, and these quadrants fly away from the lander. Propulsion is provided by a 3400-pound-second solid rocket with an I_{sp} of 270 and the capability of providing a velocity increment of 220 ft/sec. Upon burnout a shaped charge connecting the yo-yo weights is severed and the lander is decelerated to approximately zero spin rate. The spent lander propulsion system and yo-yo despin system are then jettisoned.

5.0 ADVANCED MARINER SUMMARY PARAMETRIC CURVES

Upon completion of the parametric evaluation phase of the Advanced Mariner study, it was found that a number of single, relatively independent parameters had been analyzed for their effects upon other dependent parameters. The degree of dependence, however, between various parameter sets was found to be sensitive to the immediate area in which the evaluation was being made. Since a particular conceptual design was to be chosen as a reference for testing the parametric results, a series of master or summary parametric curves were evolved which would show the effects of certain discrete variables on as many as possible of the major design parameters in the immediate neighborhood of the reference design. Mission characteristics and objectives were responsible for selection of the conceptual design payload and hence selection of the required vehicle parameters. The summary parametric curves reflect these basic mission philosophies and requirements.

The significance of the summary parametric curves in most cases therefore lies not in the absolute numerical values that are shown, but in their indication of the relative impact of the basic study constraints upon the selected design. The early availability of better Martian atmospheric data will certainly aid in the future optimization of a Mars entry vehicle design but is not necessary to prove the feasibility of such a mission, as this study shows. Throughout this investigation the worst case philosophy has prevailed. Yet, in spite of the overall pessimism of the assumptions, a state-of-the-art design has proven to be practicable with quite reasonable expenditure of manpower and time.

In the following paragraphs an attempt will be made to interpret the summary parametric curves which are felt to be of most importance. The conceptual design which was chosen is shown schematically in figure 23.

A brief description of the entry vehicle flight profile will aid in understanding the following underlined notation which is used on figure 23 and those to follow.

> ENTRY WEIGHT is that weight at which the planetary atmospheric entry vehicle begins its penetration into the Martian sensible atmosphere at an altitude of approximately 800,000 feet. The structure, thermal control, and heat shield systems carry the aerodynamic and thermal loads as the vehicle is decelerated. Measurements of vehicle acceleration, temperatures, and pressures are made and stored for later data playback via relay communication links to the flyby/bus. At a suitably low Mach number, $M \leq 2.5$ a drogue parachute is deployed, further decelerating the vehicle. As a high subsonic velocity is reached, a shaped charge is initiated which splits the entry vehicle circumferentially near its largest diameter.

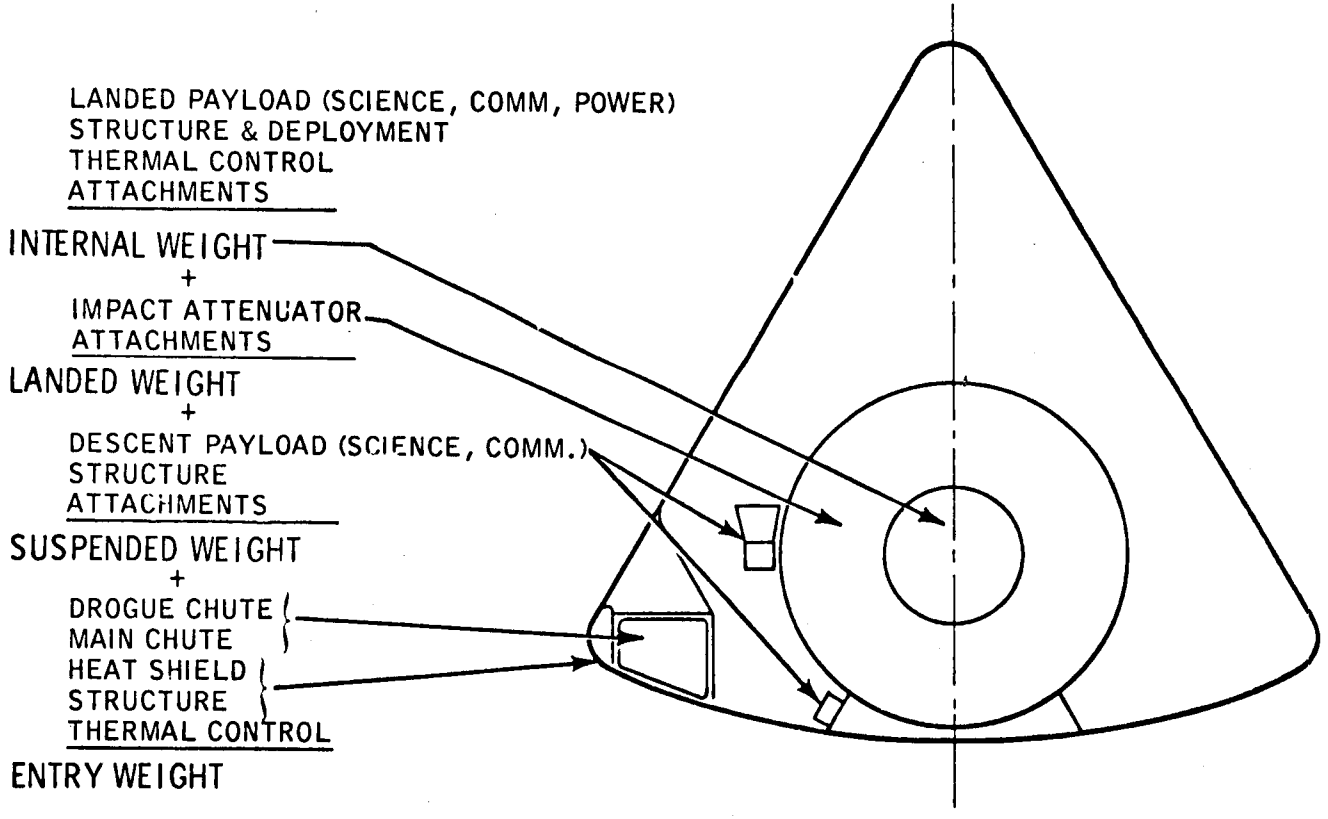

Figure 23 - PAYLOAD TERMINOLOGY DEFINITION

The drogue parachute and afterbody are jettisoned and as they pull away, the main parachute is deployed, exerting enough drag to pull the SUSPENDED WEIGHT clear of the structural nose cap. During descent on the main parachute, the descent payload science measures atmospheric temperatures and pressures and transmits these back to the flyby bus via the descent communication relay link. The data stored prior to main parachute deployment is also played out during this period. Prior to impact with the Martian surface and after a predetermined time interval from main parachute (predicated on worst atmospheric conditions and vehicle trajectory characteristics), the descent payload is jettisoned. At ground contact the main parachute is detached, allowing the LANDED WEIGHT to dissipate its kinetic energy by crushing of the impact attenuator. A preset impact initiated delay timer deploys the crushed impact attenuator and its attachments after allowing suitable time for motion to cease. The INTERNAL WEIGHT, thus deposited safely on the planetary surface, is ready to begin its landed mission. Anchored to the ground by the deployment devices and protected from the Martian environment by the thermal control system, the landed payload, supported from the structure by its attachments, deploys its sensors and establishes contact with both the Earth and the flyby bus via its communications systems.

From a parametric standpoint this descent payload with its attendant structure and attachments could vary upwards in weight from a minimum of zero. The conceptual design study, however, investigated and assigned a define value. In the interests of making the summary parametric results more meaningful, the curves which follow have been drawn showing the conceptual Design Point, as well as the Available Internal Weight with No External Weight, i. e., without descent payload and descent payload structure. In the immediate neighborhood of the conceptual design and for descent payloads other than that specified for the conceptual design (or for any other non-impact protected weight), the available internal weight variation may be found by using the explicit relations developed elsewhere in this report for the various determinate systems. Those weights not specifically defined by parametric studies may be approximated using the "structural fractions" and other such implicit relationships, as demonstrated by the conceptual design example.

5.1 TRAJECTORY SUMMARY PARAMETRIC CURVES

The choice of a launch window with suitable characteristics at both ends of the trajectory is of prime importance. For the 1969 opportunity several pertinent trends are evident from a study of figures 24, 25, and 26. Trajectory studies show that a near minimum departure velocity is realizable for fixed arrival dates of mid-October 1969 through late November 1969 (figure 24) using launch window dates from mid-January through mid-February (figure 25). Choice of arrival date is based upon Martian seasonal variations, i. e., arrival at or

near the peak of the wave of darkening at the chosen Syrtis Major landing site. Use of the unfloxed Atlas-Centaur as a launch vehicle, combined with the departure velocity requirements, implies a certain range of payloads, as shown by the abscissa of figures 24, 25, and 26. At planetary arrival, the considered trajectory range engenders a ZAP angle variation shown by the ordinates of the aforementioned curves. By definition of the ZAP angle (i. e., the angle subtended between the approach asymptote and the Sun-planet line and in their common plane), it is apparent that keeping this value near 90 degrees allows for optimum planetary surface observation by the flyby bus. Flying the bus between the Sun and the planet and utilizing the planet's rotation allows the lander to operate in the sunlight and in view of the bus for a longer period of time. Figure 24 shows payload capability and ZAP angle for various fixed arrival dates. Figure 25 shows the same data for various launch dates, and figure 26 combines the data from two previous curves. For any launch during the approximately month-long opportunity, four fixed arrival dates were chosen. The heavy dark lines on figure 26 show the selected arrival date window. Launching later in the window, in general, allows larger payload, but degrades the ZAP angle. The selected window is a compromise between arrival date, ZAP angle, and payload.

As an example, combining the path of the fixed arrival dates on 15, 21, 27 October and 2 November 1969 (figure 24) with the launch date data trajectories (figure 25), we see (from figure 26) that the window chosen allows a ZAP angle between 72 and 83 degrees, a payload between 1342 and 1494 pounds, and a launch date between 10 January 1969, and 11 February 1969. Flight time is from 278 to 264 days.

For the 1971 launch opportunity, as shown by figure 27 (in a manner similar to figure 26), a single fixed arrival date (12 November 1971) has been chosen. The launch date window extends between 2 May 1971, and 3 June 1971. The payload varies from 1550 to 1660 pounds, the ZAP angle from 133 to 130 degrees, and the time of flight from 194 to 162 days.

5. 2 SCIENCE AND DATA REQUIREMENTS--SUMMARY PARAMETRIC CURVES

Parameters of great importance for the lander involve the landed science mission. Figure 28 shows the interdependence of the science experiments and the power required to run them with the total bit content of landed data which is to be transmitted. These parameters are plotted against the required internal weight for the landed package. The conceptual design point chosen has a 5000-bit total content, a constant transmission bit rate of 14 bits/sec, and transmitter RF power of 30 watts. These were used to determine data transmission times and communication power weights. Constant mission duration was assumed. The variation in science and science power weight assumed a constant average power usage per pound of science equipment, based on the reference design. As an example, let us investigate the alternative possibilities of either doubling the transmitted science bit content or doubling the science and science power

landed weight. Taken about the design point (14.0 pounds for science and science power, 5000 bits, and 124 pounds required internal weight), we see that doubling the bit content to 10,000 raises the required internal weight to 127 pounds. (This change may be done most simply by increasing the sampling rate of the scientific instruments.) Doubling the science and science power landed weight to 28.0 pounds and maintaining the bit content at 5000 total bits, the required internal weight goes up to 139 pounds, changing only a small amount more than the equipment weight change. (This is indicative of the effect of high packaging density (here in the range of 2.0 to 3.0 slug/ft^3), where components require only minimal structural weight, being packaged so tightly as to almost support one another.)

Another possible tradeoff is indicated on figure 29 where the surface mission time of the lander has been varied about the nominal value of 5 hours (requiring a landed transmission time of 18 minutes and having a required internal weight of 124 pounds). When the surface mission time is varied, say to 10 hours, the landed science data bit generation rate is assumed constant, necessitating a proportional increase in the total landed transmission time of 25-plus minutes. The required internal weight increases to 196 pounds, reflecting additional power requirements for scientific instrument and radio system operation. A constant data transmission bit rate (14 bits/sec) and transmitter RF power level (30 watts) are assumed. Missions longer than 10 hours, due to landed antenna look angles to Earth, require either considerably increased transmitter RF power, decreased bit rate with lengthened transmission times, or a non-fixed antenna pointing angle (gimballed antenna driven to look at Earth). It must be kept in mind that, because of the Martian planetary rotation rate of almost 15 deg/hr about its axis, a mission can be in view of Earth for only about 11-1/2 hours (except for polar landing sites). The zero offset of the ordinate of landed transmission time is due to the post-landing playback of descent payload data at the start of the first landed transmission.

A further variation can be seen in figure 30, where the surface mission time is again varied, but the landed transmission time is held constant at several different levels. (The total landed data bit content remains constant along the constant transmission time lines.) If a 5-hour surface mission time is maintained, increasing the transmission time from 18 (124 pounds required internal weight) to 60 minutes changes the required internal weight to 140 pounds. Both bit rate (14 bits/sec) and transmitter RF power (30 watts) were held constant. A total of three landed transmissions were assumed with their attendant warmup and Earth-based acquisition times.

5.3 COMMUNICATIONS LINK SUMMARY PARAMETRICS

Direct communication with Earth is accomplished using a 30-watt RF power S-band transmitter. The landed antenna transmission center line axis is assumed to be pointing up along the local vertical at the planetary impact point. Antenna look angles to Earth vary according to impact point

dispersions as shown on figure 31 and also due to initial impact time variations and planetary rotation effects. All curves on figure 31 show a planetary impact at sunrise. Syrtis Major is the nominal aim point. Earth line latitude variations relative to Mars are the bounds for the shaded areas, which depict impact point latitude dispersions, based on three-sigma limits with a 150-km bus tracking error at lander separation. Also shown is the Earth occultation limit line. The small inset map of Syrtis Major shows the appropriate relative size of the impact point dispersion ellipse. Indicated on the curve is the limiting case which sized the transmitter power requirement, based on a horn antenna having a 74-degree total beamwidth between its half-power points. DSIF receiver characteristics were assumed to be as stated in Volume III (The Lander) of this report. Impact time variations can be accommodated by moving the abscissa (time scale) to the left or right, as required. For surface mission times greater than 5 hours or for optimum transmission characteristics, the impact time can also be varied to suit particular cases.

The direct link power requirement having been established, we may now check the usage of this communication system in the relay mode back to the flyby bus. Using the landed transmitter concurrently for both links allows for a redundancy in data paths and a checkout-by-comparison capability. Figure 32 shows various trajectory points at their relay link communication ranges and net lander and bus antenna gains. The diagonal lines are constant net lander and bus antenna gains. The points plotted are for 1969 and 1971 mission opportunities and are based on a 45-degree trajectory inclination to the planetary equator. At lander planetary entry (at an altitude of 800,000 feet), data points are shown for various periapsis altitude trajectory geometries. Similar data points are plotted at times equivalent to lander entry plus 3 hours and lander entry plus 5 hours, with the lander on the planetary surface. At the right hand side of the plot is a vertical line of constant available landed transmitter power, 30 watts, as previously chosen for the Earth direct link. All relay link points require less power than this; therefore, a margin exists for the relay link. The choice of a nominal 5-hour slowdown of the bus relative to the lander (ΔV_{bus} = 912 ft/sec at 10^6 km planetary range) allows increasing relay link margin as the 5-hour mission progresses. The optimum relay link for these cases exists at the end of the surface mission, since the bus periapsis point occurs near that time. The (1969) 6500-km periapsis point at lander entry has an 0.5×10^6 km planetary range at lander separation and bus slowdown, resulting in about a 2-hour slowdown for the same velocity increment as before. Relay communications for this particular case exist for only about 2 hours after entry before the flyby bus vanishes over the lander's planetary horizon. Earth link communications are not affected, of course, by these flyby-lander geometries.

5.4 LANDER CONFIGURATIONAL, ENVIRONMENTAL, AND SUBSYSTEM OPERATIONAL CONSTRAINT SUMMARY PARAMETRICS

Definition of the conceptual design is dependent on the establishment of certain configurational and environmental constraints or ground rules. The various

subsystems also have operational limitations which constrain the problem. A general discussion of the lander vehicle performance, as prescribed by the aforementioned characteristics, follows.

Selection of any entry vehicle shape is a function of aerodynamic, thermal protection, structural, and packaging considerations. Various widely differing families of shapes were investigated prior to the selection of an Apollo shape with a modified afterbody cone angle. Attainment of satisfactory aerodynamic performance and stability characteristics at low structural weight fractions were the realized goals of this study. Figure 33 shows the variation of lander entry weight with lander diameter for several ballistic parameter (m/C_DA) values. A hypersonic drag coefficient (C_D) of 1.45 was used. The conceptual design point is shown at an entry weight of 500 pounds for a lander diameter of 90 inches, and at an m/C_DA of 0.244 slug/ft^2. The selection of these numbers resulted from the parametric evaluation of interactions between the bus, lander, and launch vehicle, as well as the performance requirements imposed by environmental and mission constraints.

In cases where a choice of atmospheric or trajectory parameters had to be made to establish the conceptual design, a "worst-case" philosophy was used. The influence of planetary surface pressure on vehicle performance is extremely significant, as can be seen from figure 34. For the selected, 90-inch-diameter modified Apollo shape, the use of an 11-millibar surface pressure, typical of the "G" and "H" model atmospheres, results in an optimum m/C_DA of 0.244 slug/ft^2 with an entry weight of 500 pounds and an available internal weight of 142 pounds if no external payload is required. The actual design point shown at 124 pounds represents the internal weight available in the conceptual design, which has 50.3 pounds of descent payload and structure. Vehicle ballistic parameter requirements have been established based on vehicle aerodynamic and parachute system performance as defined by the minimum or optimum weight two-parachute system with drogue chute deployment at Mach 2.5, main chute deployment at Mach 0.8, and a minimum main chute deployment altitude of 8000 feet. Increasing the minimum predicted surface pressure to 20 millibars would allow for m/C_DA of 0.464 slug/ft^2, an entry weight of 960 pounds, and an available internal weight with no external weight of 390 pounds.

Estimates of the surface wind velocity also play a significant role in the determination of the available internal weight. Figure 35 shows that for a surface wind velocity of 200 ft/sec, a 1500 Earth g impact shock pulse maximum, and a 65 ft/sec main parachute vertical descent velocity, there are 124 pounds of available internal weight at the conceptual design point. If no external weight were required, i.e., no descent payload, there would be 142 pounds of available internal weight. Reducing the surface wind to 100 ft/sec, while maintaining all other parameter values, would increase the available internal weight to 220 pounds with no external weight.

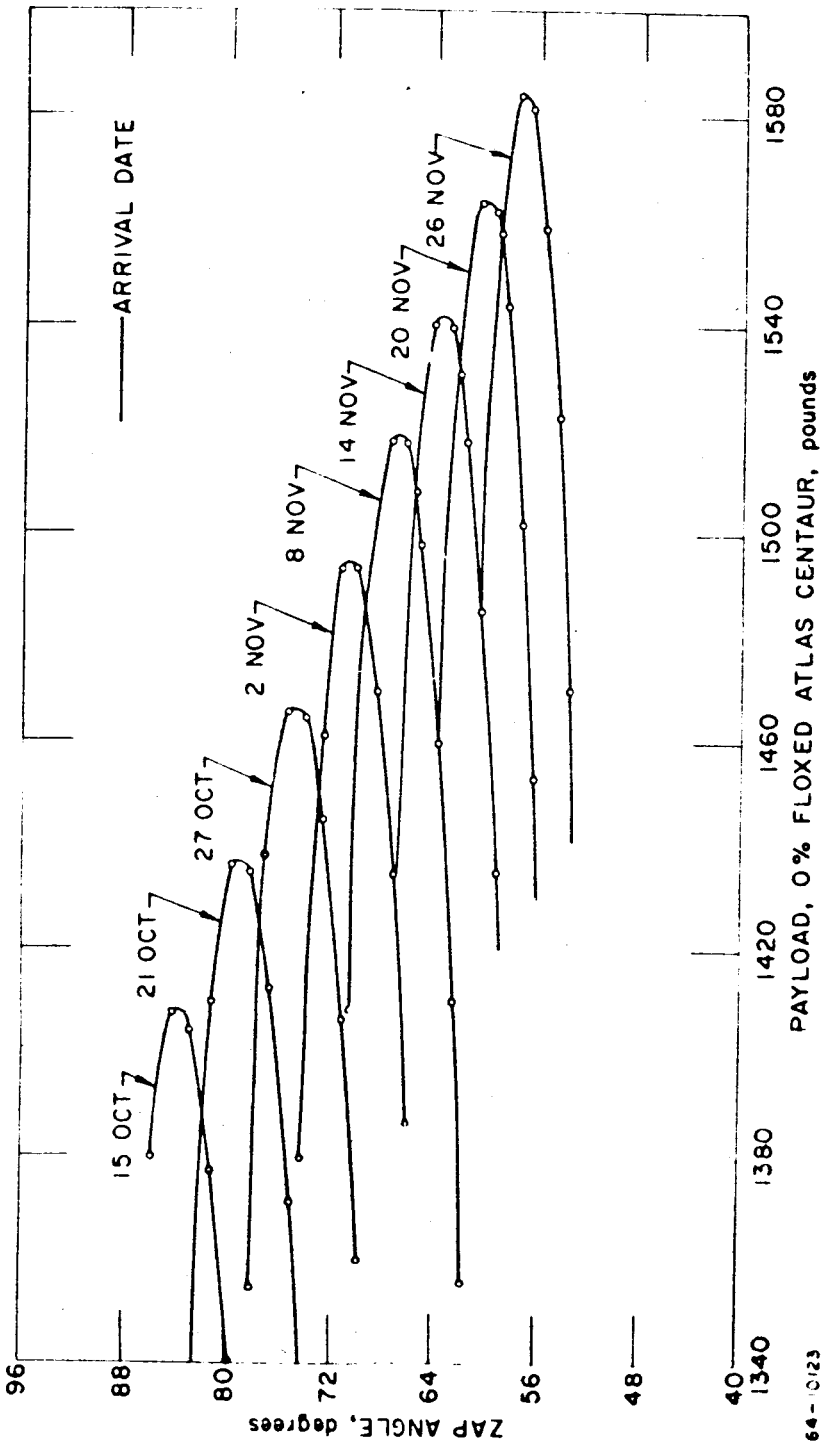

Figure 24 - 1969 LAUNCH OPPORTUNITY RELATIONS-ARRIVAL DATES

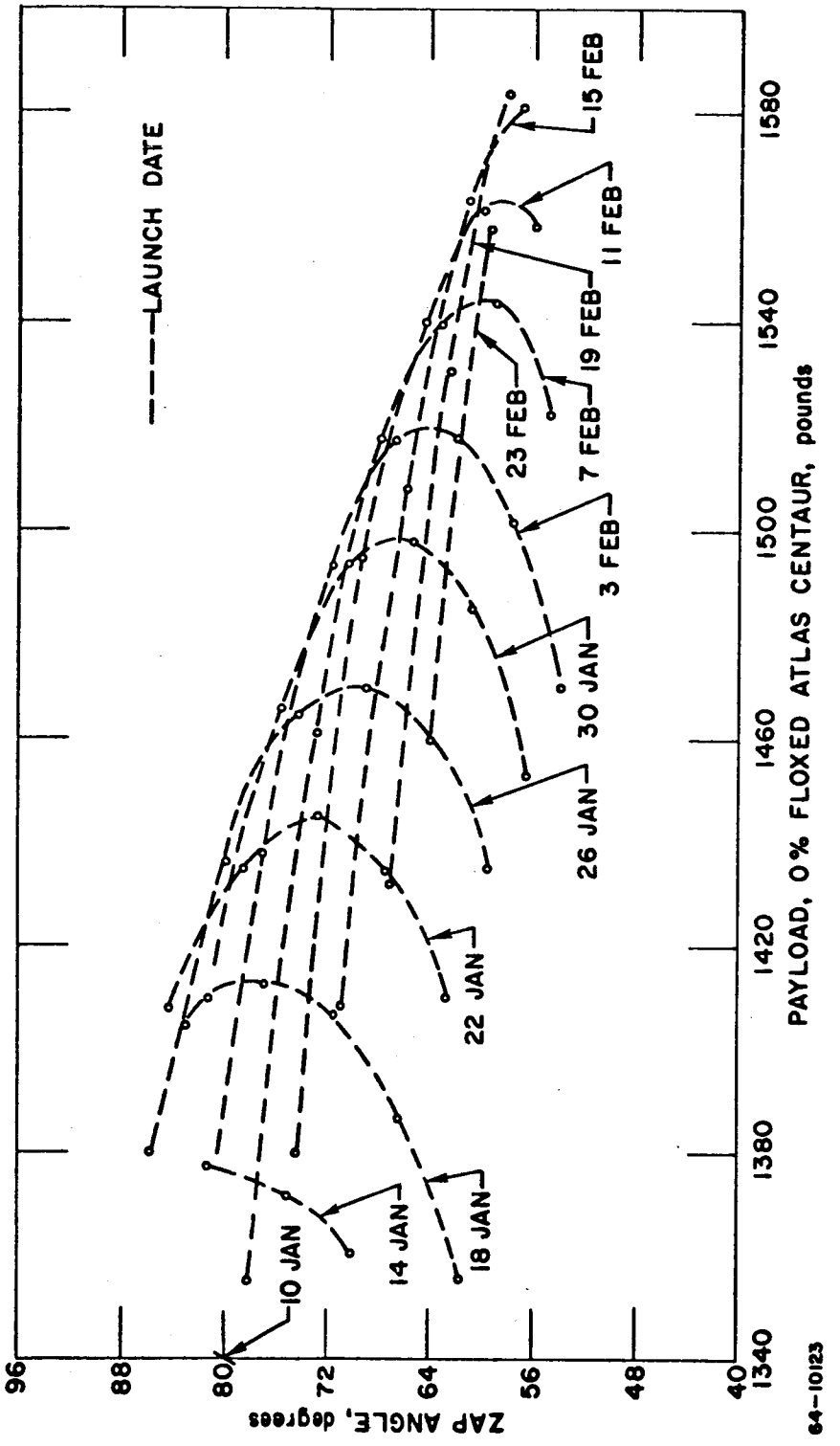

Figure 25 - 1969 LAUNCH OPPORTUNITY RELATION-LAUNCH DATES

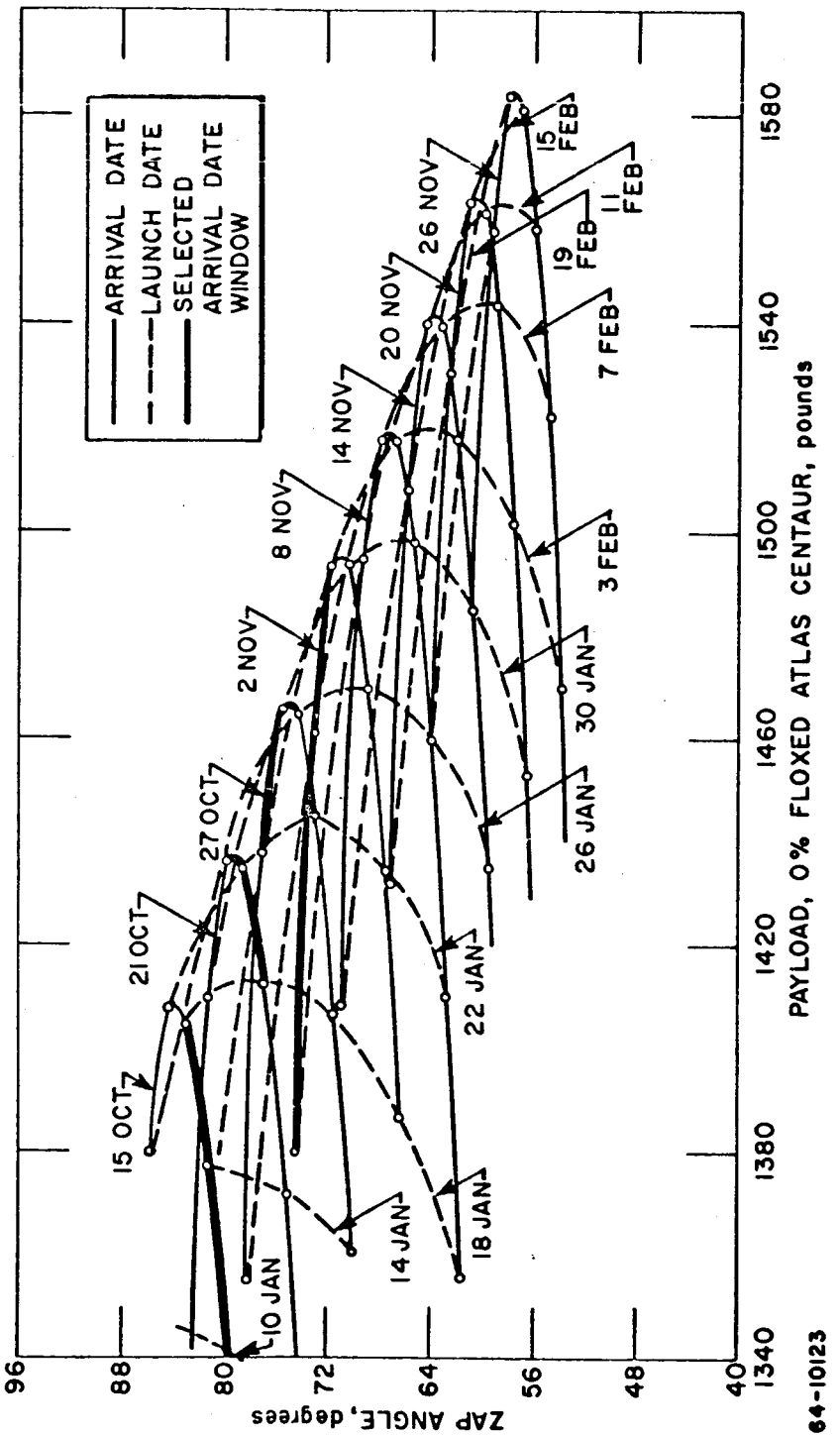

Figure 26 - 1969 LAUNCH OPPORTUNITY RELATIONS

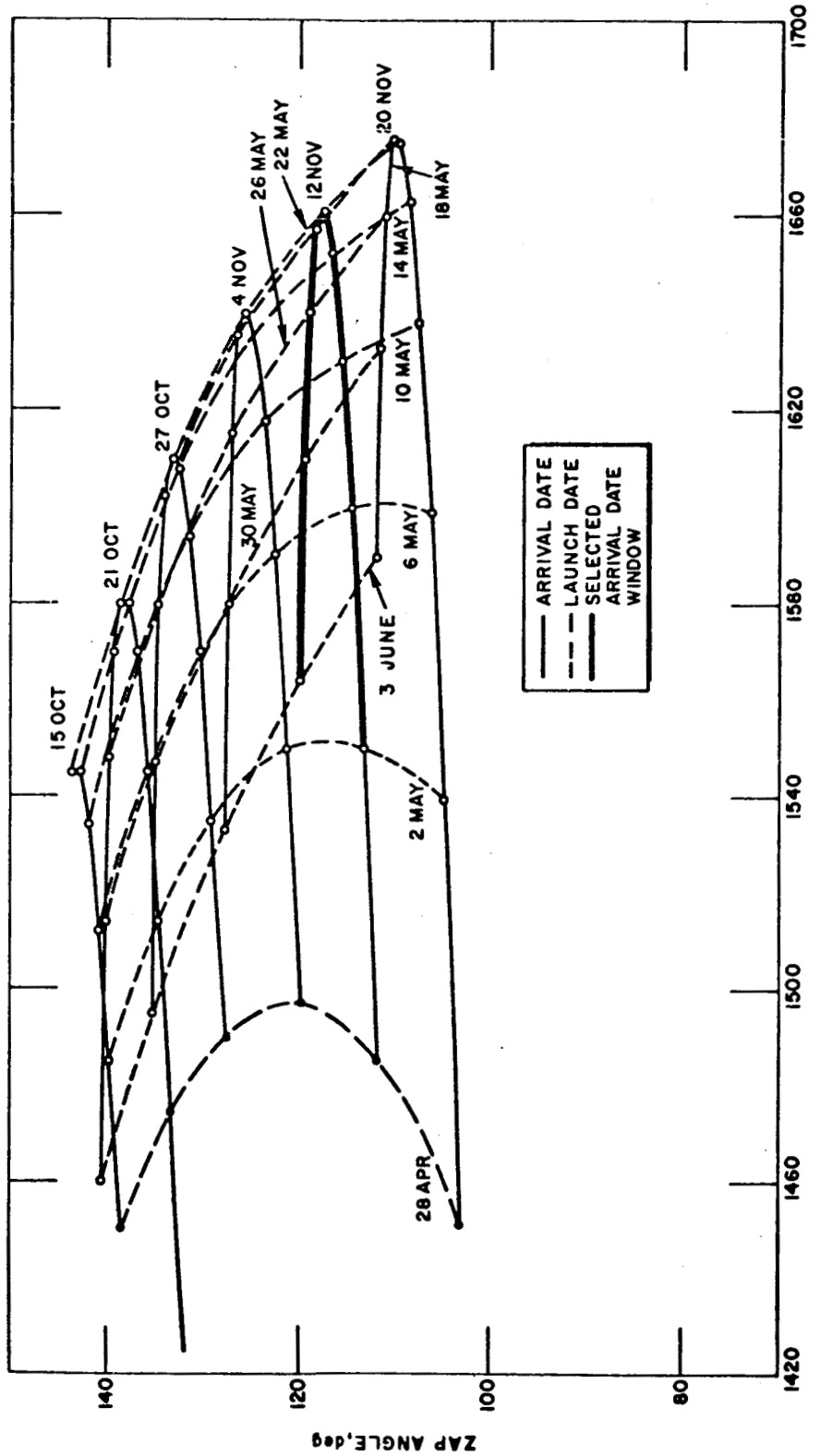

Figure 27 - 1971 LAUNCH OPPORTUNITY RELATIONS

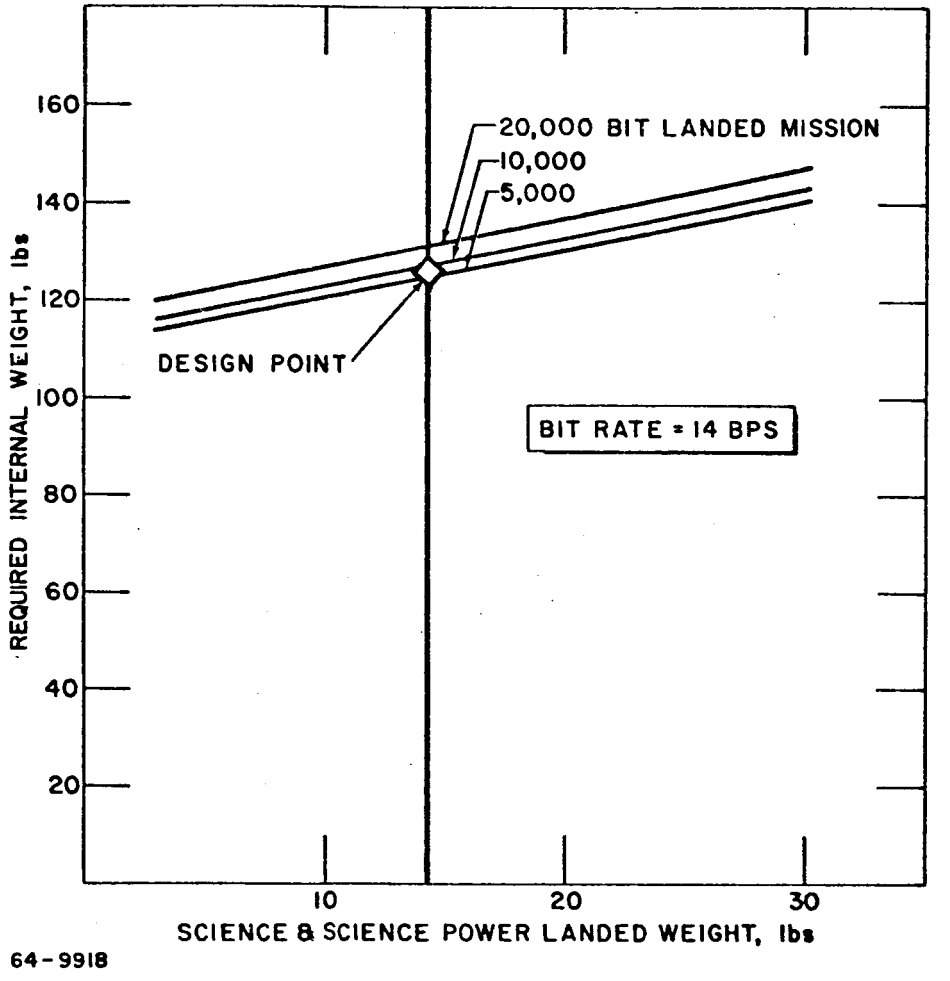

Figure 28 - REQUIRED INTERNAL WEIGHT VERSUS SCIENCE AND SCIENCE POWER LANDED WEIGHT FOR VARIOUS LANDED MISSION BIT CONTENTS

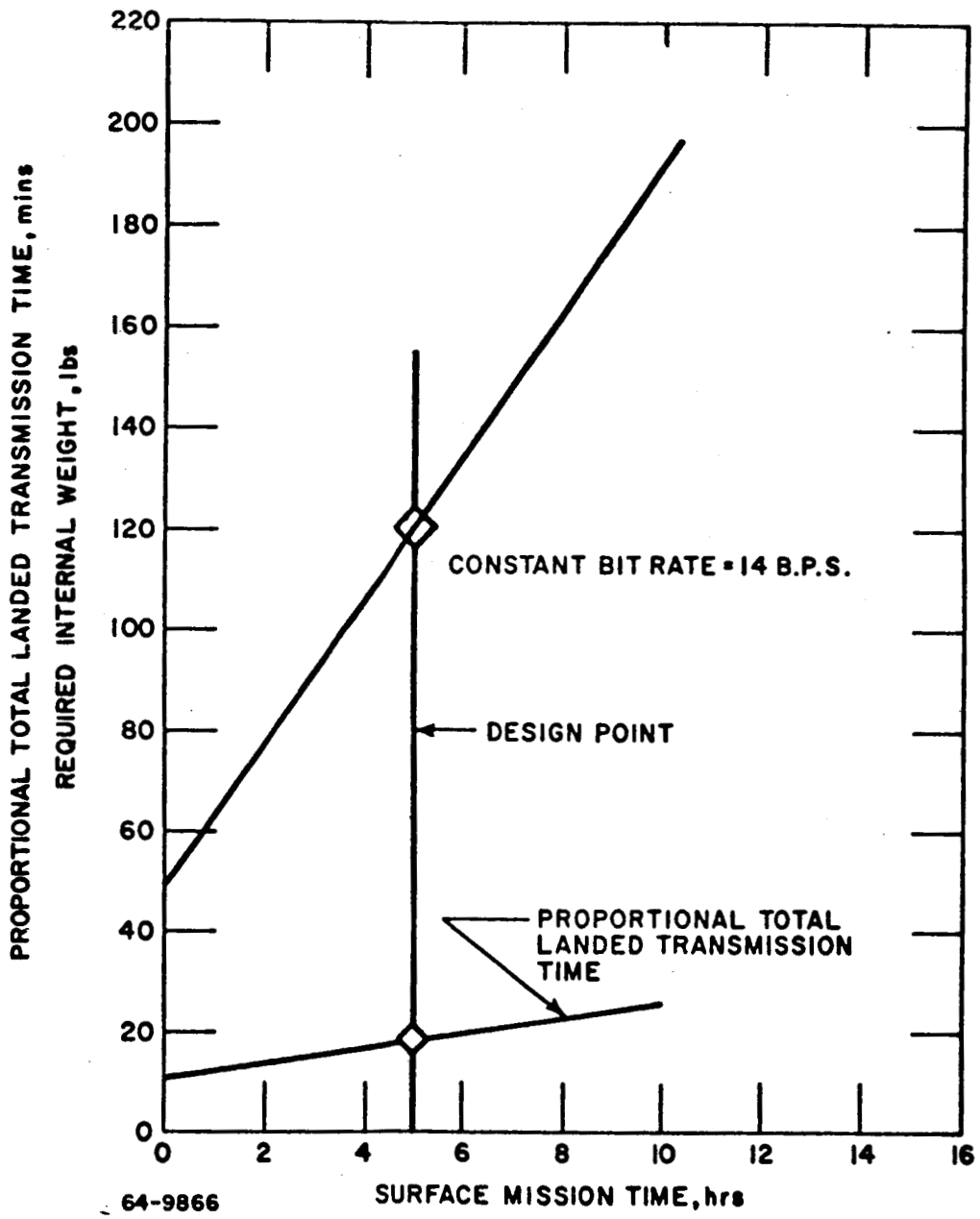

Figure 29 - REQUIRED INTERNAL WEIGHT AND PROPORTIONAL TOTAL LANDED TRANSMISSION TIME VERSUS SURFACE MISSION TIME

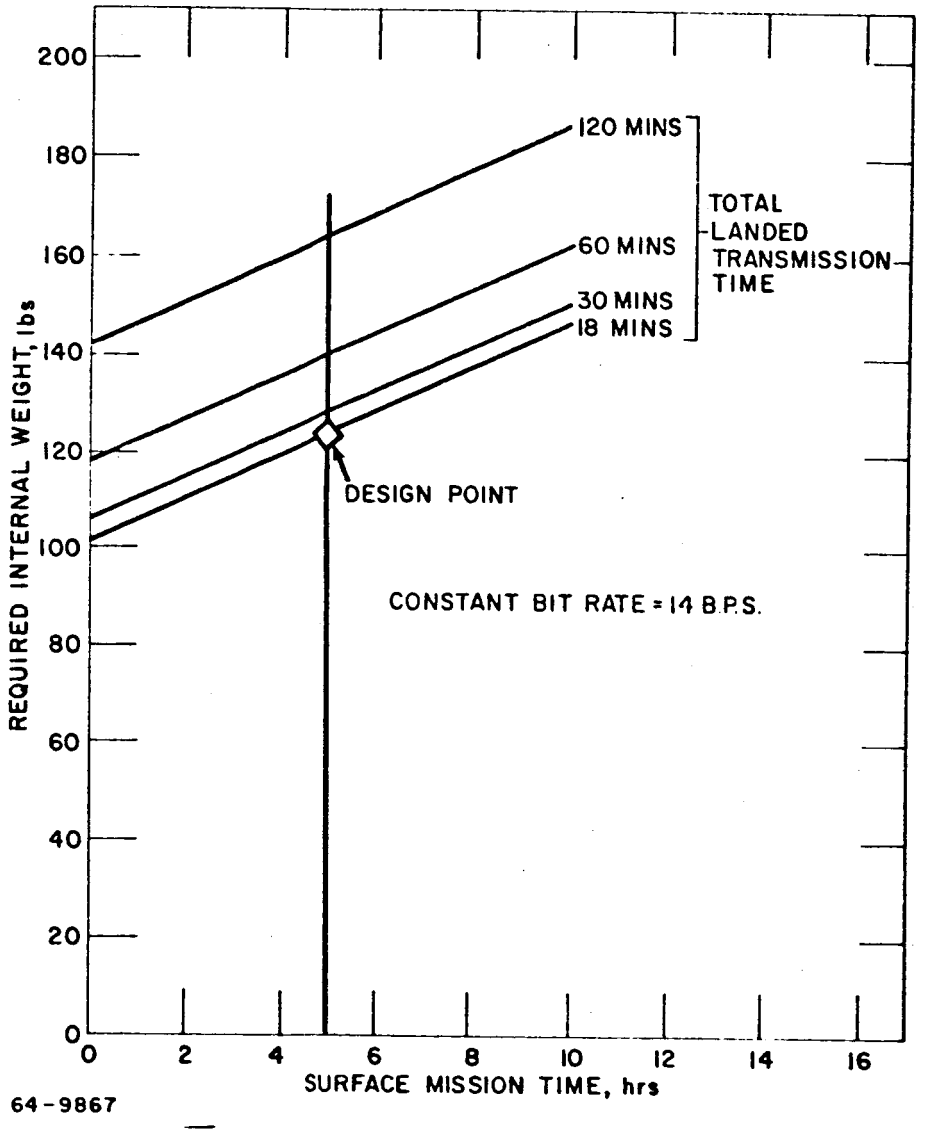

Figure 30 - REQUIRED INTERNAL WEIGHT VERSUS SURFACE MISSION TIME

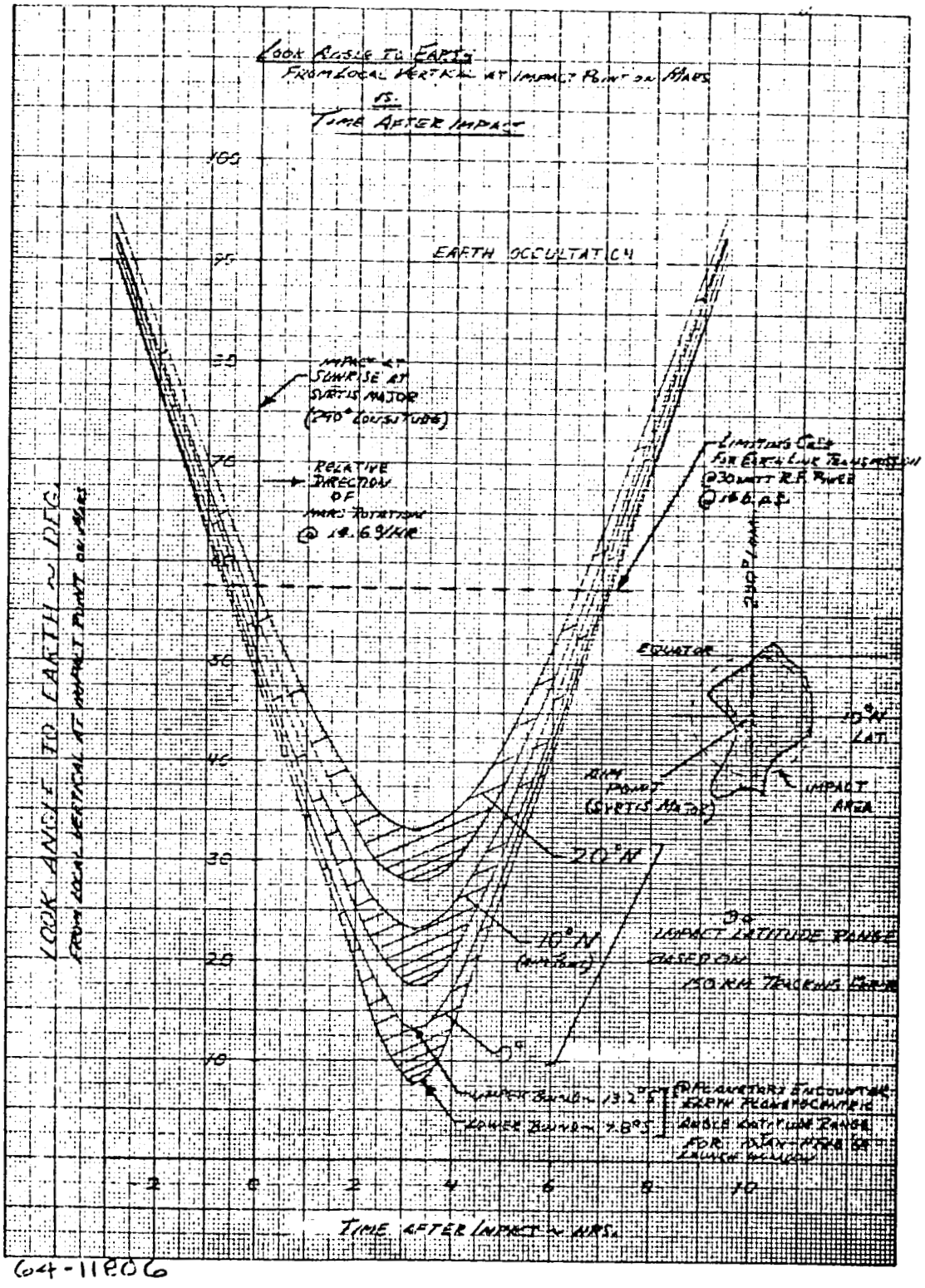

Figure 31 - LOOK ANGLE TO EARTH VERSUS TIME AFTER IMPACT

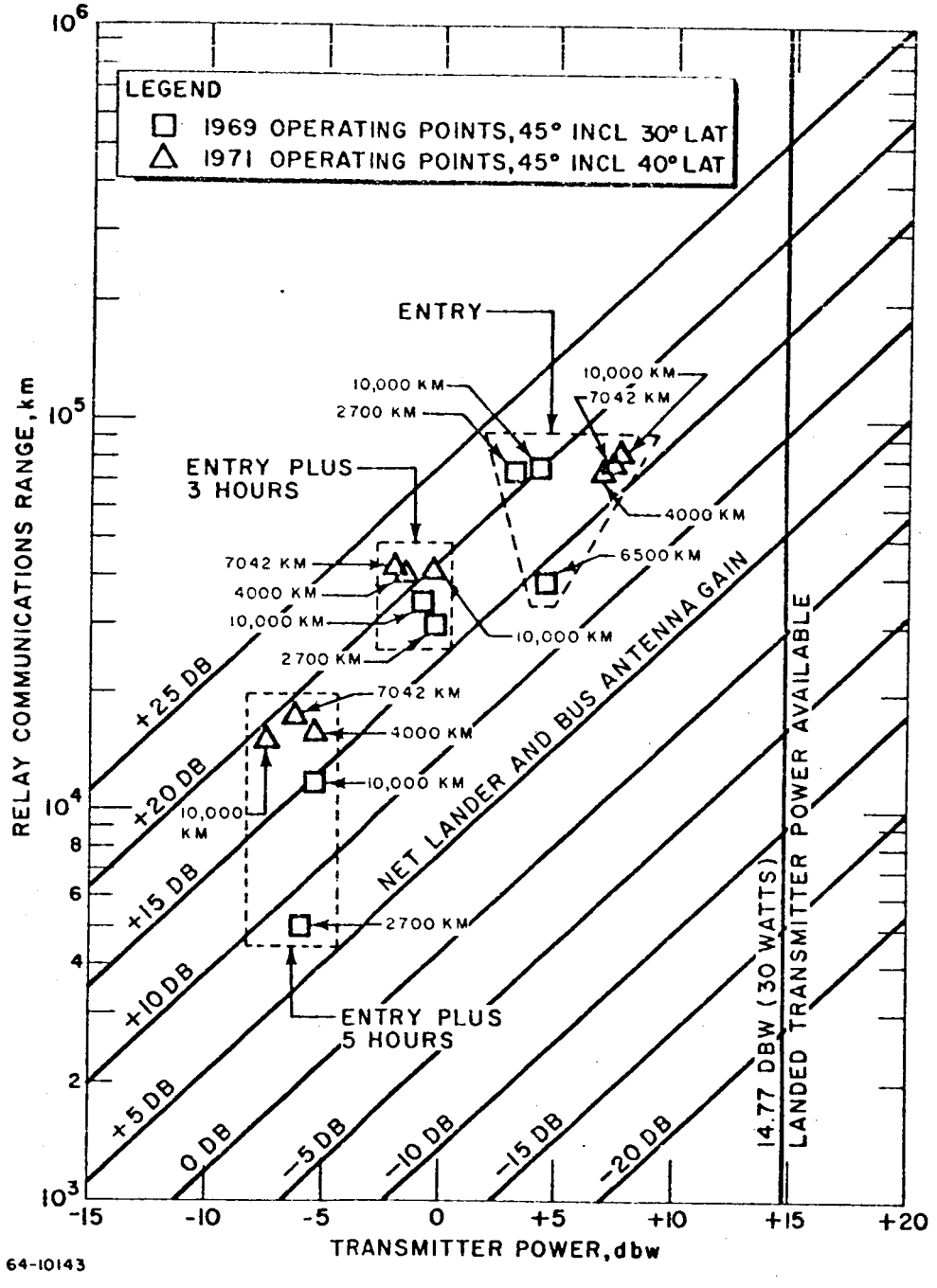

Figure 32 - RELAY COMMUNICATION RANGE VERSUS TRANSMITTER POWER AT VARIOUS NET LANDER AND BUS ANTENNA GAINS

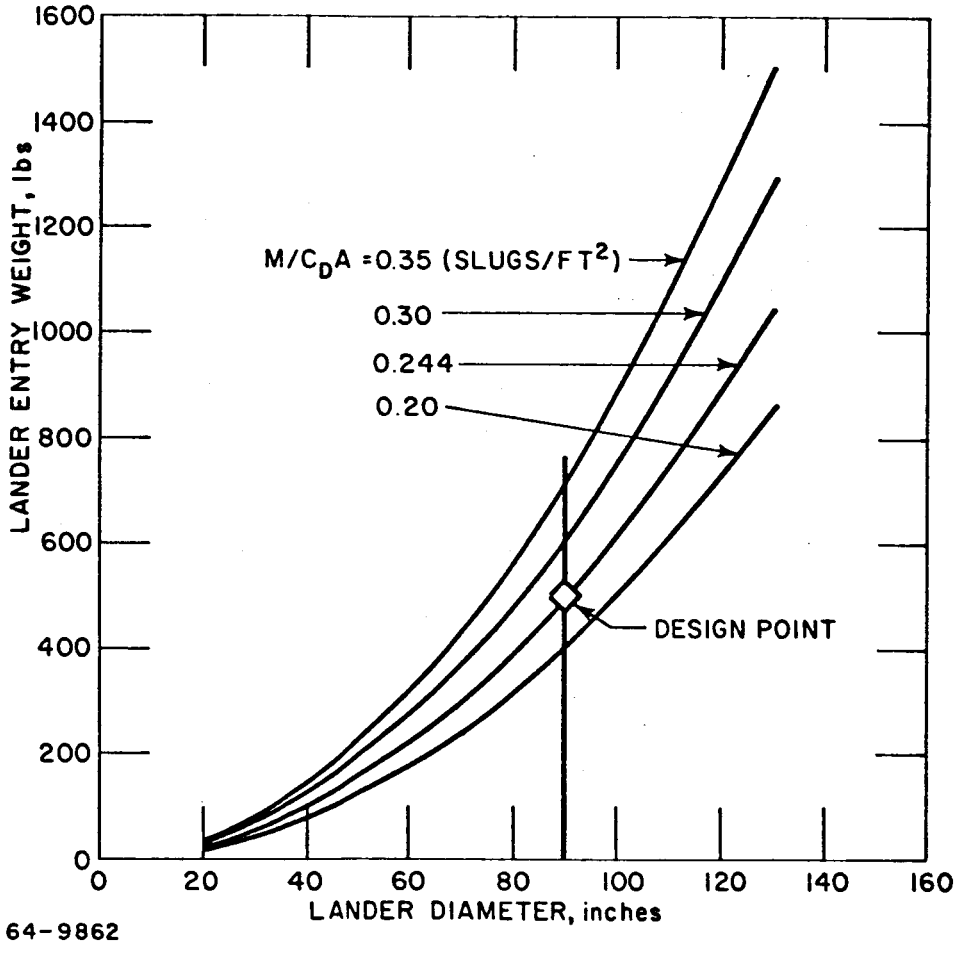

Figure 33 - LANDER ENTRY WEIGHT VERSUS LANDER DIAMETER

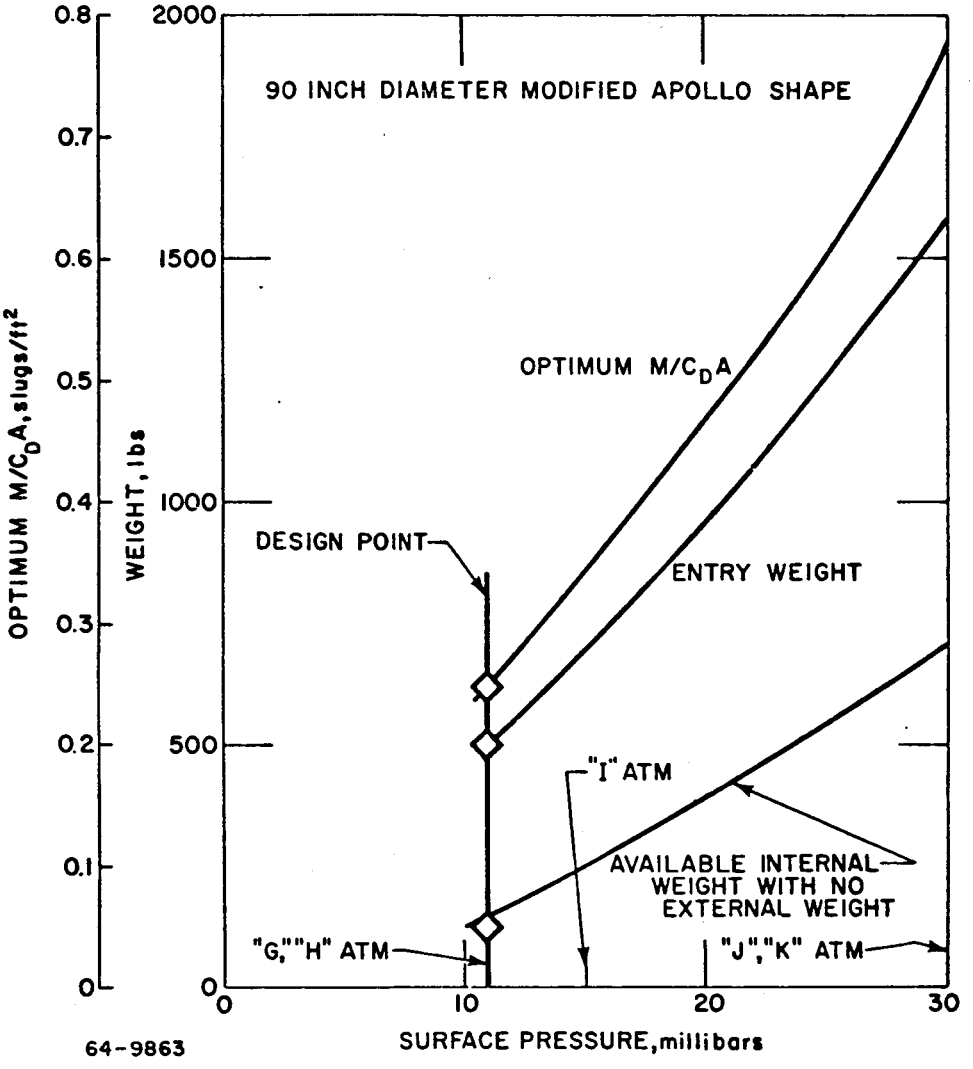

Figure 34 - OPTIMUM M/C_DA, ENTRY WEIGHT, AVAILABLE INTERNAL WEIGHT VERSUS SURFACE PRESSURE

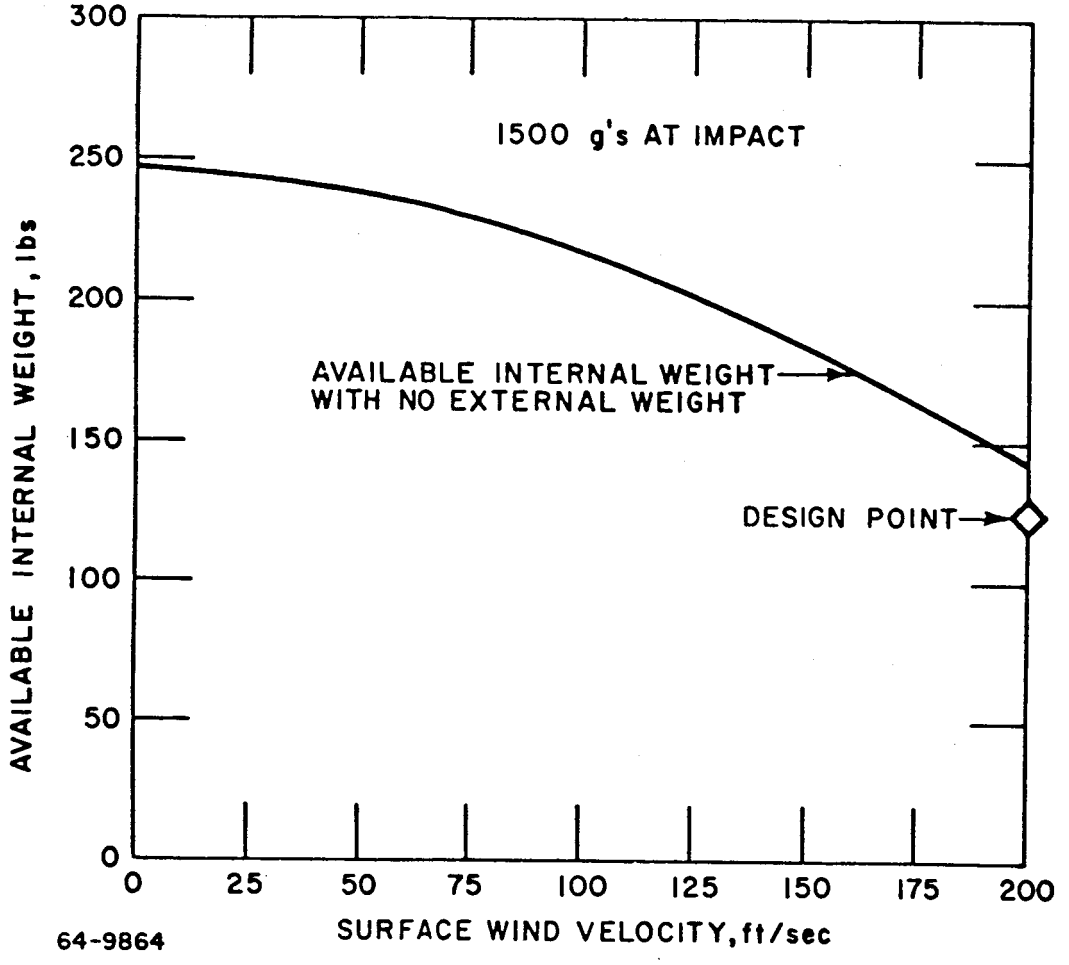

Figure 35 - AVAILABLE INTERNAL WEIGHT VERSUS SURFACE WIND VELOCITY

Increasing the maximum impact deceleration as shown on figure 36 is another means by which the available internal weight may be increased. Holding the impact velocity constant at 210 ft/sec (the vector sum of a horizontal surface wind component of 200 ft/sec and a vertical descent velocity of 65 ft/sec on the main parachute), the impact attenuator aluminum honeycomb density and impact g level may be increased with shorter deceleration strokes and increased available internal weight. Alternatively, the crushup density may be decreased with decreased impact g's, longer strokes allowed, and available internal weight decreased. A lower geometric limit exists for this case, however; namely, the largest outer diameter impact attenuator which can be packaged within the prescribed diameter lander vehicle. The effect of increased g levels on the internal equipment cannot be shown on this curve, but should be kept in mind. Equipment reliability estimates are not currently available much beyond the 1500-g level, but a general statement can be made that higher g levels usually result in lower equipment reliability, a direction not particularly compatible with the objectives of the Advanced Mariner program.

Selection of a main parachute deployment altitude has an effect on the vehicle ballistic parameter (m/C_DA) as previously noted in figure 34. The table shown in figure 37 shows the optimum ballistic parameter value as discussed heretofore, as well as the descent time after main chute deployment for various main chute deployment altitudes. The field of figure 37 further expands the data presented to include the effect of lander entry vehicle diameter. The conceptual design point is again shown for both available internal weight and lander entry weight. A main chute deployment altitude of 8000 feet was chosen as a design point to allow sufficient descent time at a terminal velocity of 65 ft/sec for playout of the data stored during entry, as well as for the measurement and transmission of atmospheric data. The main parachute terminal velocity resulted from a two-parachute weight optimization study for the 11-millibar surface pressure atmospheres. Uncertainties in surface feature elevation, as well as tolerances in the various sensing and actuation systems, were also considered in the choice of main parachute deployment altitude.

Figure 38 illustrates the variation in entry vehicle weight and available internal weight with nominal entry angle. The abscissa, nominal entry angle, implies a computed 3-sigma variation in entry angle tolerances and off-design conditions. The ballistic parameter has been varied to reflect the optimum, as for the examples shown in figures 34 and 37 (to allow an 8000-foot, Mach 0.8, main parachute deployment).

5.5 FLYBY BUS SUMMARY PARAMETRIC CURVES

The primary mission objectives for the flyby bus are to transport the lander and to obtain scientific information. With regard to the latter, figure 39 shows two trends, namely, the variation of bus weight with bus science payload weight, and the variation of bus weight with total stored encounter science data to be sent to Earth by telemetry. The first of the curves is based upon an average

of cruise mode scientific instruments fixed to the spacecraft and encounter mode science instruments mounted on the planetary scanning platform. Design constraints for the second curve include an Earth-link transmission power margin of 5.6 db, a constant playout time after completion of the planetary encounter phase of the mission, and a variable bit rate and transmitter power level to accommodate the total bit content variation. Transmitter size, solar panel area, and storage device weights have been considered for a nominal Earth communication range of 200×10^6 km. The record mode read-in rate of the storage unit has been increased directly as the total number of bits, allowing the increased bit acquisition to take place during a constant encounter time period. This assumption was made to allow for the fact that most of the bits stored are television picture data, which are of interest only in the near-periapsis region.

The effect of the flyby bus slowdown velocity increment on flyby/bus total weight at launch is shown in figure 40. Although no strong variation is evident, it is of interest to note the range of values and the possibility of off-loading or on-loading of bus slowdown propellant to make fine adjustments to the launch weight. An I_{sp} of 280 seconds and a λ of 0.7 were used for this calculation.

Finally, figure 41 shows the effect of lander diameter on lander entry weight (at constant m/C_DA), bus weight, and upon their sum, spacecraft weight. The bus weight variation with lander diameter includes sterilization canister and lander rocket weight variations, as well as bus structural weight changes to allow for different launching loads due to the lander weight dependence on diameter. As can be seen from figure 41, the lander entry weight change with lander diameter is predominant, overshadowing the effects of lander diameter on bus weight.

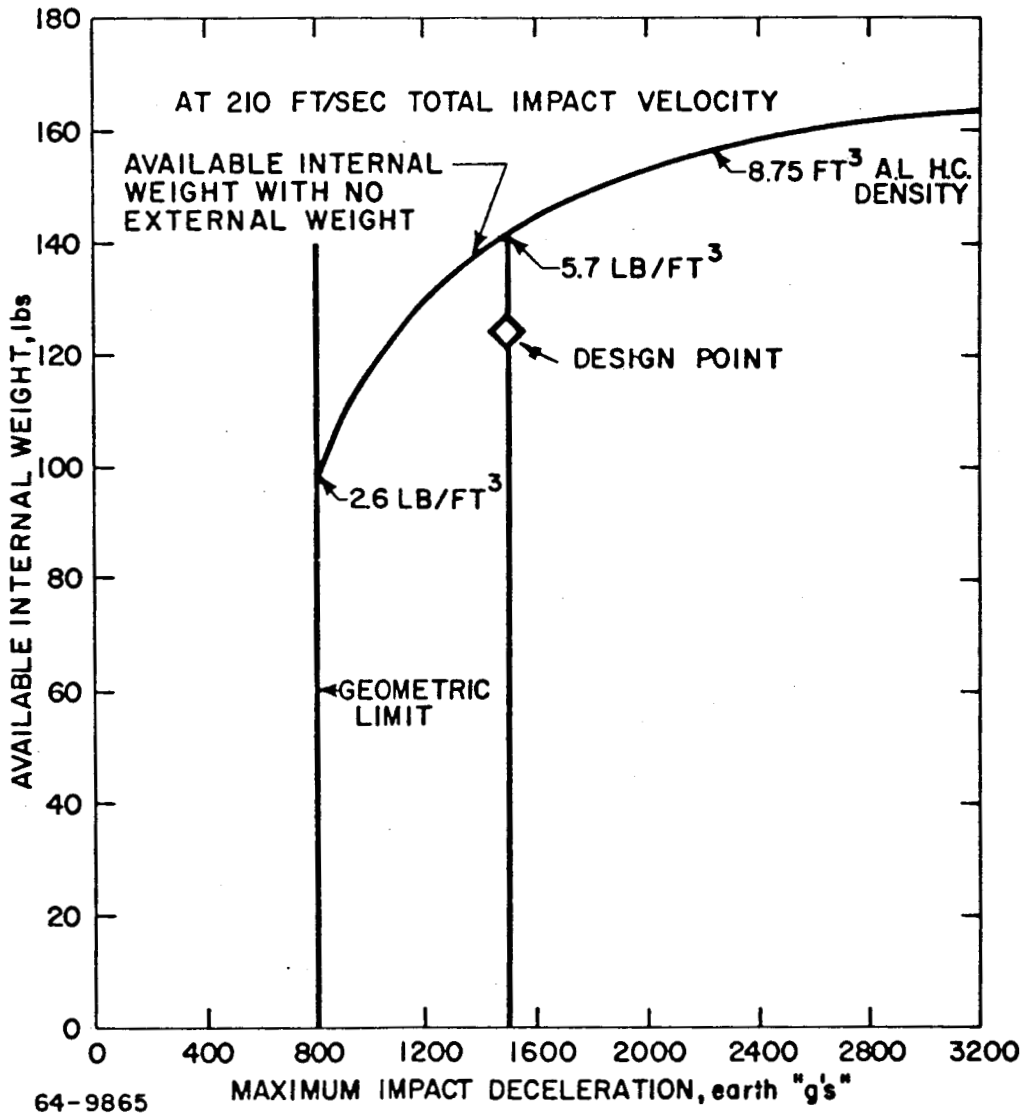

Figure 36 - AVAILABLE INTERNAL WEIGHT VERSUS MAXIMUM IMPACT DECELERATION

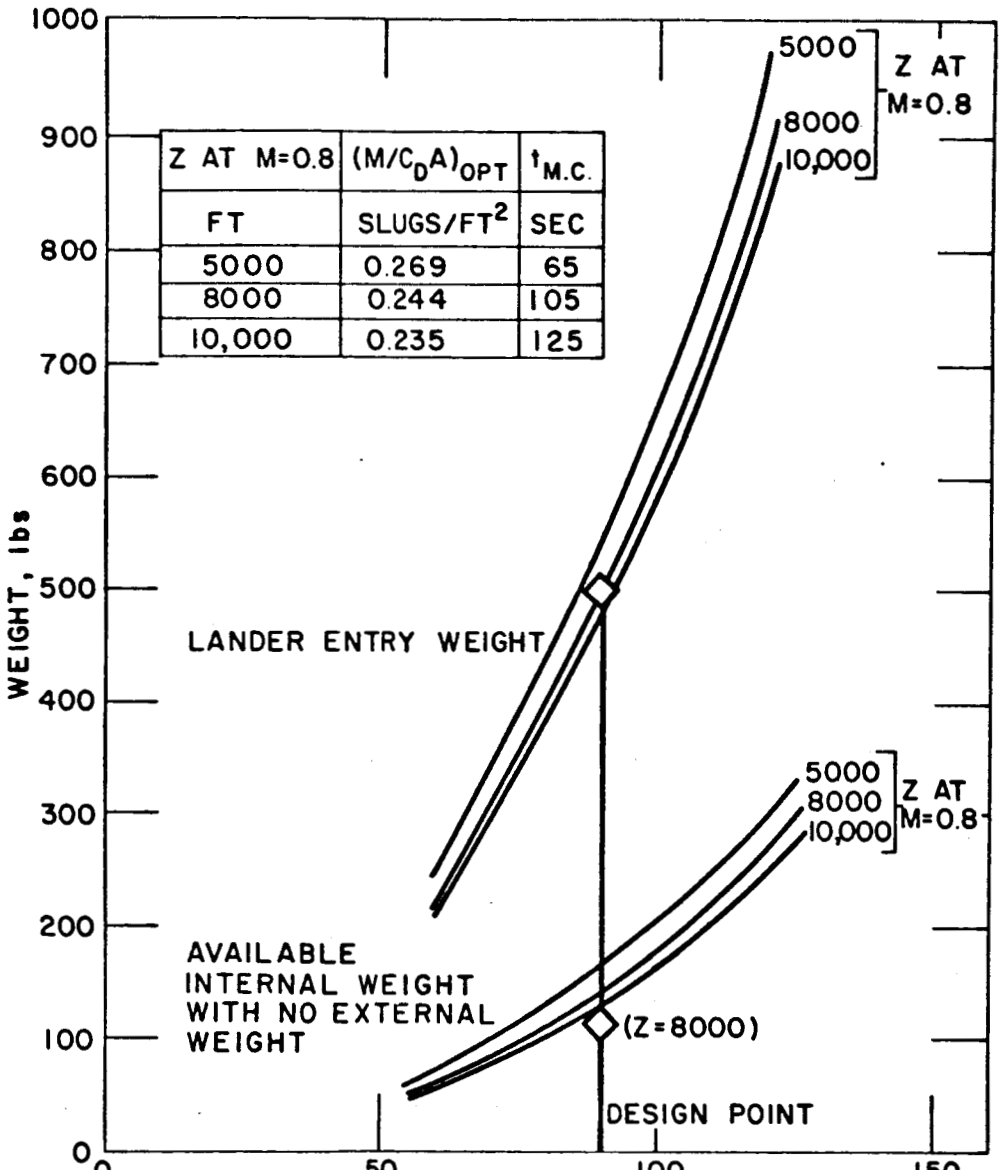

Figure 37 - LANDER ENTRY WEIGHT AND AVAILABLE INTERNAL WEIGHT VERSUS LANDER DIAMETER (AT VARIOUS MAIN CHUTE DEPLOYMENT ATTITUDES)

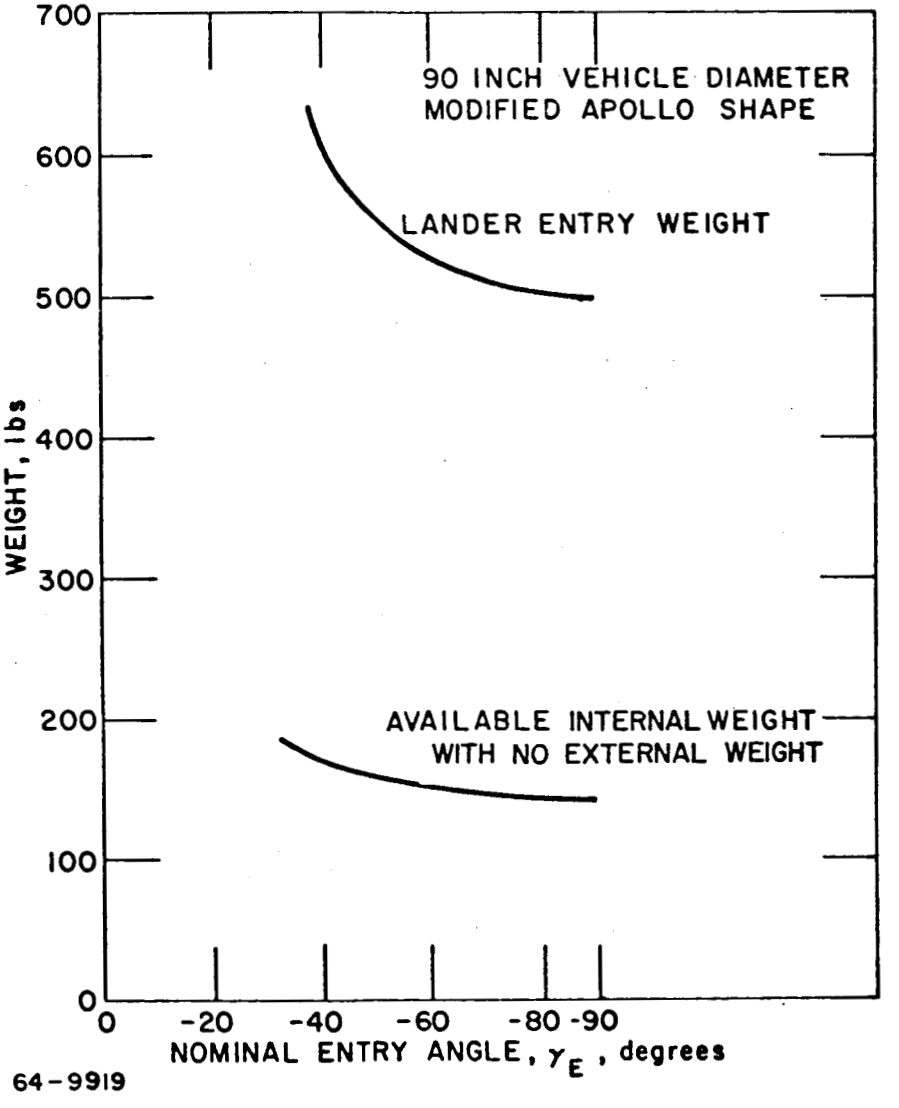

Figure 38 - LANDER ENTRY WEIGHT AND AVAILABLE INTERNAL WEIGHT VERSUS NOMINAL ENTRY ANGLE

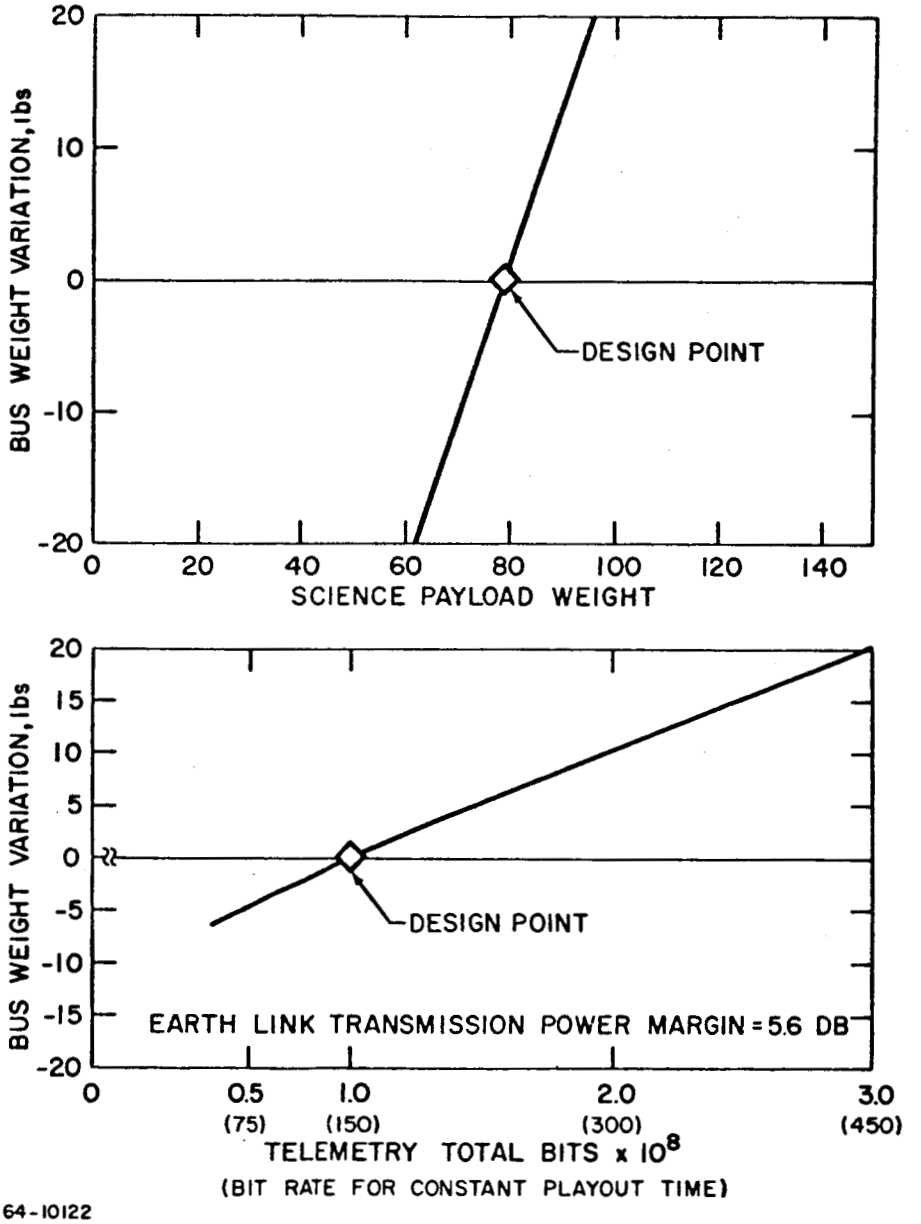

Figure 39 - BUS WEIGHT VARIATION VERSUS SCIENCE PAYLOAD WEIGHT AND TELEMETRY TOTAL BITS

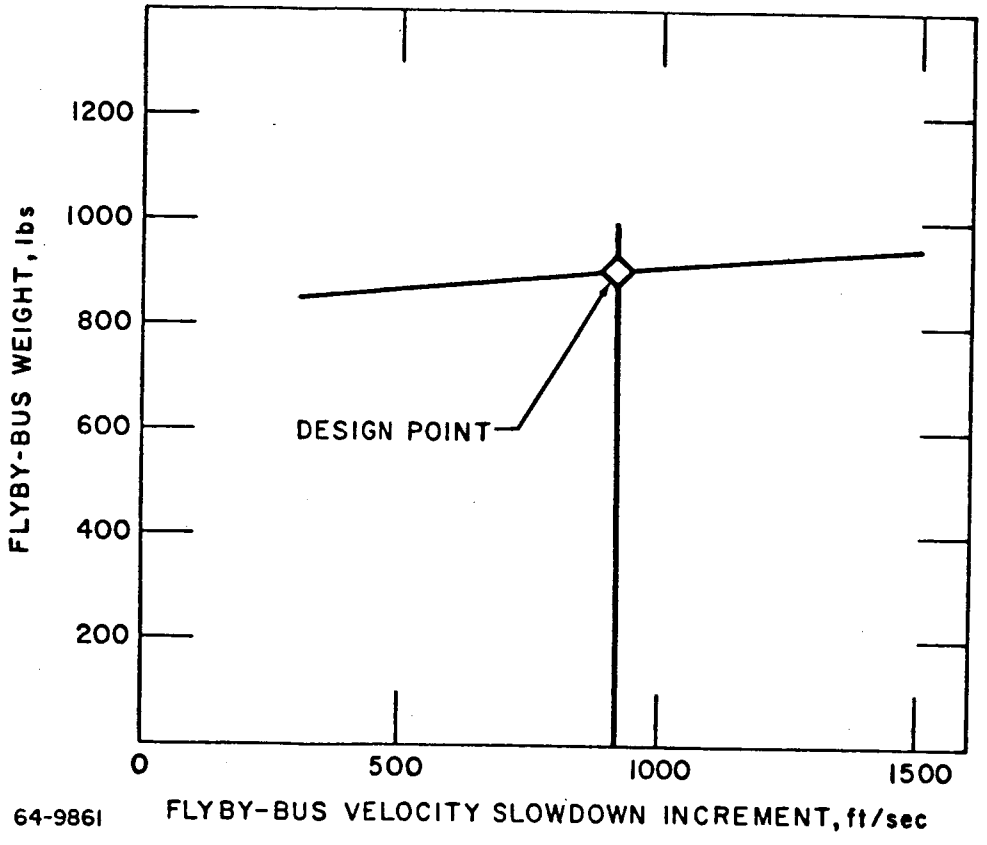

Figure 40 - FLYBY BUS WEIGHT (AT LAUNCH) VERSUS FLYBY BUS VELOCITY SLOWDOWN INCREMENT

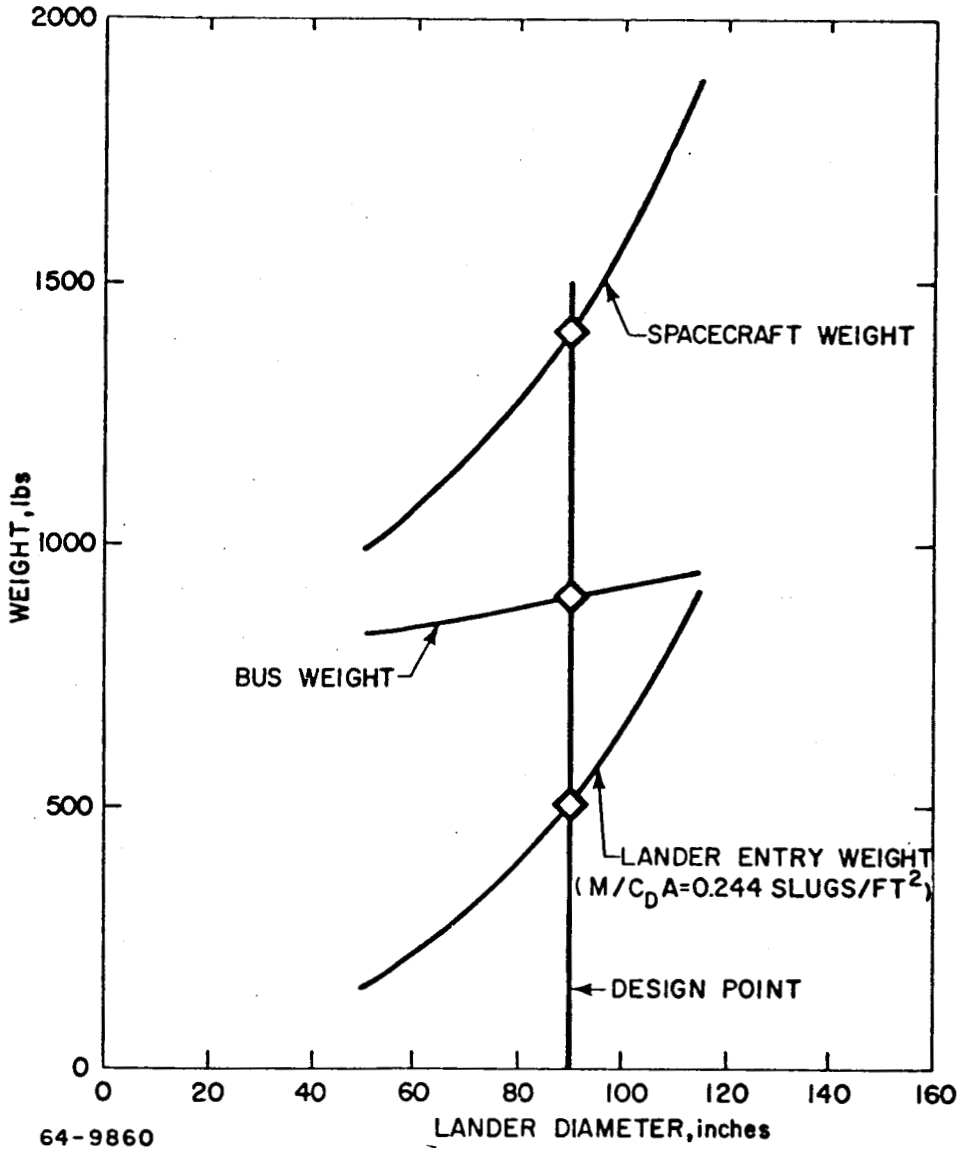

Figure 41 - SPACECRAFT, BUS, AND LANDER ENTRY WEIGHT VERSUS LANDER DIAMETER

6.0 DEVELOPMENT PLAN

The purpose of the Development Plan is to identify, organize, and discuss the major efforts required to carry out a program resulting in the successful completion of the 1969 and 1971 Mars Advanced Mariner missions, according to the schedule shown in figure 42, and using the flyby bus and lander concepts presented in volumes III and IV.

The plan covers the time span from the beginning of the preliminary design in March 1965 through the follow-up activities after the 1971 launch.

The hardware covered by the Development Plan includes the bus, lander and bus/booster interface only. For the 1969 launch a total of 9 vehicles are required; five vehicles for system test and four vehicles (two flight and two spare) for flight hardware.

For the 1971 launch, a total of 5 vehicles are required; one vehicle for system test and four vehicles (two flight and two spare) for flight hardware.

The schedule shown in figure 42 indicates the relationships of the major program activities and the path of constraining activities. It is organized first to assure that the 1969 launch date can be met, and second to maximize the time available for the conduct of subsystem development programs. In view of the fact that no development is scheduled for the 1971 launch, that portion of the schedule is not critical and is not shown here. It is shown, however, in volume V.

Preliminary design is expected to start on 1 March 1965, being awarded to two prime contractor candidates. The awards are expected to result from a normal RFP-proposal exchange; the activity will last 5 months, terminating by 1 August 1965. JPL will closely monitor the activities of these contractors and perform appropriate analyses throughout the period, so that the prime contractor selection can be made on 1 August 1965. The winning contractor would then continue into the final design stage.

Selection of the prime contractor actually governs the start of the subsystem development programs, since it will take 5 months of final system design to produce subsystem requirement specification adequate to initiate subsystem development activities.

For the bust, two of the more critical development programs are the attitude control program and the separation program. The first is scheduled tightly because the lead times necessary for developing such components as propellant tanks are characteristically long. The second is thought to be critical because of its technical and operational complexity; pyrotechnic procurement is a long-lead procurement item.

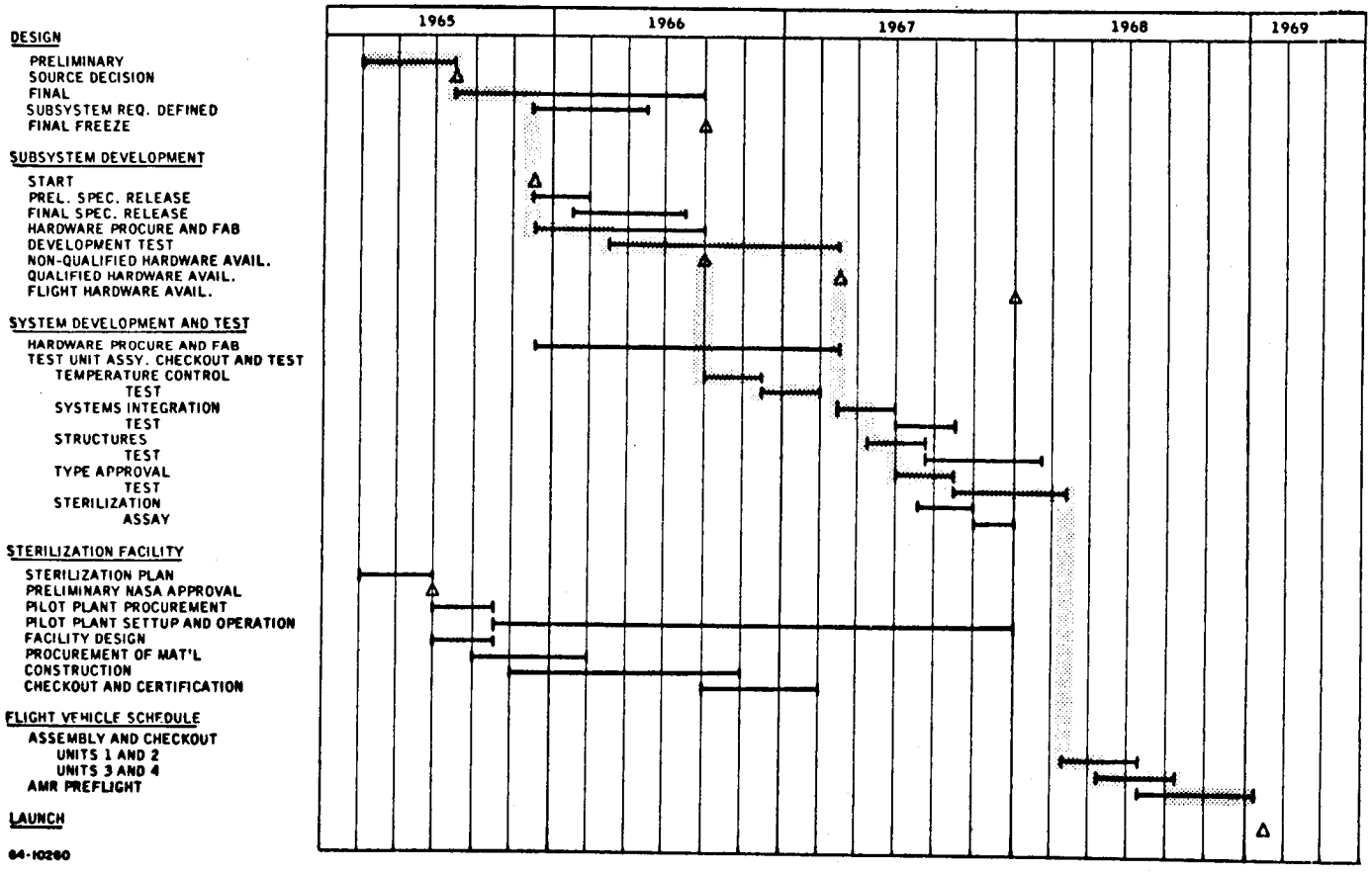

Figure 42 - ADVANCED MARINER MILESTONE SCHEDULE

A generally critical item for the lander is the requirement that all its components must be heat sterilizable. There is nothing in the conceptual design which is not considered sterilizable, but the severity of the requirement makes likely the possibility of problems in this area.

The subsystem development programs continue until the end of March 1967 and must be complete by that time because of constraining activities later in the program.

Five system test units are planned, the last four of which are to be assembled from qualified subsystems. The minimum fabrication schedule for these four govern the initiation of systems test, and of these, the system type approval test is the controlling one, extending through March 1968.

It is reasoned that assembly of the flight hardware and spares should not start until the type approval testing is complete. In this way it is assured that no major retrofits will be required on flight hardware.

Flight vehicles are assembled in pairs, with the two spare spacecraft being the governing factor on the initiation of assembly of the flight spacecraft. In order for the spare spacecraft to be available for backup, they need 4 months at the launch site for checkout and preflight mating and testing before the launch date. The 2-month overlap between assembly activities is considered minimum.

The program elements chiefly constraining the subsystem development programs are therefore the following:

1. Spacecraft flight units need 4 months at launch site.

2. Assembly of flight units must start by 1 April 1968.

3. Type approval testing must be complete by 1 April 1968.

4. Assembly of test vehicles controls initiation of type approval testing.

5. Development programs must provide qualified hardware for system test unit assembly.

In an effort to shorten the AMR preflight activities, the launch site compatibility and integration program will use the system type approval unit after the type approval tests are complete. The flight units and spares will then require only the usual launch site check out and preflight and booster integration activities at ETR, which are estimated to require 4 months.

In figure 42, sterilization is shown as a separate line item to emphasize its overall importance to the program and to demonstrate that it is a long lead item. The underlying constraint in the sterilization schedule is the clean room

and terminal sterilization facilities which must be available by 1 April 1967 for assembly of the four systems test units to be constructed from qualified subsystems. The indicated schedule requires that sterilization planning parallel the preliminary design. At about the same time that the prime contractor is chosen, the sterilization plan will be approved to allow immediate acquisition of both pilot plant and sterilization facilities. The facility schedule indicated is considered realistic; the pilot plant activities are carried on through the completion of the sterilization assay.

7.0 COST PLAN

The purpose of the cost plan is to estimate the cost of the development effort specified in the Development Plan.

The summary costs are indicated in table 10 which is a presentation of the total costs of both 1969 and 1971 launches. These costs, as well as the others presented in volume V, are based upon several ground rules which are:

1. The cost estimates do not allow for contingencies in the development or manufacture of the spacecraft. This is never completely true, but allows the reader to judge the impact of unanticipated contingencies based on his own experience.

2. Hardware covered: bus, lander, and bus/booster interface only; number of units covered--1969 launch: system test, five vehicles; and flight, four vehicles (two flight and two spare); number of units covered--1971 launch: system test, one vehicle; and flight, four vehicles (two flight and two spare).

3. Subsystem Development is carried out for the 1969 launch but not for the 1971 launch. Vehicles used in 1971 are identical to those used in 1969.

4. Hardware costs are those associated with fabrication and quality control of flight units; fabrication and quality control of flight hardware GSE; acceptance tests of flight hardware; and spacecraft field support.

5. Development costs include all the other program costs which are subdivided as follows: (a) costs associated with the system test units, and (b) support costs, such as management, reliability, quality assurance, and documentation; and (c) subsystem development costs.

6. The cost estimate is in terms of contract cost less fee.

The single most expensive year is 1966, since most of the development activities are in process. While the 1965 costs may seem high, most of the costs occur after the start of fiscal year 1966. The only costs occurring earlier are the preliminary design and sterilization planning of the two competing contractors. Most of the manufacturing costs are incurred in 1967 and 1968.

Table 11 is a summary of the total costs indicated in the cost plan. There is a significant reduction in the 1971 costs, primarily because no subsystem development is planned for that opportunity. Bus hardware costs are about double per unit those of the lander. This is principally because of the greater payload complexity of the bus, including the solar panels. The hardware cost

decreases slightly in 1971, since the GSE can be re-used after refurbishment. Bus development costs are actually about the same as lander development costs, but appear higher in this summary since five sets of system test hardware are included. The bus systems test hardware is considerably more expensive than that for lander systems test.

TABLE 10

1969 and 1971 LAUNCHES - TOTAL PROGRAM COST
($ x 10^{-3})

	CALENDAR YEAR								
	1965	1966	1967	1968	1969	1970	1971	1972	Total
Prel. Design	2,397								2,397
Syst. Anal. & Int.		1,344	1,925	2,093	2,067	1,941	1,240	434	11,044
Final Design	2,607	4,710	3,161	1,081	94	56			11,709
Devel. Prog:									
Bus									
TV		1,380	685						2,065
Payload Plat.		405	53	39	10				507
Comm. & Pwr		2,787	437						3,224
Attitude Cont.		1,122	1,320						2,442
Propulsion		2,240	1,600						3,840
Temp. Cont.		330	350	117					797
B/L Sep. Syst.		1,550	580						2,130
Science Liaison		17	17	17					51
Lander:									
Aerodynamics		892							892
Comm. & Pwr		2,663	333						2,996
Structures		548	430						978
Thermo & Mat'l		1,116	420	33	3	3			1,575
Parachute		1,990							1,990
Impact		1,833							1,833
Propulsion		421	421						842
Temp. Cont.		245	155	99					499
Sterilization	2,700	1,800	1,800						6,300
Science Liaison		27	27	26					80
Mfr & Q.C.		11,572	23,404	9,669	16,144	7,092	1,035	68	68,984
GSE		4,956	2,362	1,063	411	108	30		8,930
Syst. Testing:									
Temp. Cont.		236	472	94					802
Syst. Integ.			280	2,255					2,535
Structural			494						494
Type Approval		26	764	112					902
Steril. Assay			429			429			858
Accept. Testing			820	820		820			2,460
Rel. & QA		1,950	2,028	962	344	140	96		5,520
Documentation		192	268	265	108	108	131		1,078
Prog. Mgmt.		146	198	194	188	93	32		851
TOTAL	7,704	46,498	45,233	18,939	19,369	10,790	2,570	502	151,605

TABLE 11

PROGRAM COST SUMMARY
($$ x 10-3)

	Launch Window		Total
	1969	1971	
Bus			
Development	53,116	5,549	58,665
Hardware	17,007	16,163	33,170
Subtotal	70,123	21,712	91,835
Lander			
Development	41,093	3,455	44,548
Hardware	8,216	7,006	15,222
Subtotal	49,309	10,461	59,770
Grand Total	119,432	32,173	151,605

DISTRIBUTION

Addressee	No. of Copies
JPL (+1 vellum)	20
Central Files	1
Research Library (+1 reproducible)	5